Auto-Regressive analysis of GWTC-3 Ringdown data

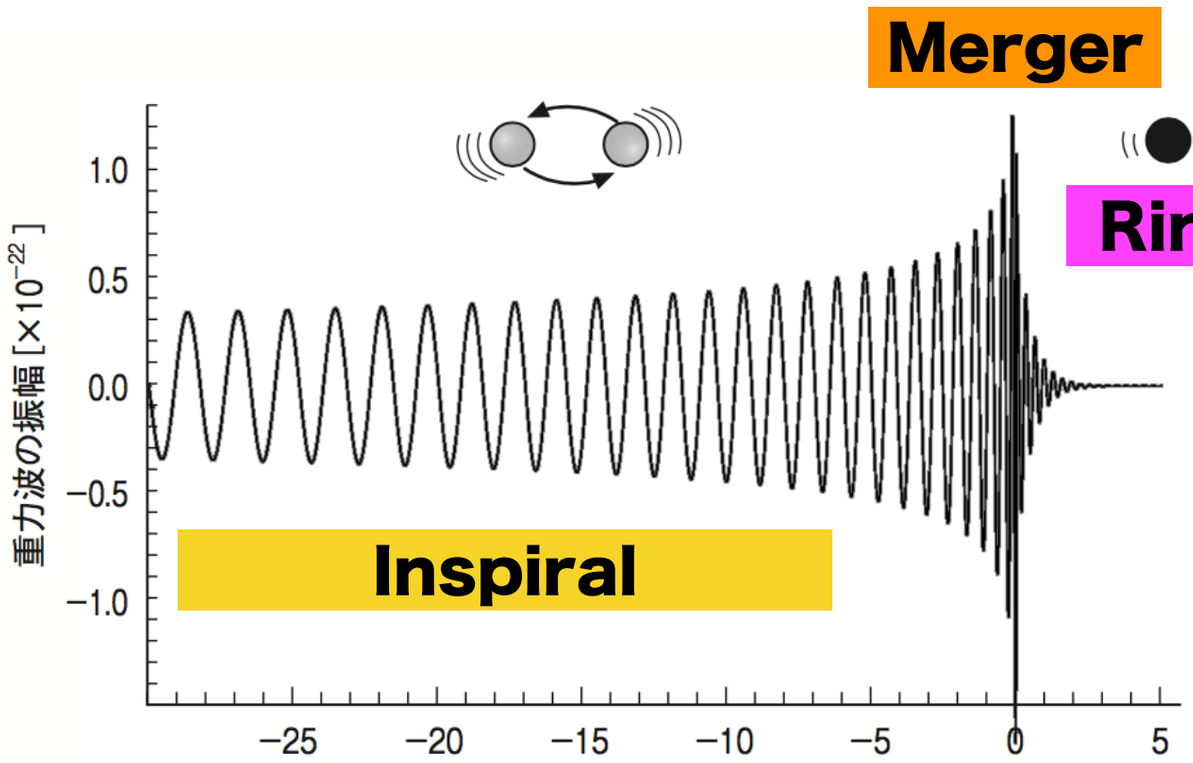

BH quasi-normal modes
⇦ BH perturbation in GR

⇨ (*M, a*)

Strong Gravity Effect
⇨ Reasonable for testing GR

“Ringdown part” is quite short (3.7 ms for 60 M_{sun}, a=0.75)
AR analysis enables to find out waveform without template

Hisaaki Shinkai (OIT)
真貝寿明（大阪工大）

http://www.oit.ac.jp/is/shinkai/

2022/1/23 A01 Boot Camp

Observation 1/2/3a/3b & 4

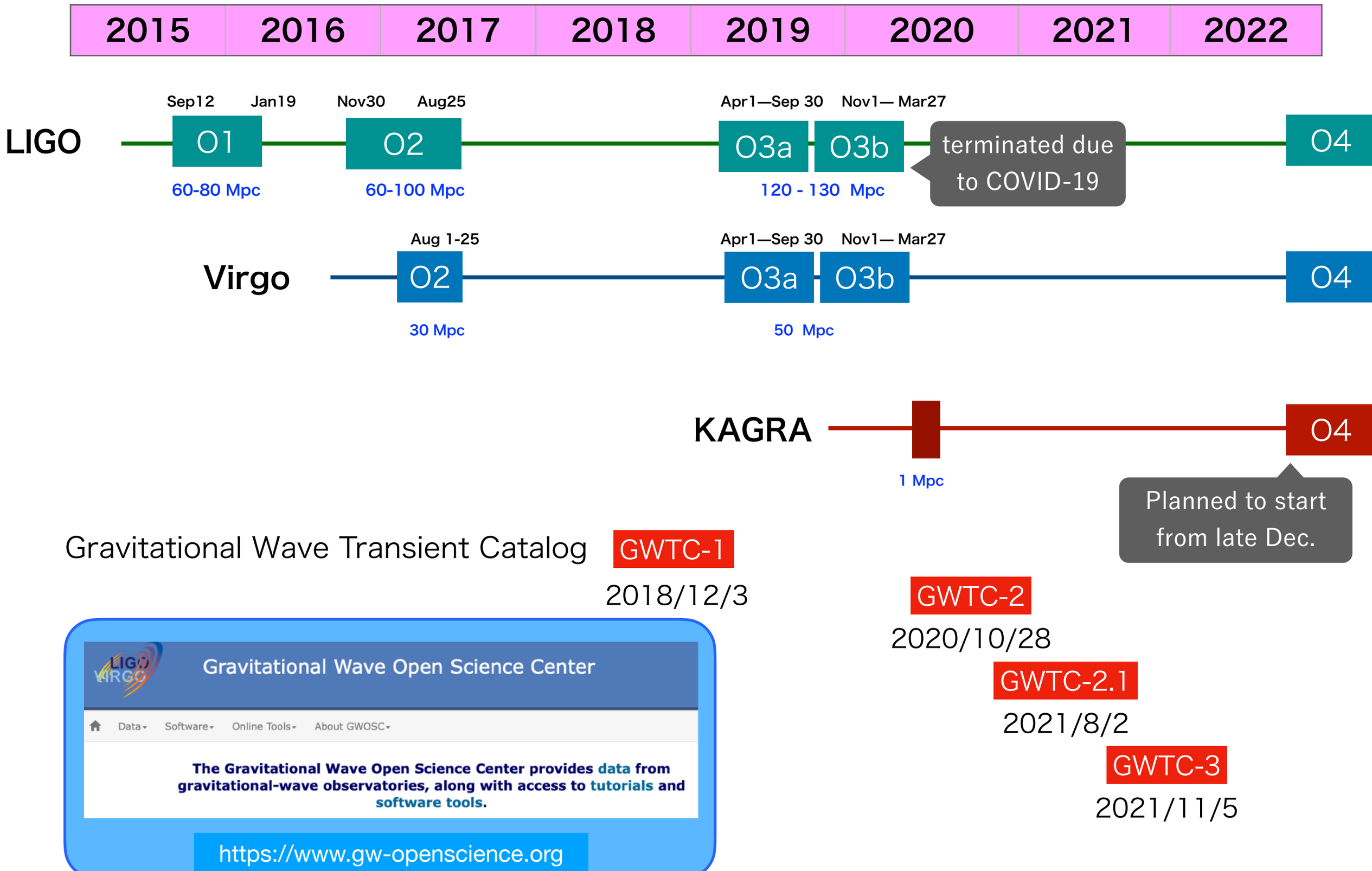

Gravitational Wave Transient Catalog GWTC-1

2018/12/3

GWTC-2

2020/10/28

GWTC-2.1

2021/8/2

GWTC-3

2021/11/5

O1 (2015/9/12 - 2016/1/19)

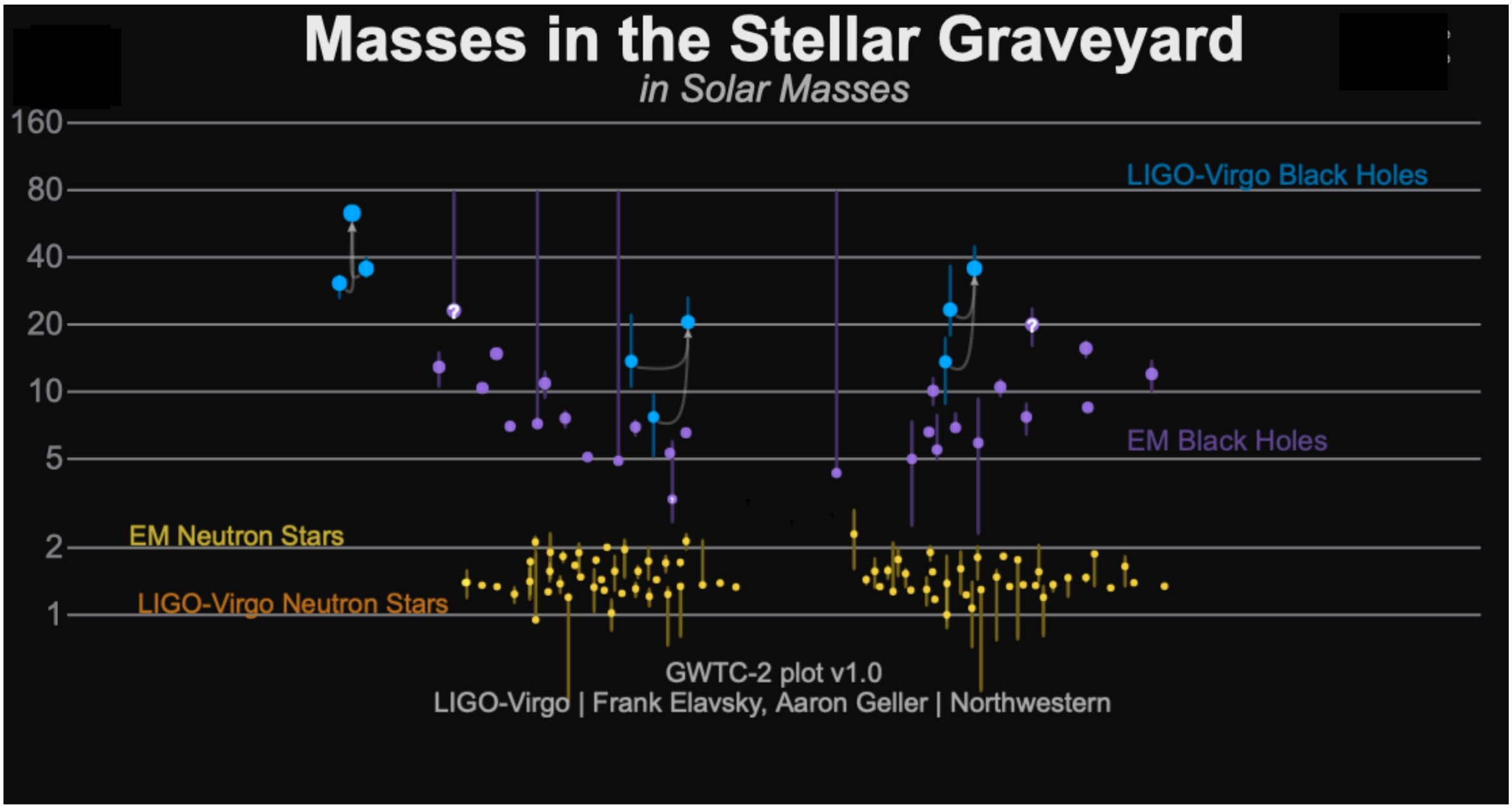

3 BHBH

GW150914: the first ever detection of gravitational waves from the merger of two black holes more than a billion light years away

https://media.ligo.northwestern.edu/gallery/mass-plot

O2 (2016/11/30 - 2017/8/25)

After O2：GWTC1 (2018/12/3 released)

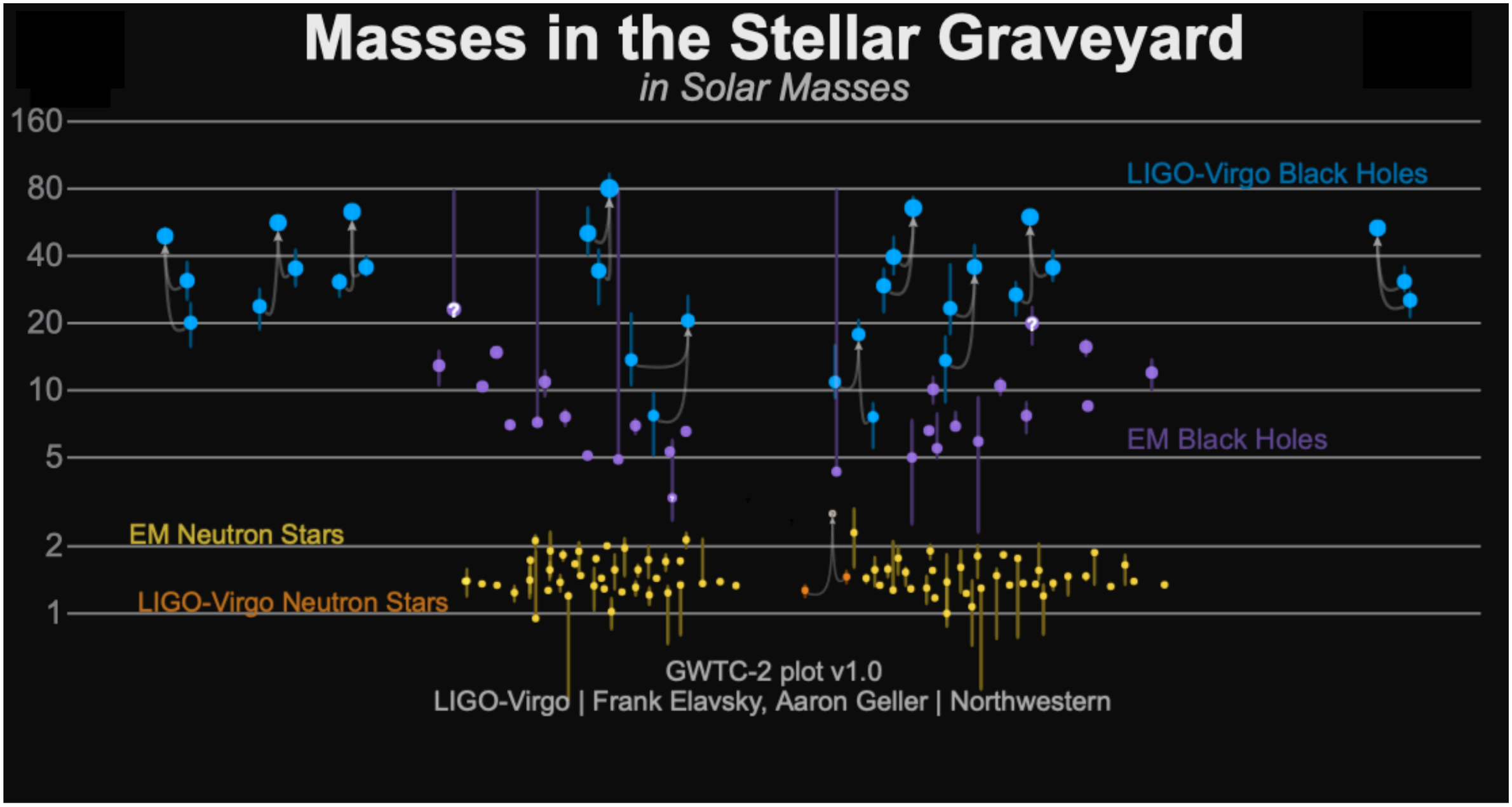

- GW170814: the first GW signal measured by the three-detector network, also from a binary black hole (BBH) merger;
- GW170817: the first GW signal measured from a binary neutron star (BNS) merger — and also the first event observed in light, by dozens of telescopes across the entire electromagnetic spectrum.

https://media.ligo.northwestern.edu/gallery/mass-plot

10 BHBH

1 NSNS

O3a (2019/4/1 - 2019/9/30)

After O3a：GWTC2 (2020/10/28 released)

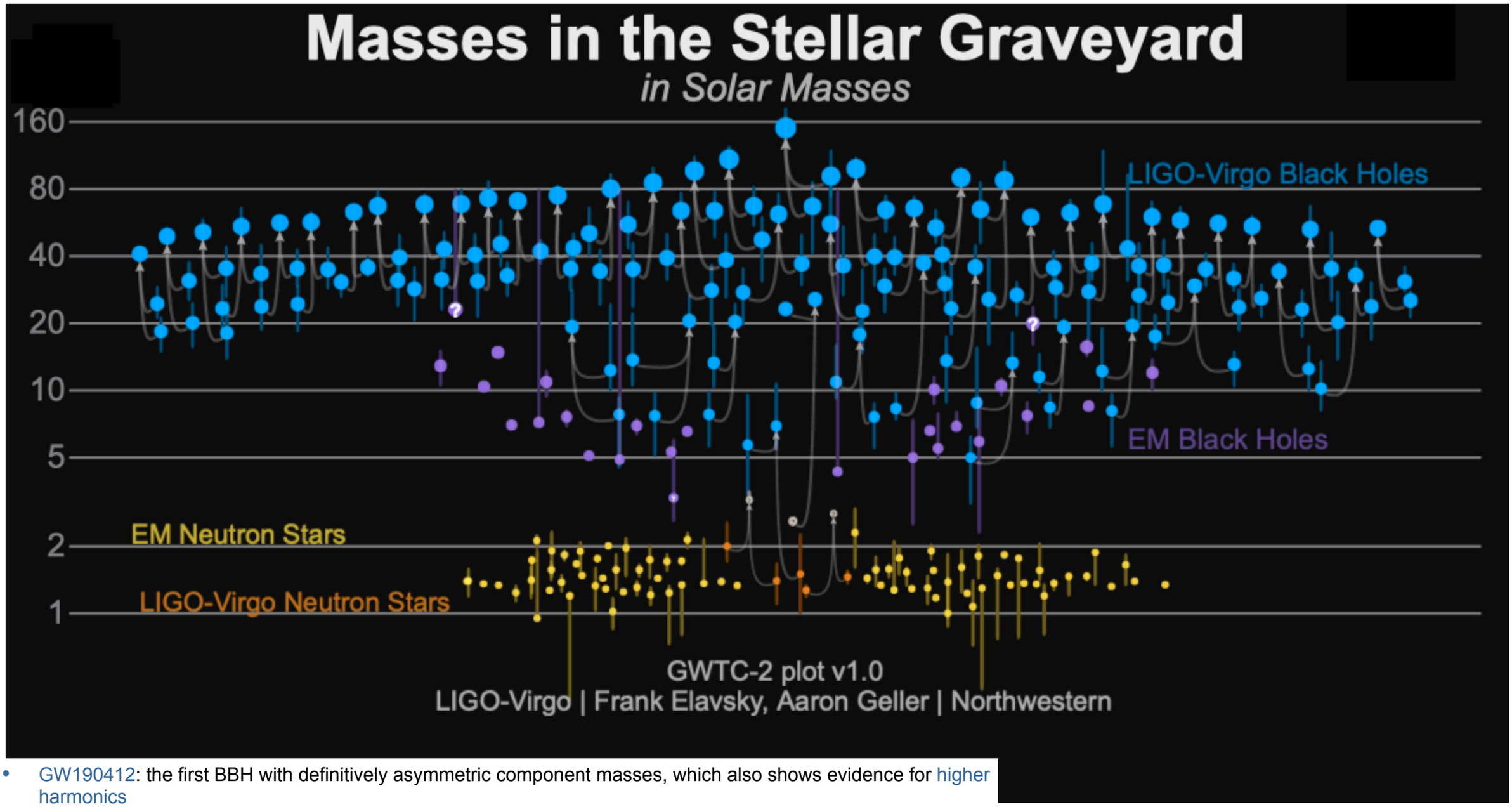

- GW190412: the first BBH with definitively asymmetric component masses, which also shows evidence for higher harmonics
- GW190425: the second gravitational-wave event consistent with a BNS, following GW170817
- GW190426_152155: a low-mass event consistent with either an NSBH or BBH
- GW190514_065416: a BBH with the smallest effective aligned spin of all O3a events
- GW190517_055101: a BBH with the largest effective aligned spin of all O3a events
- GW190521: a BBH with total mass over 150 times the mass of the Sun
- GW190814: a highly asymmetric system of ambiguous nature, corresponding to the merger of a 23 solar mass black hole with a 2.6 solar mass compact object, making the latter either the lightest black hole or heaviest neutron star observed in a compact binary
- GW190924_021846: likely the lowest-mass BBH, with both black holes exceeding 3 solar masses

46 BHBH

2 NSNS

2 BH+?

O3b (2019/11/1 - 2020/3/27)

After O3b：GWTC3 (2021/11/7 released)

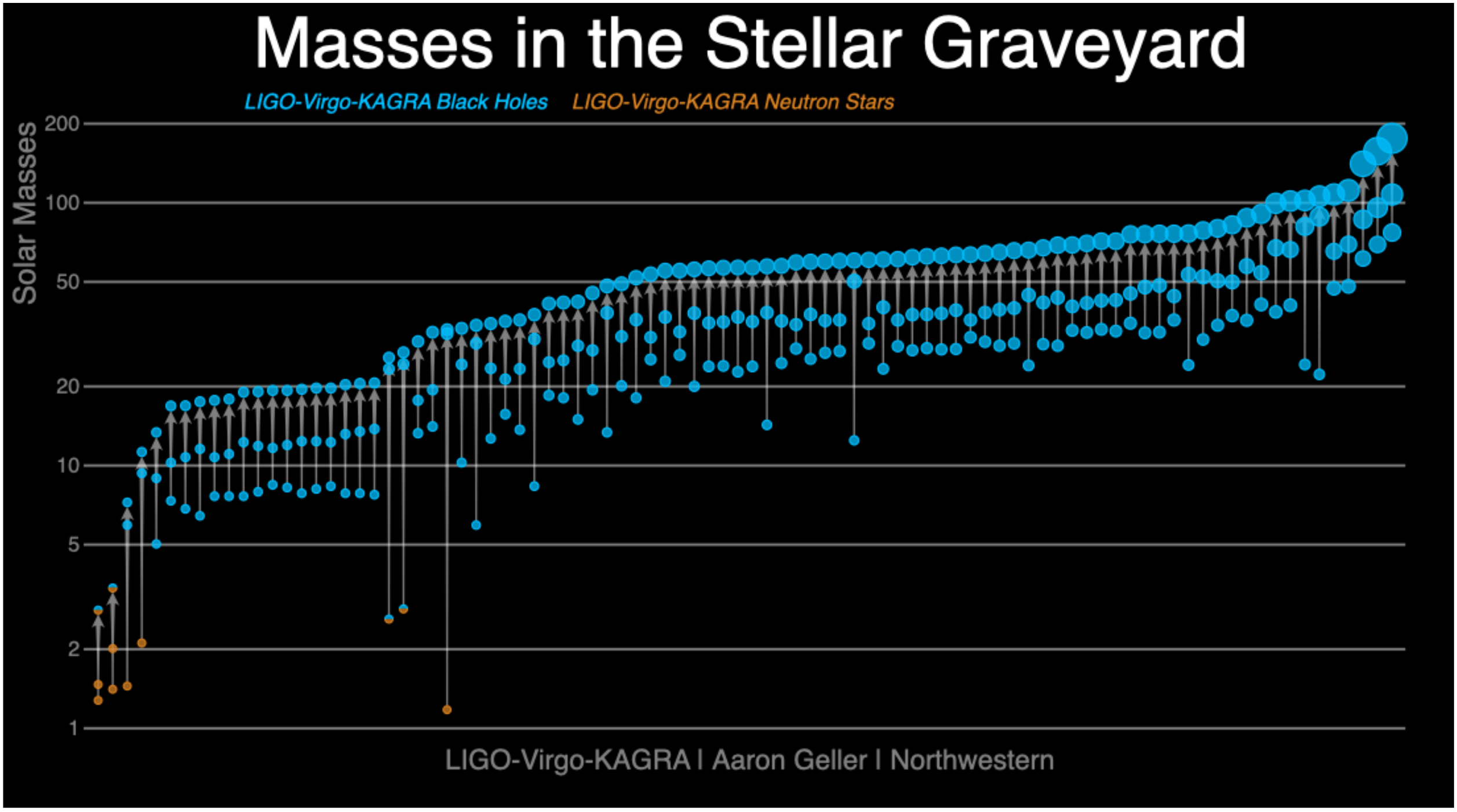

GWTC-1 (O1/O2)

Event	$m_1/M_\odot$	$m_2/M_\odot$	$\mathcal{M}/M_\odot$	$\chi_{\rm eff}$	$M_f/M_\odot$	a_f	$E_{\rm rad}/(M_\odot c^2)$	$\ell_{\rm peak}/({\rm erg\,s^{-1}})$	$d_L/{\rm Mpc}$	z	$\Delta\Omega/{\rm deg}^2$
GW150914	$35.6^{+4.7}_{-3.1}$	$30.6^{+3.0}_{-4.4}$	$28.6^{+1.7}_{-1.5}$	$-0.01^{+0.12}_{-0.13}$	$63.1^{+3.4}_{-3.0}$	$0.69^{+0.05}_{-0.04}$	$3.1^{+0.4}_{-0.4}$	$3.6^{+0.4}_{-0.4}\times10^{56}$	440^{+150}_{-170}	$0.09^{+0.03}_{-0.03}$	182
GW151012	$23.2^{+14.9}_{-5.5}$	$13.6^{+4.1}_{-4.8}$	$15.2^{+2.1}_{-1.2}$	$0.05^{+0.31}_{-0.20}$	$35.6^{+10.8}_{-3.8}$	$0.67^{+0.13}_{-0.11}$	$1.6^{+0.6}_{-0.5}$	$3.2^{+0.8}_{-1.7}\times10^{56}$	1080^{+550}_{-490}	$0.21^{+0.09}_{-0.09}$	1523
GW151226	$13.7^{+8.8}_{-3.2}$	$7.7^{+2.2}_{-2.5}$	$8.9^{+0.3}_{-0.3}$	$0.18^{+0.20}_{-0.12}$	$20.5^{+6.4}_{-1.5}$	$0.74^{+0.07}_{-0.05}$	$1.0^{+0.1}_{-0.2}$	$3.4^{+0.7}_{-1.7}\times10^{56}$	450^{+180}_{-190}	$0.09^{+0.04}_{-0.04}$	1033
GW170104	$30.8^{+7.3}_{-5.6}$	$20.0^{+4.9}_{-4.6}$	$21.4^{+2.2}_{-1.8}$	$-0.04^{+0.17}_{-0.21}$	$48.9^{+5.1}_{-4.0}$	$0.66^{+0.08}_{-0.11}$	$2.2^{+0.5}_{-0.5}$	$3.3^{+0.6}_{-1.0}\times10^{56}$	990^{+440}_{-430}	$0.20^{+0.08}_{-0.08}$	921
GW170608	$11.0^{+5.5}_{-1.7}$	$7.6^{+1.4}_{-2.2}$	$7.9^{+0.2}_{-0.2}$	$0.03^{+0.19}_{-0.07}$	$17.8^{+3.4}_{-0.7}$	$0.69^{+0.04}_{-0.04}$	$0.9^{+0.0}_{-0.1}$	$3.5^{+0.4}_{-1.3}\times10^{56}$	320^{+120}_{-110}	$0.07^{+0.02}_{-0.02}$	392
GW170729	$50.2^{+16.2}_{-10.2}$	$34.0^{+9.1}_{-10.1}$	$35.4^{+6.5}_{-4.8}$	$0.37^{+0.21}_{-0.25}$	$79.5^{+14.7}_{-10.2}$	$0.81^{+0.07}_{-0.13}$	$4.8^{+1.7}_{-1.7}$	$4.2^{+0.9}_{-1.5}\times10^{56}$	2840^{+1400}_{-1360}	$0.49^{+0.19}_{-0.21}$	1041
GW170809	$35.0^{+8.3}_{-5.9}$	$23.8^{+5.1}_{-5.2}$	$24.9^{+2.1}_{-1.7}$	$0.08^{+0.17}_{-0.17}$	$56.3^{+5.2}_{-3.8}$	$0.70^{+0.08}_{-0.09}$	$2.7^{+0.6}_{-0.6}$	$3.5^{+0.6}_{-0.9}\times10^{56}$	1030^{+320}_{-390}	$0.20^{+0.05}_{-0.07}$	308
GW170814	$30.6^{+5.6}_{-3.0}$	$25.2^{+2.8}_{-4.0}$	$24.1^{+1.4}_{-1.1}$	$0.07^{+0.12}_{-0.12}$	$53.2^{+3.2}_{-2.4}$	$0.72^{+0.07}_{-0.05}$	$2.7^{+0.4}_{-0.3}$	$3.7^{+0.4}_{-0.5}\times10^{56}$	600^{+150}_{-220}	$0.12^{+0.03}_{-0.04}$	87
GW170817	$1.46^{+0.12}_{-0.10}$	$1.27^{+0.09}_{-0.09}$	$1.186^{+0.001}_{-0.001}$	$0.00^{+0.02}_{-0.01}$	≤ 2.8	≤ 0.89	≥ 0.04	$\geq 0.1\times10^{56}$	40^{+7}_{-15}	$0.01^{+0.00}_{-0.00}$	16
GW170818	$35.4^{+7.5}_{-4.7}$	$26.7^{+4.3}_{-5.2}$	$26.5^{+2.1}_{-1.7}$	$-0.09^{+0.18}_{-0.21}$	$59.4^{+4.9}_{-3.8}$	$0.67^{+0.07}_{-0.08}$	$2.7^{+0.5}_{-0.5}$	$3.4^{+0.5}_{-0.7}\times10^{56}$	1060^{+420}_{-380}	$0.21^{+0.07}_{-0.07}$	スクリ
GW170823	$39.5^{+11.2}_{-6.7}$	$29.0^{+6.7}_{-7.8}$	$29.2^{+4.6}_{-3.6}$	$0.09^{+0.22}_{-0.26}$	$65.4^{+10.1}_{-7.4}$	$0.72^{+0.09}_{-0.12}$	$3.3^{+1.0}_{-0.9}$	$3.6^{+0.7}_{-1.1}\times10^{56}$	1940^{+970}_{-900}	$0.35^{+0.15}_{-0.15}$	1666

TABLE V. KL divergences (in bits) between the prior and posterior for the effective aligned spin $\chi_{\rm eff}$ and the effective precession spin χ_p. For the computation of the KL divergence for χ_p, we quote the KL divergence with the prior conditioned on the $\chi_{\rm eff}$ posterior, $D^{\chi_p}_{\rm KL}(\chi_{\rm eff})$, and without conditioning, $D^{\chi_p}_{\rm KL}$. For GW170817, $D^{\chi_p}_{\rm KL}$ is given for the high spin prior. The median and 90% interval for the KL divergences is estimated by computing the statistic for repeated draws of a subset of the posterior and prior PDFs. Single-detector optimal SNRs from parameter-estimation analyses for Hanford (H), Livingston (L), and Virgo (V).

Event	GW150914	GW151012	GW151226	GW170104	GW170608	GW170729	GW170809	GW170814	GW170817	GW170818	GW170823
$D^{\chi_{\rm eff}}_{\rm KL}$	$0.71^{+0.04}_{-0.03}$	$0.23^{+0.03}_{-0.02}$	$1.32^{+0.11}_{-0.06}$	$0.54^{+0.03}_{-0.03}$	$0.97^{+0.03}_{-0.05}$	$1.83^{+0.07}_{-0.09}$	$0.71^{+0.03}_{-0.03}$	$0.99^{+0.05}_{-0.07}$	$2.32^{+0.08}_{-0.10}$	$0.50^{+0.04}_{-0.03}$	$0.32^{+0.04}_{-0.03}$
$D^{\chi_p}_{\rm KL}$	$0.16^{+0.03}_{-0.02}$	$0.09^{+0.03}_{-0.02}$	$0.17^{+0.03}_{-0.04}$	$0.05^{+0.01}_{-0.01}$	$0.07^{+0.01}_{-0.02}$	$0.09^{+0.02}_{-0.02}$	$0.05^{+0.01}_{-0.01}$	$0.02^{+0.01}_{-0.01}$	$0.19^{+0.04}_{-0.03}$	$0.06^{+0.02}_{-0.01}$	$0.03^{+0.01}_{-0.01}$
$D^{\chi_p}_{\rm KL}(\chi_{\rm eff})$	$0.09^{+0.02}$	$0.08^{+0.02}$	$0.12^{+0.05}$	$0.07^{+0.02}$	$0.08^{+0.02}$	$0.03^{+0.01}$	$0.06^{+0.01}$	$0.13^{+0.03}$	$0.07^{+0.01}$	$0.09^{+0.02}$	$0.03^{+0.01}$
H SNR	$20.6^{+1.6}_{-1.6}$	$6.4^{+1.3}_{-1.3}$	$9.8^{+1.5}_{-1.4}$	$9.5^{+1.3}_{-1.6}$	$12.1^{+1.6}_{-1.6}$	$5.9^{+1.1}_{-1.1}$	$5.9^{+1.4}_{-1.4}$	$9.3^{+1.0}_{-1.2}$	$18.9^{+1.0}_{-1.0}$	$4.6^{+0.9}_{-0.8}$	$6.8^{+1.4}_{-1.2}$
L SNR	$14.2^{+1.6}_{-1.4}$	$5.8^{+1.2}_{-1.2}$	$6.9^{+1.2}_{-1.1}$	$9.9^{+1.5}_{-1.3}$	$9.2^{+1.5}_{-1.2}$	$8.3^{+1.4}_{-1.4}$	$10.7^{+1.6}_{-1.8}$	$14.3^{+1.5}_{-1.4}$	$26.3^{+1.4}_{-1.3}$	$9.7^{+1.5}_{-1.5}$	$9.2^{+1.7}_{-1.5}$
V SNR	...	...	...	...	...	$1.7^{+1.0}_{-1.1}$	$1.1^{+1.2}_{-0.8}$	$4.1^{+1.1}_{-1.1}$	$3.0^{+0.2}_{-0.2}$	$4.2^{+0.8}_{-0.7}$	...

GWTC-2 (O3a)

Event	$M\ (M_\odot)$	$\mathcal{M}\ (M_\odot)$	$m_1\ (M_\odot)$	$m_2\ (M_\odot)$	$\chi_{\rm eff}$	D_L (Gpc)	z	$M_f\ (M_\odot)$	χ_f	$\Delta\Omega$ (deg^2)	SNR
GW190408_181802	$43.0^{+4.2}_{-3.0}$	$18.3^{+1.9}_{-1.2}$	$24.6^{+5.1}_{-3.4}$	$18.4^{+3.3}_{-3.6}$	$-0.03^{+0.14}_{-0.19}$	$1.55^{+0.40}_{-0.60}$	$0.29^{+0.06}_{-0.10}$	$41.1^{+3.9}_{-2.8}$	$0.67^{+0.06}_{-0.07}$	150	$15.3^{+0.2}_{-0.3}$
GW190412	$38.4^{+3.8}_{-3.7}$	$13.3^{+0.4}_{-0.3}$	$30.1^{+4.7}_{-5.1}$	$8.3^{+1.6}_{-0.9}$	$0.25^{+0.08}_{-0.11}$	$0.74^{+0.14}_{-0.17}$	$0.15^{+0.03}_{-0.03}$	$37.3^{+3.9}_{-3.8}$	$0.67^{+0.05}_{-0.06}$	21	$18.9^{+0.2}_{-0.3}$
GW190413_052954	$58.6^{+13.3}_{-9.7}$	$24.6^{+5.5}_{-4.1}$	$34.7^{+12.6}_{-8.1}$	$23.7^{+7.3}_{-6.7}$	$-0.01^{+0.29}_{-0.34}$	$3.55^{+2.27}_{-1.66}$	$0.59^{+0.29}_{-0.24}$	$56.0^{+12.5}_{-9.2}$	$0.68^{+0.12}_{-0.13}$	1500	$8.9^{+0.4}_{-0.7}$
GW190413_134308	$78.8^{+17.4}_{-11.9}$	$33.0^{+8.2}_{-5.4}$	$47.5^{+13.5}_{-10.7}$	$3.18^{+11.7}_{-10.8}$	$-0.03^{+0.25}_{-0.29}$	$4.45^{+2.48}_{-2.12}$	$0.71^{+0.31}_{-0.30}$	$75.5^{+16.4}_{-11.4}$	$0.68^{+0.10}_{-0.12}$	730	$10.0^{+0.4}_{-0.5}$
GW190421_213856	$72.9^{+13.4}_{-9.2}$	$31.2^{+5.9}_{-4.2}$	$41.3^{+10.4}_{-6.9}$	$31.9^{+8.0}_{-8.8}$	$-0.06^{+0.22}_{-0.27}$	$2.88^{+1.37}_{-1.38}$	$0.49^{+0.19}_{-0.21}$	$69.7^{+12.5}_{-8.7}$	$0.67^{+0.10}_{-0.11}$	1200	$10.7^{+0.2}_{-0.4}$
GW190424_180648	$72.6^{+13.3}_{-10.7}$	$31.0^{+5.8}_{-4.6}$	$40.5^{+11.1}_{-7.3}$	$31.8^{+7.6}_{-7.7}$	$0.13^{+0.22}_{-0.22}$	$2.20^{+1.58}_{-1.16}$	$0.39^{+0.23}_{-0.19}$	$68.9^{+12.4}_{-10.1}$	$0.74^{+0.09}_{-0.09}$	2800	$10.4^{+0.2}_{-0.4}$
GW190425	$3.4^{+0.3}_{-0.1}$	$1.44^{+0.02}_{-0.02}$	$2.0^{+0.6}_{-0.3}$	$1.4^{+0.02}_{-0.02}$	$0.06^{+0.11}_{-0.05}$	$0.16^{+0.07}_{-0.07}$	$0.03^{+0.01}_{-0.02}$	...	...	1000	$12.4^{+0.3}_{-0.4}$
GW190426_152155	$7.2^{+3.5}_{-1.5}$	$2.41^{+0.08}_{-0.08}$	$5.7^{+3.9}_{-2.3}$	$1.5^{+0.8}_{-0.5}$	$-0.03^{+0.32}_{-0.30}$	$0.37^{+0.32}_{-0.30}$	$0.08^{+0.04}_{-0.03}$	...	...	1300	$8.7^{+0.5}_{-0.6}$
GW190503_185404	$71.7^{+9.4}_{-8.3}$	$30.2^{+4.2}_{-4.2}$	$43.3^{+9.2}_{-8.1}$	$28.4^{+7.7}_{-8.0}$	$-0.03^{+0.20}_{-0.26}$	$1.45^{+0.69}_{-0.63}$	$0.27^{+0.11}_{-0.11}$	$68.6^{+8.8}_{-7.7}$	$0.66^{+0.09}_{-0.12}$	94	$12.4^{+0.2}_{-0.3}$
GW190512_180714	$35.9^{+3.8}_{-3.5}$	$14.6^{+1.3}_{-1.0}$	$23.3^{+5.3}_{-5.8}$	$12.6^{+3.6}_{-2.5}$	$0.03^{+0.12}_{-0.13}$	$1.43^{+0.55}_{-0.55}$	$0.27^{+0.09}_{-0.10}$	$34.5^{+3.8}_{-3.5}$	$0.65^{+0.07}_{-0.07}$	220	$12.2^{+0.2}_{-0.4}$
GW190513_205428	$53.9^{+8.6}_{-5.9}$	$21.6^{+3.8}_{-1.9}$	$35.7^{+9.5}_{-9.2}$	$18.0^{+7.7}_{-4.1}$	$0.11^{+0.28}_{-0.17}$	$2.06^{+0.88}_{-0.80}$	$0.37^{+0.13}_{-0.13}$	$51.6^{+8.2}_{-5.8}$	$0.68^{+0.14}_{-0.12}$	520	$12.9^{+0.3}_{-0.4}$
GW190514_065416	$67.2^{+18.7}_{-10.8}$	$28.5^{+7.9}_{-4.8}$	$39.0^{+14.7}_{-8.2}$	$28.4^{+9.3}_{-8.8}$	$-0.19^{+0.29}_{-0.32}$	$4.13^{+2.65}_{-2.17}$	$0.67^{+0.33}_{-0.31}$	$64.5^{+17.9}_{-10.4}$	$0.63^{+0.11}_{-0.15}$	3000	$8.2^{+0.3}_{-0.6}$
GW190517_055101	$63.5^{+9.6}_{-9.6}$	$26.6^{+4.0}_{-4.0}$	$37.4^{+11.7}_{-7.6}$	$25.3^{+7.0}_{-7.3}$	$0.52^{+0.19}_{-0.19}$	$1.86^{+1.62}_{-0.84}$	$0.34^{+0.24}_{-0.14}$	$59.3^{+9.1}_{-8.9}$	$0.87^{+0.05}_{-0.07}$	470	$10.7^{+0.4}_{-0.6}$
GW190519_153544	$106.6^{+13.5}_{-14.8}$	$44.5^{+6.4}_{-7.1}$	$66.0^{+10.7}_{-12.0}$	$40.5^{+11.0}_{-11.1}$	$0.31^{+0.20}_{-0.22}$	$2.53^{+1.83}_{-0.92}$	$0.44^{+0.25}_{-0.14}$	$101.0^{+12.4}_{-13.8}$	$0.79^{+0.07}_{-0.13}$	860	$15.6^{+0.2}_{-0.3}$
GW190521	$163.9^{+39.2}_{-23.5}$	$69.2^{+17.0}_{-10.6}$	$95.3^{+28.7}_{-18.9}$	$69.0^{+22.7}_{-23.1}$	$0.03^{+0.32}_{-0.39}$	$3.92^{+2.19}_{-1.95}$	$0.64^{+0.28}_{-0.28}$	$156.3^{+36.8}_{-22.4}$	$0.71^{+0.12}_{-0.16}$	1000	$14.2^{+0.3}_{-0.3}$
GW190521_074359	$74.7^{+7.0}_{-4.8}$	$32.1^{+3.2}_{-2.5}$	$42.2^{+5.9}_{-4.8}$	$32.8^{+5.4}_{-6.4}$	$0.09^{+0.10}_{-0.13}$	$1.24^{+0.40}_{-0.57}$	$0.24^{+0.07}_{-0.10}$	$71.0^{+6.5}_{-4.4}$	$0.72^{+0.05}_{-0.07}$	550	$25.8^{+0.1}_{-0.2}$
GW190527_092055	$59.1^{21.3}_{-9.8}$	$24.3^{+9.1}_{-4.2}$	$36.5^{+16.4}_{-9.0}$	$22.6^{+10.5}_{-8.1}$	$0.11^{+0.28}_{-0.28}$	$2.49^{+2.48}_{-1.24}$	$0.44^{+0.34}_{-0.20}$	$56.4^{+20.2}_{-9.3}$	$0.71^{+0.12}_{-0.16}$	3700	$8.1^{+0.3}_{-0.9}$
GW190602_175927	$116.3^{+19.0}_{-15.6}$	$49.1^{+9.1}_{-8.5}$	$69.1^{+15.7}_{-13.0}$	$47.8^{+14.3}_{-17.4}$	$0.07^{+14.3}_{-0.24}$	$2.69^{+1.79}_{-1.12}$	$0.47^{+0.25}_{-0.17}$	$11.0^{+17.7}_{-14.9}$	$0.70^{+0.10}_{-0.14}$	690	$12.8^{+0.2}_{-0.3}$
GW190620_030421	$92.1^{18.5}_{-13.1}$	$38.3^{+8.3}_{-6.5}$	$57.1^{+16.0}_{-12.7}$	$35.5^{+12.2}_{-12.3}$	$0.33^{+0.22}_{-0.25}$	$2.81^{+1.68}_{-1.31}$	$0.49^{+0.23}_{-0.20}$	$87.2^{+16.8}_{-12.1}$	$0.79^{+0.08}_{-0.15}$	7200	$12.1^{+0.3}_{-0.4}$
GW190630_185205	$59.1^{+4.6}_{-4.8}$	$24.9^{+2.1}_{-2.1}$	$35.1^{+6.9}_{-5.6}$	$23.7^{+5.2}_{-5.1}$	$0.10^{+0.12}_{-0.13}$	$0.89^{+0.56}_{-0.37}$	$0.18^{+0.10}_{-0.07}$	$56.4^{+4.4}_{-4.6}$	$0.70^{+0.05}_{-0.07}$	1200	$15.6^{+0.2}_{-0.3}$
GW190701_203306	$94.3^{+12.1}_{-9.5}$	$40.3^{+5.4}_{-4.9}$	$53.9^{+11.8}_{-8.0}$	$40.8^{+8.7}_{-12.0}$	$-0.07^{+0.23}_{-0.29}$	$2.06^{+0.76}_{-0.73}$	$0.37^{+0.11}_{-0.12}$	$90.2^{+11.3}_{-8.9}$	$0.66^{+0.09}_{-0.13}$	46	$11.3^{+0.2}_{-0.3}$

GWTC-2 (O3a) continued

Event	$M\ (M_\odot)$	$\mathcal{M}\ (M_\odot)$	$m_1\ (M_\odot)$	$m_2\ (M_\odot)$	$\chi_{\rm eff}$	D_L (Gpc)	z	$M_f\ (M_\odot)$	χ_f	$\Delta\Omega$ (deg^2)	SNR
GW190706_222641	$104.1^{+20.2}_{-13.9}$	$42.7^{+10.0}_{-7.0}$	$67.0^{+14.6}_{-16.2}$	$38.2^{+14.6}_{-13.3}$	$0.28^{+0.26}_{-0.29}$	$4.42^{+2.59}_{-1.93}$	$0.71^{+0.32}_{-0.27}$	$99.0^{+18.3}_{-13.5}$	$0.78^{+0.09}_{-0.18}$	650	$12.6^{+0.2}_{-0.4}$
GW190707_093326	$20.1^{+1.9}_{-1.3}$	$8.5^{+0.6}_{-0.5}$	$11.6^{+3.3}_{-1.7}$	$8.4^{+1.4}_{-1.7}$	$-0.05^{+0.10}_{-0.08}$	$0.77^{+0.38}_{-0.37}$	$0.16^{+0.07}_{-0.07}$	$19.2^{+1.9}_{-1.3}$	$0.66^{+0.03}_{-0.04}$	1300	$13.3^{+0.2}_{-0.4}$
GW190708_232457	$30.9^{+2.5}_{-1.8}$	$13.2^{+0.9}_{-0.6}$	$17.6^{+4.7}_{-2.3}$	$13.2^{+2.0}_{-2.7}$	$0.02^{+0.10}_{-0.08}$	$0.88^{+0.33}_{-0.39}$	$0.18^{+0.06}_{-0.07}$	$29.5^{+2.5}_{-1.8}$	$0.69^{+0.04}_{-0.04}$	14000	$13.1^{+0.2}_{-0.3}$
GW190719_215514	$57.8^{+18.3}_{-10.7}$	$23.5^{+6.5}_{-4.0}$	$36.5^{+18.0}_{-10.3}$	$20.8^{+9.0}_{-7.2}$	$0.32^{+0.29}_{-0.31}$	$3.94^{+2.59}_{-2.00}$	$0.64^{+0.33}_{-0.29}$	$54.9^{+17.3}_{-10.2}$	$0.78^{+0.11}_{-0.17}$	2900	$8.3^{+0.3}_{-0.8}$
GW190720_000836	$21.5^{+4.3}_{-2.3}$	$8.9^{+0.5}_{-0.8}$	$13.4^{+6.7}_{-3.0}$	$7.8^{+2.3}_{-2.2}$	$0.18^{+0.14}_{-0.12}$	$0.79^{+0.69}_{-0.32}$	$0.16^{+0.12}_{-0.06}$	$20.4^{+4.5}_{-2.2}$	$0.72^{+0.06}_{-0.05}$	460	$11.0^{+0.3}_{-0.7}$
GW190727_060333	$67.1^{+11.7}_{-8.0}$	$28.6^{+5.3}_{-3.7}$	$38.0^{+9.5}_{-6.2}$	$29.4^{+7.1}_{-8.4}$	$0.11^{+0.26}_{-0.25}$	$3.30^{+1.54}_{-1.50}$	$0.55^{+0.21}_{-0.22}$	$63.8^{+10.9}_{-7.5}$	$0.73^{+0.10}_{-0.10}$	830	$11.9^{+0.3}_{-0.5}$
GW190728_064510	$20.6^{+4.5}_{-1.3}$	$8.6^{+0.5}_{-0.3}$	$12.3^{+7.2}_{-2.2}$	$8.1^{+1.7}_{-2.6}$	$0.12^{+0.20}_{-0.07}$	$0.87^{+0.26}_{-1.37}$	$0.18^{+0.05}_{-0.07}$	$19.6^{+4.7}_{-1.3}$	$0.71^{+0.04}_{-0.04}$	400	$13.0^{+0.2}_{-0.4}$
GW190731_140936	$70.1^{+15.8}_{-11.3}$	$29.5^{+7.1}_{-5.2}$	$41.5^{+12.2}_{-9.0}$	$28.8^{+9.7}_{-9.5}$	$0.06^{+0.24}_{-0.24}$	$3.30^{+2.39}_{-1.72}$	$0.55^{+0.31}_{-0.26}$	$67.0^{+14.6}_{-10.8}$	$0.70^{+0.10}_{-0.13}$	3400	$8.7^{+0.2}_{-0.5}$
GW190803_022701	$64.5^{+12.6}_{-9.0}$	$27.3^{+5.7}_{-4.1}$	$37.3^{+10.6}_{-7.0}$	$27.3^{+7.8}_{-8.2}$	$-0.03^{+0.24}_{-0.27}$	$3.27^{+1.95}_{-1.58}$	$0.55^{+0.26}_{-0.24}$	$61.7^{+11.8}_{-8.5}$	$0.68^{+0.10}_{-0.11}$	1500	$8.6^{+0.3}_{-0.5}$
GW190814	$25.8^{+1.0}_{-0.9}$	$6.09^{+0.06}_{-0.06}$	$23.2^{+1.1}_{-1.0}$	$2.59^{+0.08}_{-0.09}$	$0.00^{+0.08}_{-0.06}$	$0.24^{+0.04}_{-0.05}$	$0.05^{+0.009}_{-0.010}$	$25.6^{+1.1}_{-0.9}$	$0.28^{+0.02}_{-0.02}$	19	$24.9^{+0.1}_{-0.2}$
GW190828_063405	$58.0^{+7.7}_{-4.8}$	$25.0^{+3.4}_{-2.1}$	$32.1^{+5.8}_{-4.0}$	$26.2^{+4.6}_{-4.8}$	$0.19^{+0.15}_{-0.16}$	$2.13^{+0.66}_{-0.93}$	$0.38^{+0.10}_{-0.15}$	$54.9^{+7.2}_{-4.3}$	$0.75^{+0.06}_{-0.07}$	520	$16.2^{+0.2}_{-0.3}$
GW190828_065509	$34.4^{+5.4}_{-4.4}$	$13.3^{+1.2}_{-1.0}$	$24.1^{+7.0}_{-7.2}$	$10.2^{+3.6}_{-2.1}$	$0.08^{+0.16}_{-0.16}$	$1.60^{+0.62}_{-0.60}$	$0.30^{+0.10}_{-1.10}$	$33.1^{+5.5}_{-4.5}$	$0.65^{+0.08}_{-0.08}$	660	$10.0^{+0.3}_{-0.5}$
GW190909_114149	$75.0^{+55.9}_{-17.6}$	$30.9^{+17.2}_{-7.5}$	$45.8^{+52.7}_{-13.3}$	$28.3^{+13.4}_{-12.7}$	$-0.06^{+0.37}_{-0.36}$	$3.77^{+3.27}_{-2.22}$	$0.62^{+0.41}_{-0.33}$	$72.0^{54.9}_{-16.8}$	$0.66^{+0.15}_{-0.20}$	4700	$8.1^{+0.4}_{-0.6}$
GW190910_112807	$79.6^{+9.3}_{-9.1}$	$34.3^{+4.1}_{-4.1}$	$43.9^{+7.6}_{-6.1}$	$35.6^{+7.6}_{-7.2}$	$0.02^{+0.18}_{-0.18}$	$1.46^{+10.3}_{-0.58}$	$0.28^{+0.16}_{-0.10}$	$75.8^{+8.5}_{-8.6}$	$0.70^{+0.08}_{-0.07}$	11000	$14.1^{+0.2}_{-0.3}$
GW190915_235702	$59.9^{+7.5}_{-6.4}$	$25.3^{+3.2}_{-2.7}$	$35.3^{+9.5}_{-6.4}$	$24.4^{+5.6}_{-6.1}$	$0.02^{+0.20}_{-0.25}$	$1.62^{+0.71}_{-0.61}$	$0.30^{+0.11}_{-0.10}$	$57.2^{+7.1}_{-6.0}$	$0.70^{+0.09}_{-0.11}$	400	$13.6^{+0.2}_{-0.3}$
GW190924_021846	$13.9^{+5.1}_{-1.0}$	$5.8^{+0.2}_{-0.2}$	$8.9^{+7.0}_{-2.0}$	$5.0^{+1.4}_{-1.9}$	$0.03^{+0.30}_{-0.09}$	$0.57^{+0.22}_{-0.22}$	$0.12^{+0.04}_{-0.04}$	$13.3^{+5.2}_{-1.0}$	$0.67^{+0.05}_{-0.05}$	360	$11.5^{+0.3}_{-0.4}$
GW190929_012149	$104.3^{+34.9}_{-25.2}$	$35.8^{+14.9}_{-8.2}$	$80.8^{+33.0}_{-33.2}$	$24.1^{+19.3}_{-10.6}$	$0.01^{+0.34}_{-0.33}$	$2.13^{+3.25}_{-1.05}$	$0.38^{+0.49}_{-0.17}$	$101.5^{+33.6}_{-25.3}$	$0.66^{+0.20}_{-0.31}$	2200	$10.1^{+0.6}_{-0.8}$
GW190930_133541	$20.3^{+8.9}_{-1.5}$	$8.5^{+0.5}_{-0.5}$	$12.3^{+12.4}_{-2.3}$	$7.8^{+1.7}_{-3.3}$	$0.14^{+0.31}_{-0.15}$	$0.76^{+0.36}_{-0.32}$	$0.15^{+0.06}_{-0.06}$	$19.4^{+9.2}_{-1.5}$	$0.72^{+0.07}_{-0.06}$	1700	$9.5^{+0.3}_{-0.5}$

GWTC-2 (O3a)

Name	Instrument	cWB		GstLAL			PyCBC			PyCBC BBH		
		FAR (yr^{-1})	SNR[a]	FAR (yr^{-1})	SNR	p_{astro}	FAR (yr^{-1})	SNR[a]	p_{astro}	FAR (yr^{-1})	SNR[a]	p_{astro}
GW190408_181802	HLV	$<9.5 \times 10^{-4}$	14.8	$< 1.0 \times 10^{-5}$	14.7	1.00	$<2.5 \times 10^{-5}$	13.5	1.00	$<7.9 \times 10^{-5}$	13.6	1.00
GW190412	HLV	$<9.5 \times 10^{-4}$	19.7	$<1.0 \times 10^{-5}$	18.9	1.00	3.1×10^{-5}	17.9	1.00	$<7.9 \times 10^{-5}$	17.8	1.00
GW190413_052954	HLV	...	...	...	...	...	...	...	...	7.2×10^{-2}	8.6	0.98
GW190413_134308	HLV	...	...	3.8×10^{-1}	10.0	0.95	...	...	...	4.4×10^{-2}	9.0	0.98
GW190421_213856	HL	3.0×10^{-1}	9.3	7.7×10^{-4}	10.6	1.00	1.9×10^{9}	10.2	0.89	6.6×10^{-3}	10.2	1.00
GW190424_180648	L			$7.8 \times 10^{-1\dagger}$	10.0	0.91						
GW190425	LV			$7.5 \times 10^{-4\dagger}$	13.0	...						
GW190426_152155	HLV	...	...	1.4×10^{0}	10.1	...	...	...	...	...	...	...
GW190503_185404	HLV	1.8×10^{-3}	11.5	$<1.0 \times 10^{-5}$	12.1	1.00	3.7×10^{-2}	12.2	1.00	$<7.9 \times 10^{-5}$	12.2	1.00
GW190512_180714	HLV	8.8×10^{-1}	10.7	$<1.0 \times 10^{-5}$	12.3	1.00	3.8×10^{-5}	12.2	1.00	$<5.7 \times 10^{-5}$	12.2	1.00
GW190513_205428	HLV	...	...	$<1.0 \times 10^{-5}$	12.3	1.00	3.7×10^{-4}	11.8	1.00	$<5.7 \times 10^{-5}$	11.9	1.00
GW190514_065416	HL	...	...	...	...	...	...	...	...	5.3×10^{-1}	8.3	0.96
GW190517_055101	HLV	6.5×10^{-3}	10.7	9.6×10^{-4}	10.6	1.00	1.8×10^{-2}	10.4	1.00	$<5.7 \times 10^{-5}$	10.2	1.00
GW190519_153544	HLV	3.1×10^{-4}	14.0	$<1.0 \times 10^{-5}$	12.0	1.00	$<1.8 \times 10^{-5}$	13.0	1.00	$<5.7 \times 10^{-5}$	13.0	1.00
GW190521	HLV	2.0×10^{-4}	14.4	1.2×10^{-3}	15.0	1.00	1.1×10^{0}	12.6	0.93	...	...	...
GW190521_074359	HL	$<1.0 \times 10^{-4}$	24.7	$<1.0 \times 10^{-5}$	24.4	1.00	$<1.8 \times 10^{-5}$	24.0	1.00	$<5.7 \times 10^{-5}$	24.0	1.00
GW190527_092055	HL	...	...	6.2×10^{-2}	8.9	0.99	...	...	...	...	...	...
GW190602_175927	HLV	1.5×10^{-2}	11.1	1.1×10^{-5}	12.1	1.00	...	...	...	...	...	...
GW190620_030421	LV			$2.9 \times 10^{-3\dagger}$	13.1	1.00						
GW190630_185205	LV			$<1.0 \times 10^{-5\dagger}$	15.6	1.00						
GW190701_203306	HLV	5.5×10^{-1}	10.2	1.1×10^{-2}	11.6	1.00	...	...	...	...	...	...
GW190706_222641	HLV	$<1.0 \times 10^{-3}$	12.7	$<1.0 \times 10^{-5}$	12.3	1.00	6.7×10^{-5}	11.7	1.00	$<4.6 \times 10^{-5}$	12.3	1.00
GW190707_093326	HL	...	...	$<1.0 \times 10^{-5}$	13.0	1.00	$<1.0 \times 10^{-5}$	12.8	1.00	$<4.6 \times 10^{-5}$	12.8	1.00
GW190708_232457	LV			$2.8 \times 10^{-5\dagger}$	13.1	1.00						
GW190719_215514	HL	...	...	...	...	...	...	...	...	1.6×10^{0}	8.0	0.82
GW190720_000836	HLV	...	...	$<1.0 \times 10^{-5}$	11.7	1.00	$<2.0 \times 10^{-5}$	10.6	1.00	$<3.7 \times 10^{-5}$	10.5	1.00
GW190727_060333	HLV	8.8×10^{-2}	11.4	$<1.0 \times 10^{-5}$	12.3	1.00	3.5×10^{-3}	11.5	1.00	$<3.7 \times 10^{-5}$	11.8	1.00
GW190728_064510	HLV	...	...	$<1.0 \times 10^{-5}$	13.6	1.00	$<1.6 \times 10^{-5}$	13.4	1.00	$<3.7 \times 10^{-5}$	13.4	1.00
GW190731_140936	HL	...	...	2.1×10^{-1}	8.5	0.97	...	...	...	2.8×10^{-1}	8.2	0.96
GW190803_022701	HLV	...	...	3.2×10^{-2}	9.0	0.99	...	...	...	2.7×10^{-2}	8.6	0.99
GW190814	LV			$<1.0 \times 10^{-5}$	22.2	1.00						
GW190828_063405	HLV	$<9.6 \times 10^{-4}$	16.6	$<1.0 \times 10^{-5}$	16.0	1.00	$<1.5 \times 10^{-5}$	15.3	1.00	$<3.3 \times 10^{-5}$	15.3	1.00
GW190828_065509	HLV	...	...	$<1.0 \times 10^{-5}$	11.1	1.00	5.8×10^{-5}	10.8	1.00	$<3.3 \times 10^{-5}$	10.8	1.00
GW190909_114149	HL	...	...	1.1×10^{0}	8.5	0.89	...	...	...	...	...	...
GW190910_112807	LV			$1.9 \times 10^{-5\dagger}$	13.4	1.00						
GW190915_235702	HLV	$<1.0 \times 10^{-3}$	12.3	$<1.0 \times 10^{-5}$	13.1	1.00	8.6×10^{-4}	13.0	1.00	$<3.3 \times 10^{-5}$	12.7	1.00
GW190924_021846	HLV	...	...	$<1.0 \times 10^{-5}$	13.2	1.00	$<6.3 \times 10^{-5}$	12.5	1.00	$<3.3 \times 10^{-5}$	12.4	1.00
GW190929_012149	HLV	...	...	2.0×10^{-2}	9.9	1.00	...	...	...	...	...	...

GWTC-2.1 (O3a)

Event	M ($M_\odot$)	$\mathcal{M}$ ($M_\odot$)	m_1 ($M_\odot$)	m_2 ($M_\odot$)	$\chi_{\rm eff}$	$D_{\rm L}$ (Gpc)	z	$M_{\rm f}$ ($M_\odot$)	$\chi_{\rm f}$	$\Delta\Omega$ (deg^2)
GW190403_051519	$110.5^{+30.6}_{-24.2}$	$36.3^{+14.4}_{-8.8}$	$88.0^{+28.2}_{-32.9}$	$22.1^{+23.8}_{-9.0}$	$0.70^{+0.15}_{-0.27}$	$8.00^{+5.88}_{-3.99}$	$1.14^{+0.64}_{-0.49}$	$105.2^{+29.1}_{-24.1}$	$0.92^{+0.04}_{-0.11}$	5600
GW190426_190642	$184.4^{+41.7}_{-36.6}$	$77.1^{+19.4}_{-17.1}$	$106.9^{+41.6}_{-25.2}$	$76.6^{+26.2}_{-33.6}$	$0.19^{+0.43}_{-0.40}$	$4.35^{+3.35}_{-2.15}$	$0.70^{+0.41}_{-0.30}$	$175.0^{+39.4}_{-34.3}$	$0.76^{+0.15}_{-0.15}$	8200
GW190725_174728	$18.2^{+4.2}_{-1.8}$	$7.4^{+0.6}_{-0.5}$	$11.5^{+6.2}_{-2.7}$	$6.4^{+2.0}_{-2.0}$	$-0.04^{+0.26}_{-0.14}$	$1.05^{+0.57}_{-0.46}$	$0.21^{+0.10}_{-0.09}$	$17.4^{+4.4}_{-1.8}$	$0.65^{+0.08}_{-0.07}$	2300
GW190805_211137	$80.1^{+22.5}_{-16.1}$	$33.5^{+10.1}_{-7.0}$	$48.2^{+17.5}_{-12.5}$	$32.0^{+13.4}_{-11.4}$	$0.35^{+0.30}_{-0.36}$	$5.31^{+4.10}_{-2.95}$	$0.82^{+0.48}_{-0.40}$	$75.8^{+21.2}_{-15.3}$	$0.81^{+0.09}_{-0.15}$	3900
GW190916_200658	$68.9^{+21.0}_{-14.0}$	$27.3^{+9.3}_{-5.5}$	$44.3^{+21.2}_{-13.3}$	$23.9^{+12.7}_{-10.2}$	$0.18^{+0.33}_{-0.29}$	$4.46^{+3.79}_{-2.52}$	$0.71^{+0.46}_{-0.36}$	$65.7^{+19.8}_{-13.4}$	$0.73^{+0.14}_{-0.23}$	4500
GW190917_114630	$11.4^{+3.0}_{-2.9}$	$3.7^{+0.2}_{-0.2}$	$9.3^{+3.4}_{-4.4}$	$2.1^{+1.5}_{-0.5}$	$-0.11^{+0.24}_{-0.49}$	$0.72^{+0.34}_{-0.31}$	$0.15^{+0.06}_{-0.06}$	$11.2^{+3.0}_{-2.9}$	$0.42^{+0.12}_{-0.06}$	2100
GW190925_232845	$37.0^{+3.8}_{-2.6}$	$15.8^{+1.1}_{-1.0}$	$21.2^{+6.9}_{-3.1}$	$15.6^{+2.6}_{-3.6}$	$0.11^{+0.17}_{-0.14}$	$0.93^{+0.38}_{-0.35}$	$0.19^{+0.07}_{-0.07}$	$35.2^{+3.8}_{-2.4}$	$0.72^{+0.07}_{-0.06}$	1200
GW190926_050336	$62.9^{+22.7}_{-11.9}$	$25.6^{+8.8}_{-5.3}$	$39.8^{+20.6}_{-11.1}$	$23.2^{+10.8}_{-9.7}$	$-0.04^{+0.28}_{-0.33}$	$3.78^{+3.17}_{-2.00}$	$0.62^{+0.40}_{-0.29}$	$60.5^{+21.8}_{-11.6}$	$0.65^{+0.14}_{-0.19}$	2500

TABLE V. Median and 90% symmetric credible intervals for the one-dimensional marginal posterior distributions on selected source parameters for the 8 events that are new to this catalog with $p_{\rm astro} > 0.5$, highlighted in bold in Table I. The columns show source total mass M, chirp mass $\mathcal{M}$ and component masses m_i, dimensionless effective inspiral spin $\chi_{\rm eff}$, luminosity distance $D_{\rm L}$, redshift z, final mass $M_{\rm f}$, final spin $\chi_{\rm f}$, and sky localization $\Delta\Omega$. The sky localization is the area of the 90% credible region. A subset of the one-dimensional posterior distributions are visualized in Fig. 3. Two-dimensional projections of the 90% credible regions in the M–q and $\mathcal{M}$–$\chi_{\rm eff}$ planes are shown in Fig. 4 and Fig. 5.

GWTC-3 (O3b)

Event	M ($M_\odot$)	$\mathcal{M}$ ($M_\odot$)	m_1 ($M_\odot$)	m_2 ($M_\odot$)	$\chi_{\rm eff}$	$D_{\rm L}$ (Gpc)	z	$M_{\rm f}$ ($M_\odot$)	$\chi_{\rm f}$	$\Delta\Omega$ deg^2)	SNR
GW191103_012549	$20.0^{+3.7}_{-1.8}$	$8.34^{+0.66}_{-0.57}$	$11.8^{+6.2}_{-2.2}$	$7.9^{+1.7}_{-2.4}$	$0.21^{+0.16}_{-0.10}$	$0.99^{+0.50}_{-0.47}$	$0.20^{+0.09}_{-0.09}$	$19.0^{+3.8}_{-1.7}$	$0.75^{+0.06}_{-0.05}$	2500	$8.9^{+0.3}_{-0.5}$
GW191105_143521	$18.5^{+2.1}_{-1.3}$	$7.82^{+0.61}_{-0.45}$	$10.7^{+3.7}_{-1.6}$	$7.7^{+1.4}_{-1.9}$	$-0.02^{+0.13}_{-0.09}$	$1.15^{+0.43}_{-0.48}$	$0.23^{+0.07}_{-0.09}$	$17.6^{+2.1}_{-1.2}$	$0.67^{+0.04}_{-0.05}$	640	$9.7^{+0.3}_{-0.5}$
GW191109_010717	112^{+20}_{-16}	$47.5^{+9.6}_{-7.5}$	65^{+11}_{-11}	47^{+15}_{-13}	$-0.29^{+0.42}_{-0.31}$	$1.29^{+1.13}_{-0.65}$	$0.25^{+0.18}_{-0.12}$	107^{+18}_{-15}	$0.61^{+0.18}_{-0.19}$	1600	$17.3^{+0.5}_{-0.5}$
GW191113_071753	$34.5^{+10.5}_{-9.8}$	$10.7^{+1.1}_{-1.0}$	29^{+12}_{-14}	$5.9^{+4.4}_{-1.3}$	$0.00^{+0.37}_{-0.29}$	$1.37^{+1.15}_{-0.62}$	$0.26^{+0.18}_{-0.11}$	34^{+11}_{-10}	$0.45^{+0.33}_{-0.11}$	3600	$7.9^{+0.5}_{-1.1}$
GW191126_115259	$20.7^{+3.4}_{-2.0}$	$8.65^{+0.95}_{-0.71}$	$12.1^{+5.5}_{-2.2}$	$8.3^{+1.9}_{-2.4}$	$0.21^{+0.15}_{-0.11}$	$1.62^{+0.74}_{-0.74}$	$0.30^{+0.12}_{-0.13}$	$19.6^{+3.5}_{-2.0}$	$0.75^{+0.06}_{-0.05}$	1400	$8.3^{+0.2}_{-0.5}$
GW191127_050227	80^{+39}_{-22}	$29.9^{+11.7}_{-9.1}$	53^{+47}_{-20}	24^{+17}_{-14}	$0.18^{+0.34}_{-0.36}$	$3.4^{+3.1}_{-1.9}$	$0.57^{+0.40}_{-0.29}$	76^{+39}_{-21}	$0.75^{+0.13}_{-0.29}$	980	$9.2^{+0.7}_{-0.6}$
GW191129_134029	$17.5^{+2.4}_{-1.2}$	$7.31^{+0.43}_{-0.28}$	$10.7^{+4.1}_{-2.1}$	$6.7^{+1.5}_{-1.7}$	$0.06^{+0.16}_{-0.08}$	$0.79^{+0.26}_{-0.33}$	$0.16^{+0.05}_{-0.06}$	$16.8^{+2.5}_{-1.2}$	$0.69^{+0.03}_{-0.05}$	850	$13.1^{+0.2}_{-0.3}$
GW191204_110529	$47.2^{+9.2}_{-8.0}$	$19.8^{+3.6}_{-3.3}$	$27.3^{+11.0}_{-6.0}$	$19.3^{+5.6}_{-6.0}$	$0.05^{+0.26}_{-0.27}$	$1.8^{+1.7}_{-1.1}$	$0.34^{+0.25}_{-0.18}$	$45.0^{+8.6}_{-7.6}$	$0.71^{+0.12}_{-0.11}$	3700	$8.8^{+0.4}_{-0.6}$
GW191204_171526	$20.21^{+1.70}_{-0.96}$	$8.55^{+0.38}_{-0.27}$	$11.9^{+3.3}_{-1.8}$	$8.2^{+1.4}_{-1.6}$	$0.16^{+0.08}_{-0.05}$	$0.65^{+0.19}_{-0.25}$	$0.13^{+0.04}_{-0.05}$	$19.21^{+1.79}_{-0.95}$	$0.73^{+0.03}_{-0.03}$	350	$17.5^{+0.2}_{-0.2}$
GW191215_223052	$43.3^{+5.3}_{-4.3}$	$18.4^{+2.2}_{-1.7}$	$24.9^{+7.1}_{-4.1}$	$18.1^{+3.8}_{-4.1}$	$-0.04^{+0.17}_{-0.21}$	$1.93^{+0.89}_{-0.86}$	$0.35^{+0.13}_{-0.14}$	$41.4^{+5.1}_{-4.1}$	$0.68^{+0.07}_{-0.07}$	530	$11.2^{+0.3}_{-0.4}$
GW191216_213338	$19.81^{+2.69}_{-0.94}$	$8.33^{+0.22}_{-0.19}$	$12.1^{+4.6}_{-2.3}$	$7.7^{+1.6}_{-1.9}$	$0.11^{+0.13}_{-0.06}$	$0.34^{+0.12}_{-0.13}$	$0.07^{+0.02}_{-0.03}$	$18.87^{+2.80}_{-0.94}$	$0.70^{+0.03}_{-0.04}$	490	$18.6^{+0.2}_{-0.2}$
GW191219_163120	$32.3^{+2.2}_{-2.7}$	$4.32^{+0.12}_{-0.17}$	$31.1^{+2.2}_{-2.8}$	$1.17^{+0.07}_{-0.06}$	$0.00^{+0.07}_{-0.09}$	$0.55^{+0.25}_{-0.16}$	$0.11^{+0.05}_{-0.03}$	$32.2^{+2.2}_{-2.7}$	$0.14^{+0.06}_{-0.06}$	1500	$9.1^{+0.5}_{-0.8}$
GW191222_033537	79^{+16}_{-11}	$33.8^{+7.1}_{-5.0}$	$45.1^{+10.9}_{-8.0}$	$34.7^{+9.3}_{-10.5}$	$-0.04^{+0.20}_{-0.25}$	$3.0^{+1.7}_{-1.7}$	$0.51^{+0.23}_{-0.26}$	$75.5^{+15.3}_{-9.9}$	$0.67^{+0.08}_{-0.11}$	2000	$12.5^{+0.2}_{-0.3}$
GW191230_180458	86^{+19}_{-12}	$36.5^{+8.2}_{-5.6}$	$49.4^{+14.0}_{-9.6}$	37^{+11}_{-12}	$-0.05^{+0.26}_{-0.31}$	$4.3^{+2.1}_{-1.9}$	$0.69^{+0.26}_{-0.27}$	82^{+17}_{-11}	$0.68^{+0.11}_{-0.13}$	1100	$10.4^{+0.3}_{-0.4}$
GW200105_162426	$11.0^{+1.5}_{-1.4}$	$3.42^{+0.08}_{-0.08}$	$9.0^{+1.7}_{-1.7}$	$1.91^{+0.33}_{-0.24}$	$0.00^{+0.13}_{-0.18}$	$0.27^{+0.12}_{-0.11}$	$0.06^{+0.02}_{-0.02}$	$10.7^{+1.5}_{-1.4}$	$0.43^{+0.05}_{-0.02}$	7900	$13.7^{+0.2}_{-0.4}$
GW200112_155838	$63.9^{+5.7}_{-4.6}$	$27.4^{+2.6}_{-2.1}$	$35.6^{+6.7}_{-4.5}$	$28.3^{+4.4}_{-5.9}$	$0.06^{+0.15}_{-0.15}$	$1.25^{+0.43}_{-0.46}$	$0.24^{+0.07}_{-0.08}$	$60.8^{+5.3}_{-4.3}$	$0.71^{+0.06}_{-0.06}$	4300	$19.8^{+0.1}_{-0.2}$

GWTC-3 (O3b) continued

Event	M ($M_\odot$)	$\mathcal{M}$ ($M_\odot$)	m_1 ($M_\odot$)	m_2 ($M_\odot$)	$\chi_{\rm eff}$	$D_{\rm L}$ (Gpc)	z	$M_{\rm f}$ ($M_\odot$)	$\chi_{\rm f}$	$\Delta\Omega$ deg^2)	SNR
GW200115_042309	$7.4^{+1.8}_{-1.7}$	$2.43^{+0.05}_{-0.07}$	$5.9^{+2.0}_{-2.5}$	$1.44^{+0.85}_{-0.29}$	$-0.15^{+0.24}_{-0.42}$	$0.29^{+0.15}_{-0.10}$	$0.06^{+0.03}_{-0.02}$	$7.2^{+1.8}_{-1.7}$	$0.42^{+0.09}_{-0.05}$	370	$11.3^{+0.3}_{-0.5}$
GW200128_022011	75^{+17}_{-12}	$32.0^{+7.5}_{-5.5}$	$42.2^{+11.6}_{-8.1}$	$32.6^{+9.5}_{-9.2}$	$0.12^{+0.24}_{-0.25}$	$3.4^{+2.1}_{-1.8}$	$0.56^{+0.28}_{-0.28}$	71^{+16}_{-11}	$0.74^{+0.10}_{-0.10}$	2600	$10.6^{+0.3}_{-0.4}$
GW200129_065458	$63.4^{+4.3}_{-3.6}$	$27.2^{+2.1}_{-2.3}$	$34.5^{+9.9}_{-3.2}$	$28.9^{+3.4}_{-9.3}$	$0.11^{+0.11}_{-0.16}$	$0.90^{+0.29}_{-0.38}$	$0.18^{+0.05}_{-0.07}$	$60.3^{+4.0}_{-3.3}$	$0.73^{+0.06}_{-0.05}$	130	$26.8^{+0.2}_{-0.2}$
GW200202_154313	$17.58^{+1.78}_{-0.67}$	$7.49^{+0.24}_{-0.20}$	$10.1^{+3.5}_{-1.4}$	$7.3^{+1.1}_{-1.7}$	$0.04^{+0.13}_{-0.06}$	$0.41^{+0.15}_{-0.16}$	$0.09^{+0.03}_{-0.03}$	$16.76^{+1.87}_{-0.66}$	$0.69^{+0.03}_{-0.04}$	170	$10.8^{+0.2}_{-0.4}$
GW200208_130117	$65.4^{+7.8}_{-6.8}$	$27.7^{+3.6}_{-3.1}$	$37.8^{+9.2}_{-6.2}$	$27.4^{+6.1}_{-7.4}$	$-0.07^{+0.22}_{-0.27}$	$2.23^{+1.00}_{-0.85}$	$0.40^{+0.15}_{-0.14}$	$62.5^{+7.3}_{-6.4}$	$0.66^{+0.09}_{-0.13}$	30	$10.8^{+0.3}_{-0.4}$
GW200208_222617	63^{+100}_{-25}	$19.6^{+10.7}_{-5.1}$	51^{+104}_{-30}	$12.3^{+9.0}_{-5.7}$	$0.45^{+0.43}_{-0.44}$	$4.1^{+4.4}_{-1.9}$	$0.66^{+0.54}_{-0.28}$	61^{+100}_{-25}	$0.83^{+0.14}_{-0.27}$	2000	$7.4^{+1.4}_{-1.2}$
GW200209_085452	$62.6^{+13.9}_{-9.4}$	$26.7^{+6.0}_{-4.2}$	$35.6^{+10.5}_{-6.8}$	$27.1^{+7.8}_{-7.8}$	$-0.12^{+0.24}_{-0.30}$	$3.4^{+1.9}_{-1.8}$	$0.57^{+0.25}_{-0.26}$	$59.9^{+13.1}_{-8.9}$	$0.66^{+0.10}_{-0.12}$	730	$9.6^{+0.4}_{-0.5}$
GW200210_092254	$27.0^{+7.1}_{-4.3}$	$6.56^{+0.38}_{-0.40}$	$24.1^{+7.5}_{-4.6}$	$2.83^{+0.47}_{-0.42}$	$0.02^{+0.22}_{-0.21}$	$0.94^{+0.43}_{-0.34}$	$0.19^{+0.08}_{-0.06}$	$26.7^{+7.2}_{-4.3}$	$0.34^{+0.13}_{-0.08}$	1800	$8.4^{+0.5}_{-0.7}$
GW200216_220804	81^{+20}_{-14}	$32.9^{+9.3}_{-8.5}$	51^{+22}_{-13}	30^{+14}_{-16}	$0.10^{+0.34}_{-0.36}$	$3.8^{+3.0}_{-2.0}$	$0.63^{+0.37}_{-0.29}$	78^{+19}_{-13}	$0.70^{+0.14}_{-0.24}$	2900	$8.1^{+0.4}_{-0.5}$
GW200219_094415	$65.0^{+12.6}_{-8.2}$	$27.6^{+5.6}_{-3.8}$	$37.5^{+10.1}_{-6.9}$	$27.9^{+7.4}_{-8.4}$	$-0.08^{+0.23}_{-0.29}$	$3.4^{+1.7}_{-1.5}$	$0.57^{+0.22}_{-0.22}$	$62.2^{+11.7}_{-7.8}$	$0.66^{+0.10}_{-0.13}$	700	$10.7^{+0.3}_{-0.5}$
GW200220_061928	148^{+55}_{-33}	62^{+23}_{-15}	87^{+40}_{-23}	61^{+26}_{-25}	$0.06^{+0.40}_{-0.38}$	$6.0^{+4.8}_{-3.1}$	$0.90^{+0.55}_{-0.40}$	141^{+51}_{-31}	$0.71^{+0.15}_{-0.17}$	3000	$7.2^{+0.4}_{-0.7}$
GW200220_124850	67^{+17}_{-12}	$28.2^{+7.3}_{-5.1}$	$38.9^{+14.1}_{-8.6}$	$27.9^{+9.2}_{-9.0}$	$-0.07^{+0.27}_{-0.33}$	$4.0^{+2.8}_{-2.2}$	$0.66^{+0.36}_{-0.31}$	64^{+16}_{-11}	$0.67^{+0.11}_{-0.14}$	3200	$8.5^{+0.3}_{-0.5}$
GW200224_222234	$72.2^{+7.2}_{-5.1}$	$31.1^{+3.2}_{-2.6}$	$40.0^{+6.9}_{-4.5}$	$32.5^{+5.0}_{-7.2}$	$0.10^{+0.15}_{-0.15}$	$1.71^{+0.49}_{-0.64}$	$0.32^{+0.08}_{-0.11}$	$68.6^{+6.6}_{-4.7}$	$0.73^{+0.07}_{-0.07}$	50	$20.0^{+0.2}_{-0.2}$
GW200225_060421	$33.5^{+3.6}_{-3.0}$	$14.2^{+1.5}_{-1.4}$	$19.3^{+5.0}_{-3.0}$	$14.0^{+2.8}_{-3.5}$	$-0.12^{+0.17}_{-0.28}$	$1.15^{+0.51}_{-0.53}$	$0.22^{+0.09}_{-0.10}$	$32.1^{+3.5}_{-2.8}$	$0.66^{+0.07}_{-0.13}$	370	$12.5^{+0.3}_{-0.4}$
GW200302_015811	$57.8^{+9.6}_{-6.9}$	$23.4^{+4.7}_{-3.0}$	$37.8^{+8.7}_{-8.5}$	$20.0^{+8.1}_{-5.7}$	$0.01^{+0.25}_{-0.26}$	$1.48^{+1.02}_{-0.70}$	$0.28^{+0.16}_{-0.12}$	$55.5^{+8.9}_{-6.6}$	$0.66^{+0.13}_{-0.15}$	6000	$10.8^{+0.3}_{-0.4}$
GW200306_093714	$43.9^{+11.8}_{-7.5}$	$17.5^{+3.5}_{-3.0}$	$28.3^{+17.1}_{-7.7}$	$14.8^{+6.5}_{-6.4}$	$0.32^{+0.28}_{-0.46}$	$2.1^{+1.7}_{-1.1}$	$0.38^{+0.24}_{-0.18}$	$41.7^{+12.3}_{-6.9}$	$0.78^{+0.11}_{-0.26}$	4600	$7.8^{+0.4}_{-0.6}$
GW200308_173609*	$50.6^{+10.9}_{-8.5}$	$19.0^{+4.8}_{-2.8}$	$36.4^{+11.2}_{-9.6}$	$13.8^{+7.2}_{-3.3}$	$0.65^{+0.17}_{-0.21}$	$5.4^{+2.7}_{-2.6}$	$0.83^{+0.32}_{-0.35}$	$47.4^{+11.1}_{-7.7}$	$0.91^{+0.03}_{-0.08}$	2000	$7.1^{+0.5}_{-0.5}$
GW200311_115853	$61.9^{+5.3}_{-4.2}$	$26.6^{+2.4}_{-2.0}$	$34.2^{+6.4}_{-3.8}$	$27.7^{+4.1}_{-5.9}$	$-0.02^{+0.16}_{-0.20}$	$1.17^{+0.28}_{-0.40}$	$0.23^{+0.05}_{-0.07}$	$59.0^{+4.8}_{-3.9}$	$0.69^{+0.07}_{-0.08}$	35	$17.8^{+0.2}_{-0.2}$
GW200316_215756	$21.2^{+7.2}_{-2.0}$	$8.75^{+0.62}_{-0.55}$	$13.1^{+10.2}_{-2.9}$	$7.8^{+1.9}_{-2.9}$	$0.13^{+0.27}_{-0.10}$	$1.12^{+0.47}_{-0.44}$	$0.22^{+0.08}_{-0.08}$	$20.2^{+7.4}_{-1.9}$	$0.70^{+0.04}_{-0.04}$	190	$10.3^{+0.4}_{-0.7}$
GW200322_091133*	55^{+37}_{-27}	$15.5^{+15.7}_{-3.7}$	34^{+48}_{-18}	$14.0^{+16.8}_{-8.7}$	$0.24^{+0.45}_{-0.51}$	$3.6^{+7.0}_{-2.0}$	$0.60^{+0.84}_{-0.30}$	53^{+38}_{-26}	$0.78^{+0.16}_{-0.17}$	6500	$6.0^{+1.7}_{-1.2}$

GWTC-3 (O3b)

Name	Inst.	cWB			GstLAL			MBTA			PyCBC-broad			PyCBC-BBH		
		FAR (yr^{-1})	SNR	p_{astro}	FAR (yr^{-1})	SNR	p_{astro}	FAR (yr^{-1})	SNR	p_{astro}	FAR (yr^{-1})	SNR	p_{astro}	FAR (yr^{-1})	SNR	p_{astro}
GW191103_012549	HL	–	–	–	–	–	–	*27*	*9.0*	*0.13*	4.8	9.3	0.77	0.46	9.3	0.94
GW191105_143521	HLV	–	–	–	*24*	*10.0*	*0.07*	0.14	10.7	> 0.99	0.012	9.8	> 0.99	0.036	9.8	> 0.99
GW191109_010717	HL	< 0.0011	15.6	> 0.99	0.0010	15.8	> 0.99	1.8×10^{-4}	15.2	> 0.99	0.096	13.2	> 0.99	0.047	14.4	> 0.99
GW191113_071753	HLV	–	–	–	–	–	–	26	9.2	0.68	*1.1×10^{4}*	*8.3*	*< 0.01*	*1.2×10^{3}*	*8.5*	*< 0.01*
GW191126_115259	HL	–	–	–	*80*	*8.7*	*0.02*	*59*	*8.5*	*0.30*	*22*	*8.5*	*0.39*	3.2	8.5	0.70
GW191127_050227	HLV	–	–	–	*0.25*	*10.3*	*0.49*	1.2	9.8	0.73	*20*	*9.5*	*0.47*	4.1	8.7	0.74
GW191129_134029	HL	–	–	–	$< 1.0 \times 10^{-5}$	13.3	> 0.99	0.013	12.7	> 0.99	$< 2.6 \times 10^{-5}$	12.9	> 0.99	$< 2.4 \times 10^{-5}$	12.9	> 0.99
GW191204_110529	HL	–	–	–	*21*	*9.0*	*0.07*	*1.3×10^{4}*	*8.1*	*< 0.01*	*980*	*8.9*	*< 0.01*	3.3	8.9	0.74
GW191204_171526	HL	8.7×10^{-4}	17.1	> 0.99	$< 1.0 \times 10^{-5}$	15.6	> 0.99	$< 1.0 \times 10^{-5}$	17.1	> 0.99	$< 1.4 \times 10^{-5}$	16.9	> 0.99	$< 1.2 \times 10^{-5}$	16.9	> 0.99
GW191215_223052	HLV	0.12	9.8	0.95	$< 1.0 \times 10^{-5}$	10.9	> 0.99	0.22	10.8	> 0.99	0.0016	10.3	> 0.99	0.28	10.2	> 0.99
GW191216_213338	HV	–	–	–	$< 1.0 \times 10^{-5}$	18.6	> 0.99	9.3×10^{-4}	17.9	> 0.99	0.0019	18.3	> 0.99	7.6×10^{-4}	18.3	> 0.99
GW191219_163120	HLV	–	–	–	–	–	–	–	–	–	4.0	8.9	0.82	–	–	–
GW191222_033537	HL	8.9×10^{-4}	11.1	> 0.99	$< 1.0 \times 10^{-5}$	12.0	> 0.99	0.0099	10.8	> 0.99	0.0021	11.5	> 0.99	9.8×10^{-5}	11.5	> 0.99
GW191230_180458	HLV	0.050	10.3	0.95	0.13	10.3	0.87	*8.1*	*9.8*	*0.40*	*52*	*9.6*	*0.29*	0.42	9.9	0.96
GW200112_155838	LV	–	–	–	$< 1.0 \times 10^{-5}$ †	17.6	> 0.99	–	–	–	–	–	–	–	–	–
GW200115_042309	HLV	–	–	–	$< 1.0 \times 10^{-5}$	11.5	> 0.99	0.0055	11.2	> 0.99	$< 1.2 \times 10^{-4}$	10.8	> 0.99	–	–	–
GW200128_022011	HL	1.3	8.8	0.63	0.022	10.1	0.97	3.3	9.4	0.98	0.63	9.8	0.95	0.0043	9.9	> 0.99
GW200129_065458	HLV	–	–	–	$< 1.0 \times 10^{-5}$	26.5	> 0.99	–	–	–	$< 2.3 \times 10^{-5}$	16.3	> 0.99	$< 1.7 \times 10^{-5}$	16.2	> 0.99
GW200202_154313	HLV	–	–	–	$< 1.0 \times 10^{-5}$	11.3	> 0.99	–	–	–	–	–	–	0.025	10.8	> 0.99
GW200208_130117	HLV	–	–	–	0.0096	10.7	0.99	0.46	10.4	> 0.99	0.18	9.6	0.98	3.1×10^{-4}	10.8	> 0.99
GW200208_222617	HLV	–	–	–	*160*	*8.2*	*< 0.01*	*420*	*8.9*	*0.02*	–	–	–	4.8	7.9	0.70
GW200209_085452	HLV	–	–	–	0.046	10.0	0.95	12	9.7	0.97	*550*	*9.2*	*0.04*	1.2	9.2	0.89
GW200210_092254	HLV	–	–	–	*1.2*	*9.5*	*0.42*	–	–	–	17	8.9	0.53	7.7	8.9	0.54
GW200216_220804	HLV	–	–	–	0.35	9.4	0.77	*2.4×10^{3}*	*8.8*	*0.02*	*970*	*9.0*	*< 0.01*	7.8	8.7	0.54
GW200219_094415	HLV	0.77	9.7	0.85	9.9×10^{-4}	10.7	> 0.99	0.18	10.6	> 0.99	1.7	9.9	0.89	0.016	10.0	> 0.99
GW200220_061928	HLV	–	–	–	–	–	–	–	–	–	–	–	–	6.8	7.5	0.62
GW200220_124850	HL	–	–	–	*150*	*8.2*	*< 0.01*	1.8×10^{3}	8.2	0.83	–	–	–	*30*	*7.8*	*0.20*
GW200224_222234	HLV	8.8×10^{-4}	18.8	> 0.99	$< 1.0 \times 10^{-5}$	18.9	> 0.99	$< 1.0 \times 10^{-5}$	19.0	> 0.99	$< 8.2 \times 10^{-5}$	19.2	> 0.99	$< 7.7 \times 10^{-5}$	18.6	> 0.99
GW200225_060421	HL	8.8×10^{-4}	13.1	> 0.99	0.079	12.9	0.93	0.0049	12.5	> 0.99	$< 1.1 \times 10^{-5}$	12.3	> 0.99	4.1×10^{-5}	12.3	> 0.99
GW200302_015811	HV	–	–	–	0.11†	10.6	0.91	–	–	–	–	–	–	–	–	–
GW200306_093714	HL	–	–	–	–	–	–	410	8.5	0.81	*3.4×10^{3}*	*7.8*	*< 0.01*	*24*	*8.0*	*0.24*
GW200308_173609	HLV	–	–	–	*680*	*8.1*	*< 0.01*	*6.9×10^{4}*	*8.3*	*0.24*	*770*	*7.9*	*< 0.01*	2.4	8.0	0.86
GW200311_115853	HLV	8.2×10^{-4}	16.2	> 0.99	$< 1.0 \times 10^{-5}$	17.7	> 0.99	$< 1.0 \times 10^{-5}$	16.5	> 0.99	$< 6.9 \times 10^{-5}$	17.0	> 0.99	$< 7.7 \times 10^{-5}$	17.4	> 0.99
GW200316_215756	HLV	–	–	–	$< 1.0 \times 10^{-5}$	10.1	> 0.99	*12*	*9.5*	*0.30*	0.20	9.3	0.98	0.58	9.3	0.98
GW200322_091133	HLV	–	–	–	–	–	–	450	9.0	0.62	*1.4×10^{3}*	*8.0*	*< 0.01*	*140*	*7.7*	*0.08*

Independent Ring-down Search (Mockdata challenge)

PHYSICAL REVIEW D **99,** 124032 (2019)

Comparison of various methods to extract ringdown frequency from gravitational wave data

Hiroyuki Nakano,[1,*] Tatsuya Narikawa,[2,3,†] Ken-ichi Oohara,[4,‡] Kazuki Sakai,[5,§] Hisa-aki Shinkai,[6,‖] Hirotaka Takahashi,[7,8,¶] Takahiro Tanaka,[3,9,**] Nami Uchikata,[2,4,††] Shun Yamamoto,[6] and Takahiro S. Yamamoto[3,‡‡]

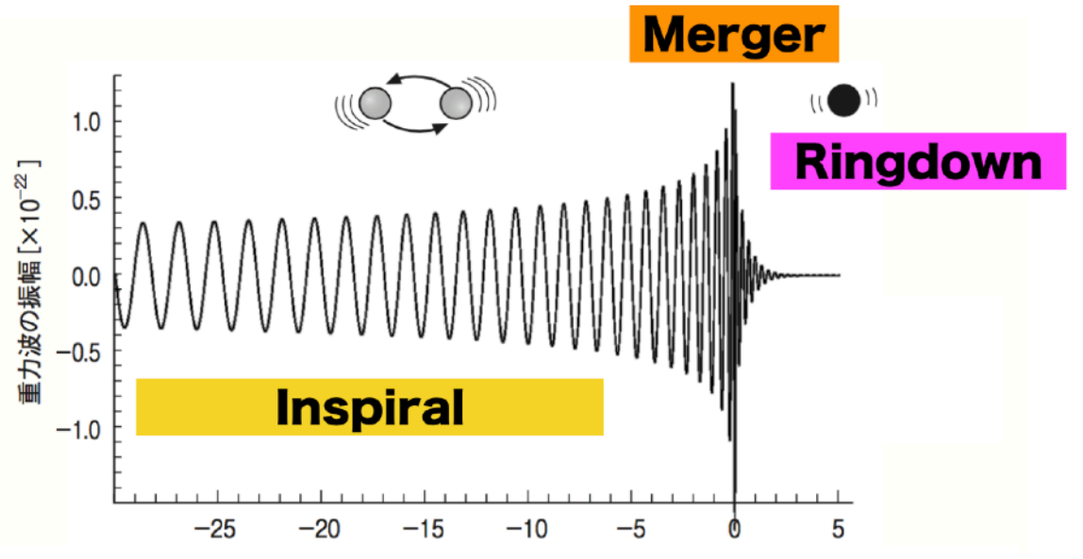

ringdown search
60 mockdata

matched filtering

Hilbert-Huan Transformation

Auto-Regression Method

Neural Network method

TABLE III. We show the values of $\overline{\delta \log f_{\rm R}}$, $\sigma(f_{\rm R})$, $\overline{\delta \log f_{\rm I}}$, and $\sigma(f_{\rm I})$ for various methods. The results limited to set A are given on the first law of each method, while those limited to set B are on the second.

		$\overline{\delta \log f_{\rm R}}(\%)$	$\sigma(f_{\rm R})(\%)$	$\overline{\delta \log f_{\rm I}}(\%)$	$\sigma(f_{\rm I})(\%)$
MF-R	A	−12.88	28.36	−71.51	97.79
	B	−0.82	27.53	−46.11	75.48
MF-MR	A	6.25 (Very good)	17.27 (Good)	−12.62 (Very good)	37.9 (Very good)
	B	2.47	10.41	7.18	27.61
HHT	A	−13.38	21.91	−44.11	61.58
	B	−8.08	19.81	−28.78	49.61
AR	A	0.2 (Excellent)	9.93 (Excellent)	4.88 (Excellent)	38.75 (Good)
	B	1.91	8.57	6.2	34.64
NN	A	−6.64 (Good)	16.48 (Very good)	−15.23 (Good)	33.96 (Excellent)
	B	−6.65	11.97	9.96	23.76

Auto-Regressive model (Method, general) I

Fitting data with linear func.

$$x_n = a_1 x_{n-1} + a_2 x_{n-2} + \cdots + a_M x_{n-M} + \varepsilon$$
$$= \sum_{j=1}^{M} a_j x_{n-j} + \varepsilon$$

e.g. $x_n = A e^{-rn\Delta t} \cos(\omega n \Delta t)$

$$Z_1 = e^{-(r-j\omega)\Delta t}$$
$$Z_2 = e^{-(r+j\omega)\Delta t}$$

$$\Rightarrow \quad x_n = \frac{A}{2}(Z_1^n + Z_2^n) = (Z_1 + Z_2)x_{n-1} - Z_1 Z_2 x_{n-2}$$

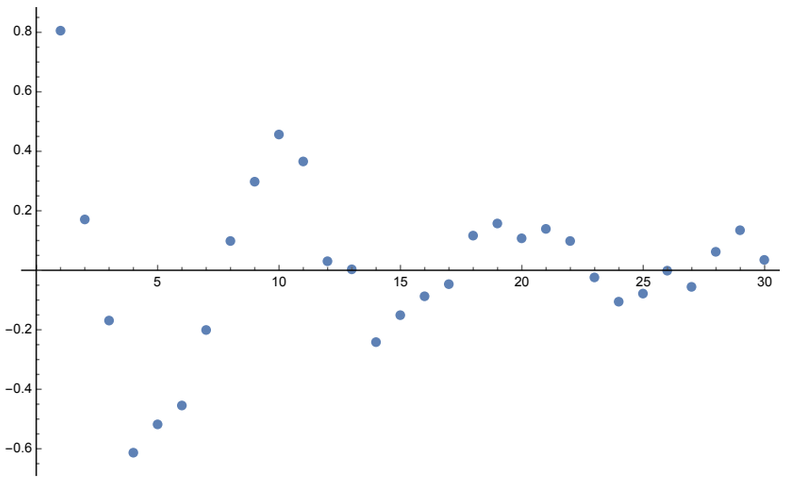

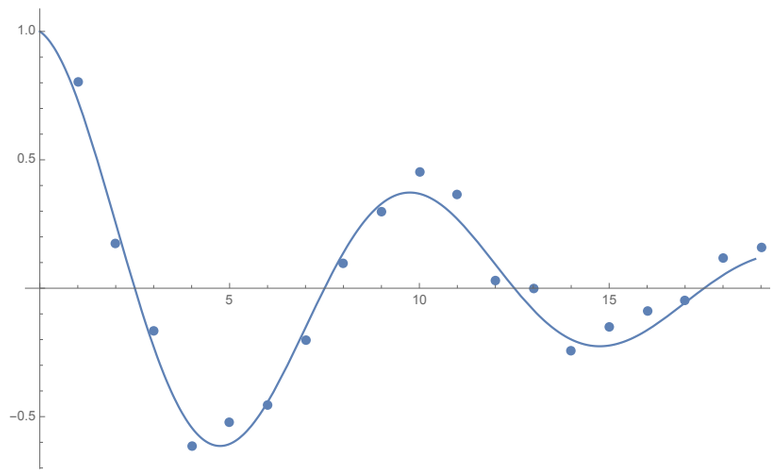

can be applied also to noisy data by adjusting *M*

Auto-Regressive model (Method, general) II

Fitting data with linear func.

$$x_n = a_1 x_{n-1} + a_2 x_{n-2} + \cdots + a_M x_{n-M} + \varepsilon$$
$$= \sum_{j=1}^{M} a_j x_{n-j} + \varepsilon$$

- find a_j (Burg method)
- find M (FPE final prediction error method)
- re-construct wave signal from fitted function
- apply FFT with arbitrary precision.

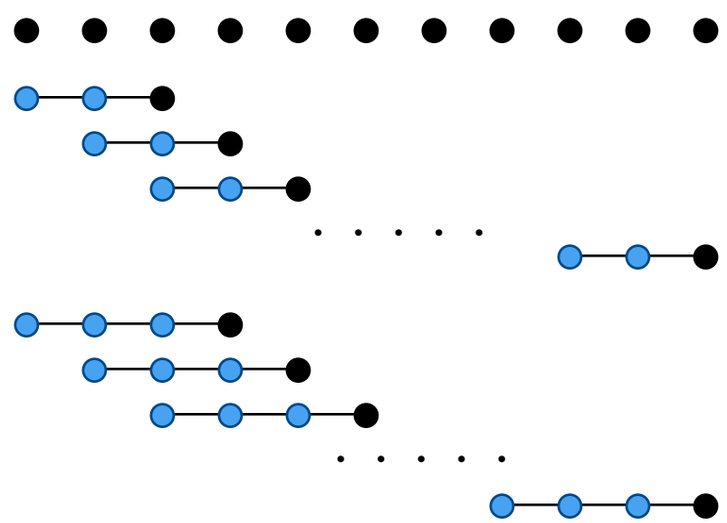

power spectrum

$$p(f) = \frac{\sigma^2}{\left| 1 - \sum_{j=1}^{M} a_j e^{-I 2\pi j f \Delta t} \right|^2}$$

Auto-Regressive model vs Short FFT

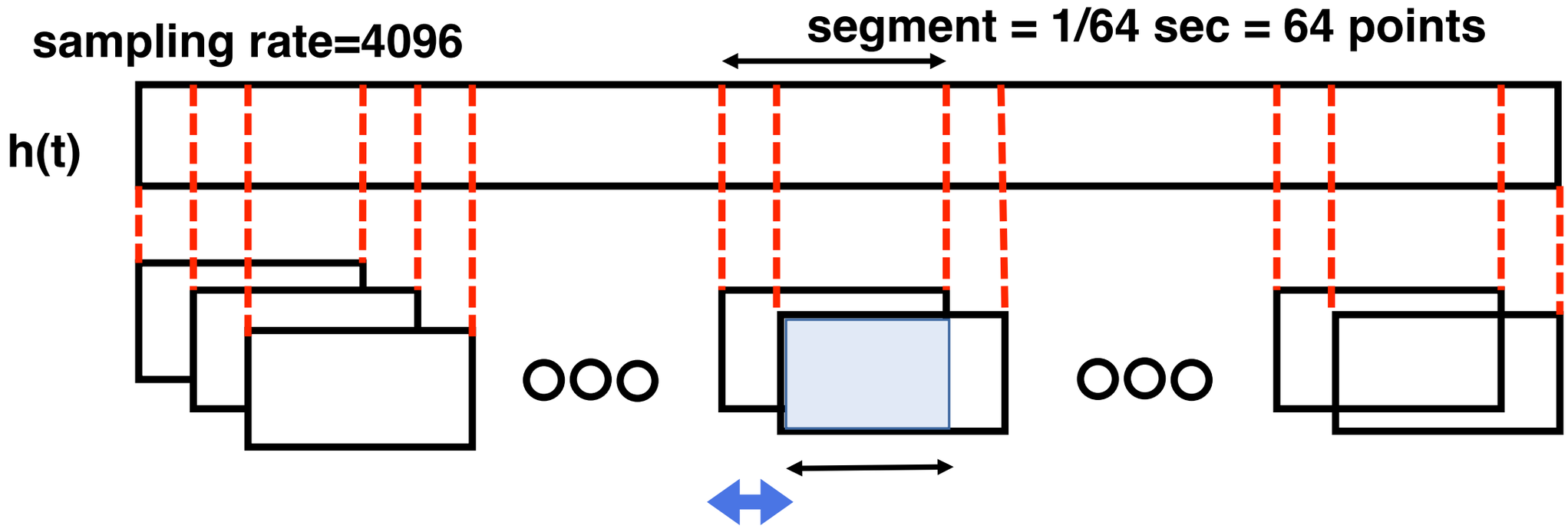

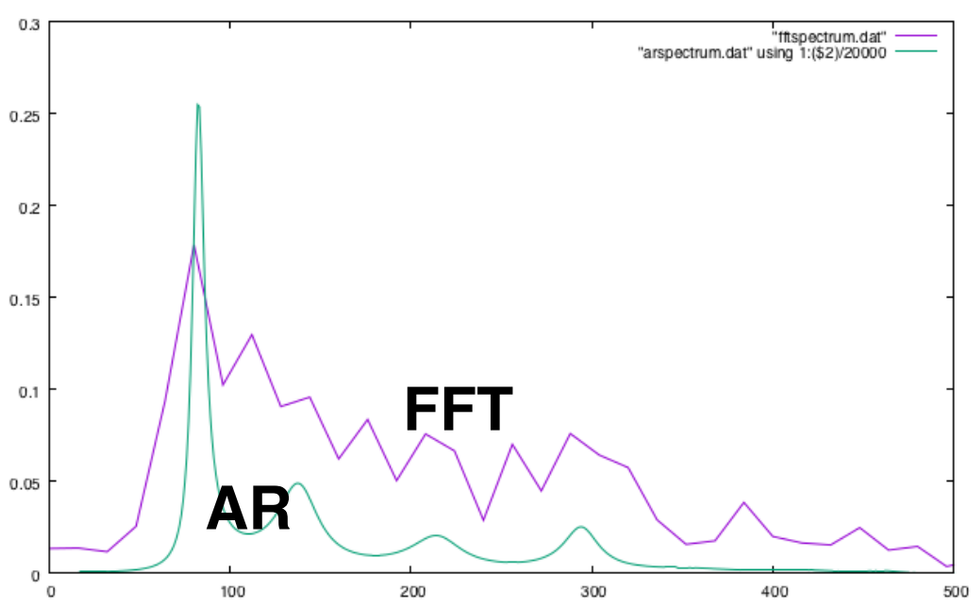

P(f)

freq. [mock data, SNR=40, inspiral part]

The order M can be fixed at 2∼8.

Even for short segment, AR model shows precise power-spectrum.

Auto-Regressive model (Method, general) III

Fitting data with linear func.

$$x_n = a_1 x_{n-1} + a_2 x_{n-2} + \cdots + a_M x_{n-M} + \varepsilon$$
$$= \sum_{j=1}^{M} a_j x_{n-j} + \varepsilon$$

- find a_j (Burg method)
- find M (FPE final prediction error method)
- re-construct wave signal from fitted function
- apply FFT with arbitrary precision.

power spectrum

$$p(f) = \frac{\sigma^2}{\left| 1 - \sum_{j=1}^{M} a_j e^{-I 2\pi j f \Delta t} \right|^2}$$

characteristic eq.

$$f(z) = 1 - \sum_{j=1}^{M} a_j z^j = 0$$

$|z_k|$ says amplitude,
$\arg(z_k)$ says frequency.

Procedures

Data —> Ringdown part

Specify (freq., damping rate) by AR method

for each segment, a couple of combinations are available.

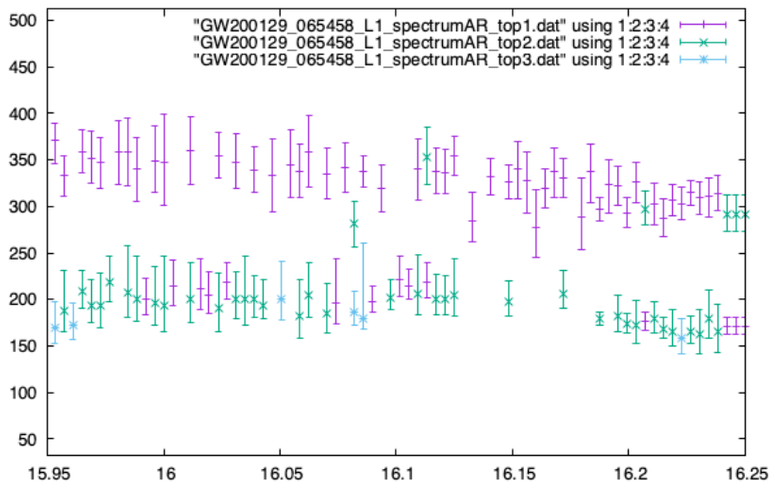

would be possible to find multi-modes

Look for the segments with constant frequencies.

Convert (freq., damping rate) to (M_final, a_final) using GR formula.

(Berti-Cardoso-Will). (Uses the redshift z by LVK catalog.)

check if three data (Hanford, Livingston, Virgo) converges

Compare with the value (M_final, a_final) by LVK catalog.

check if the analysis is consistent with GR

or having a shift

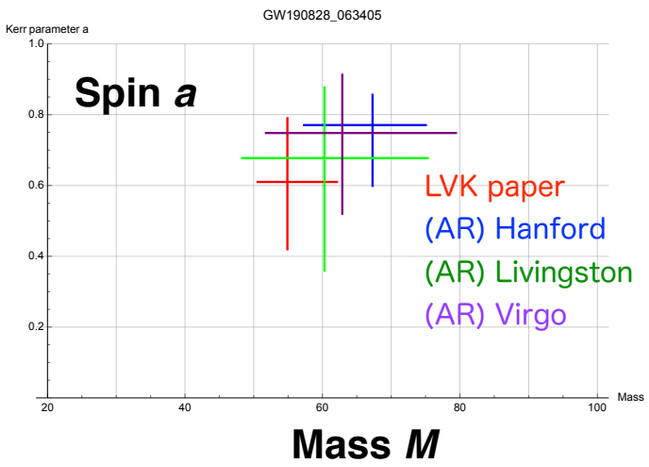

GW150914

LIGO paper

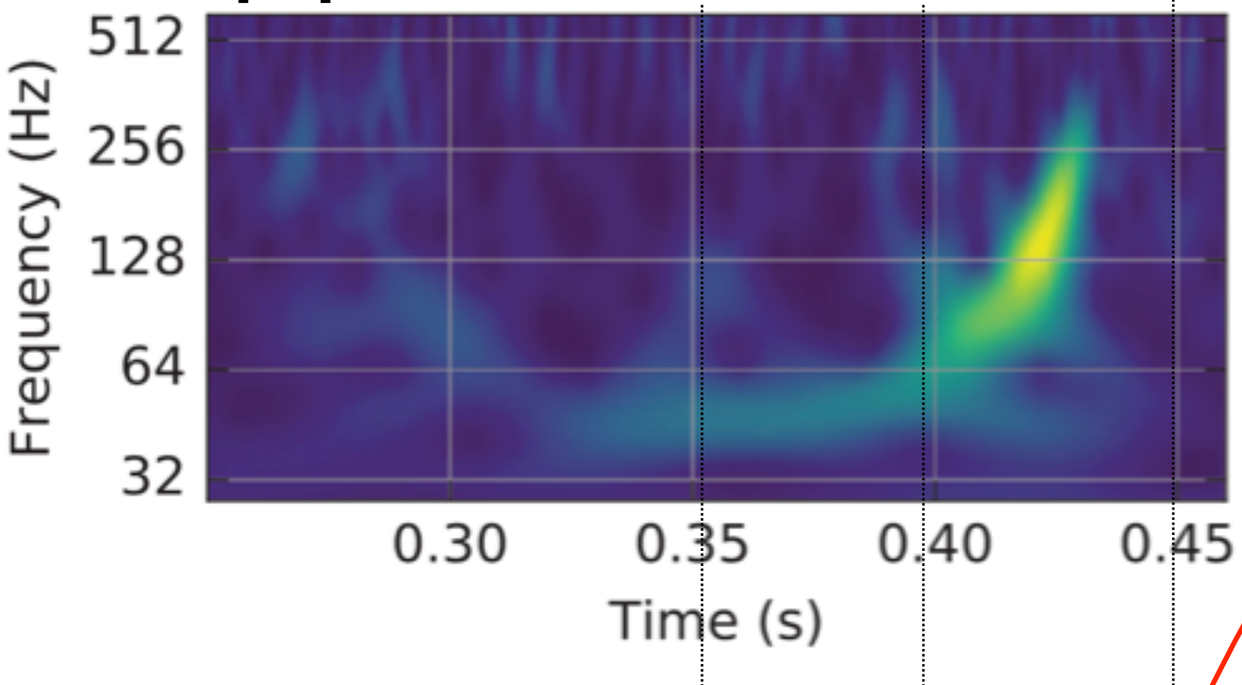

AR model Hanford

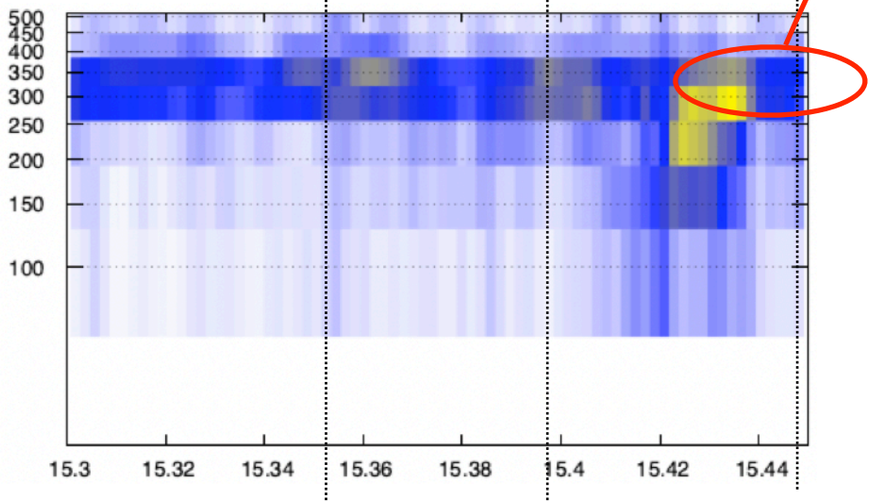

4096 sampling rate
150-450 Hz filter
1 segment = 1/64 sec= 64 points
1 shift = 1/512 sec = 8 points

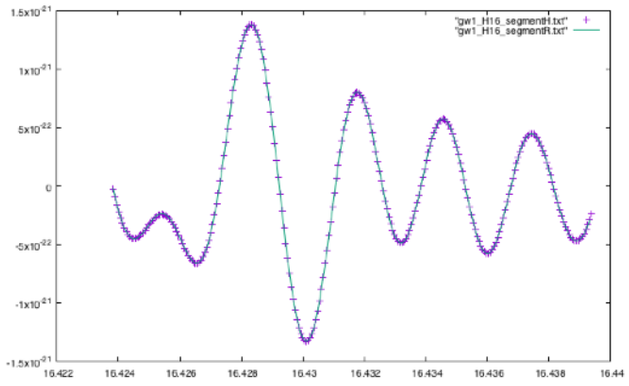

freq [Hz]

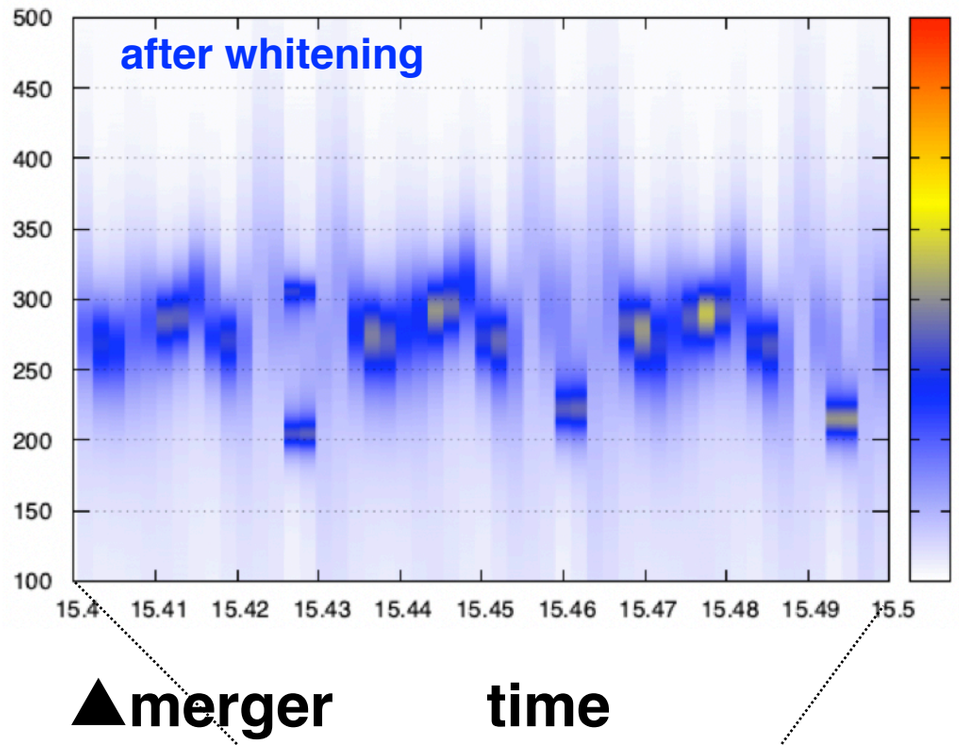

▲merger time

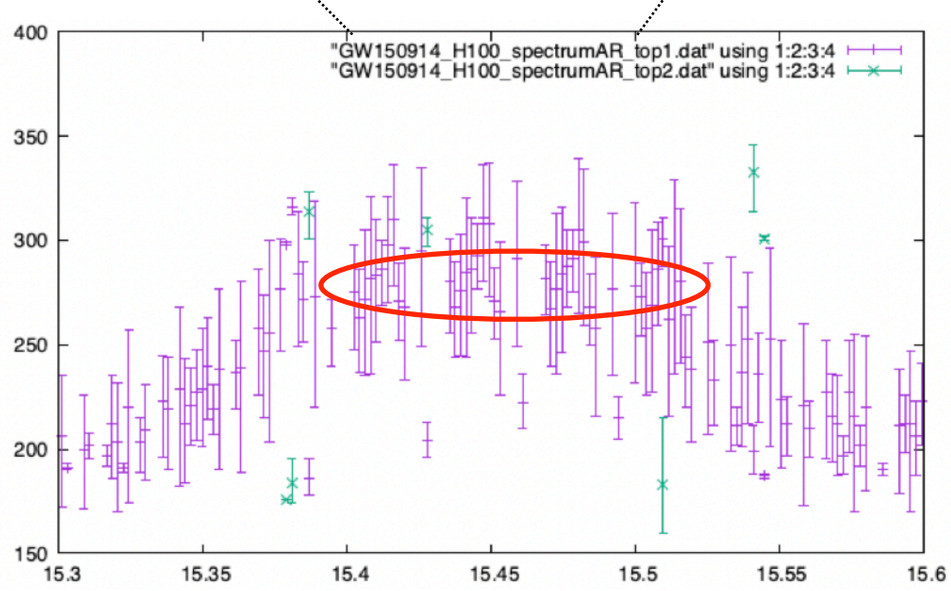

GW150914

Hanford (SNR=20.6)

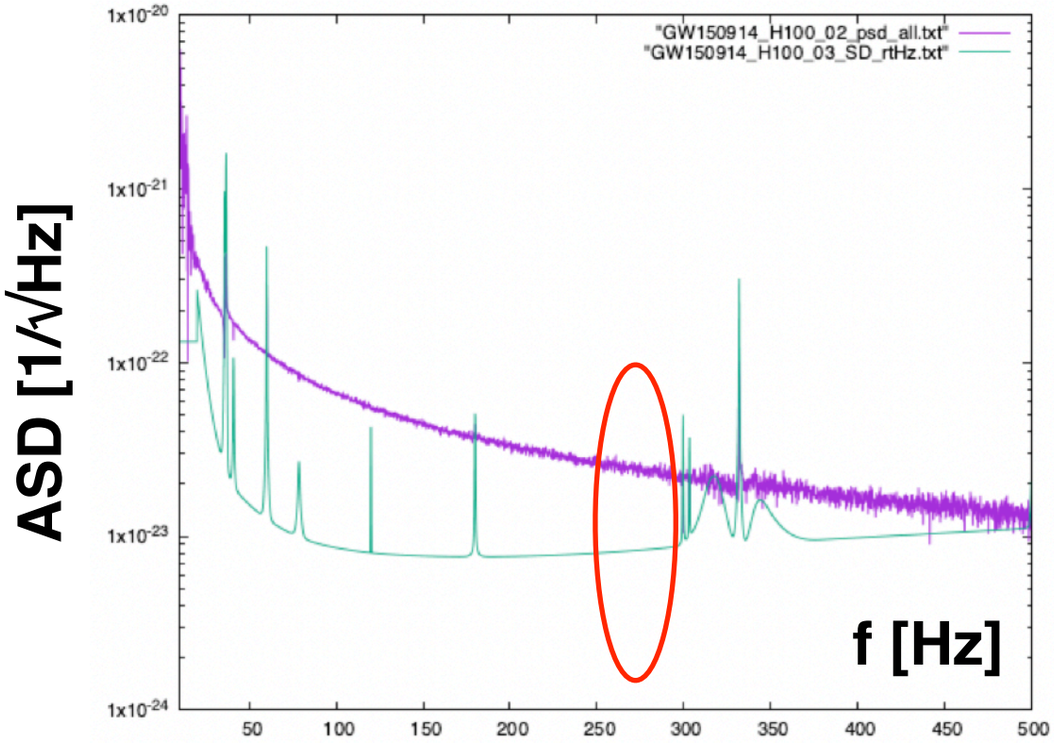

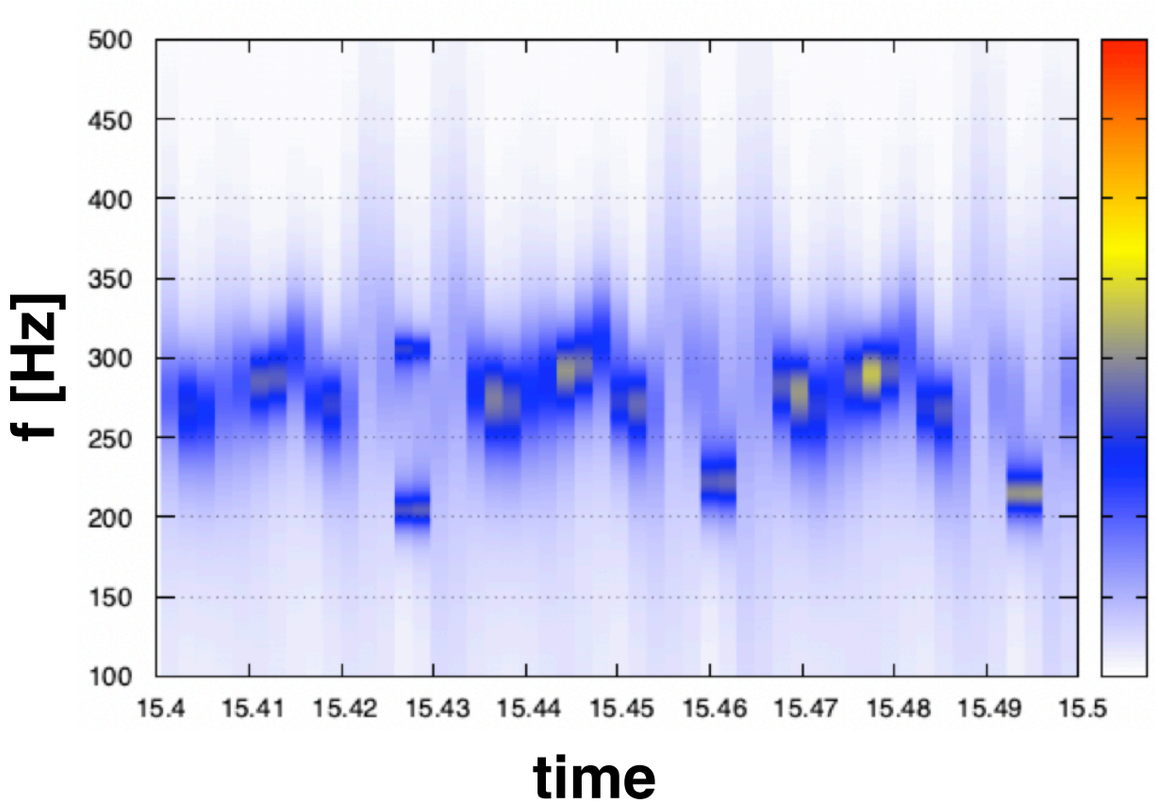

Livingston (SNR=14.2)

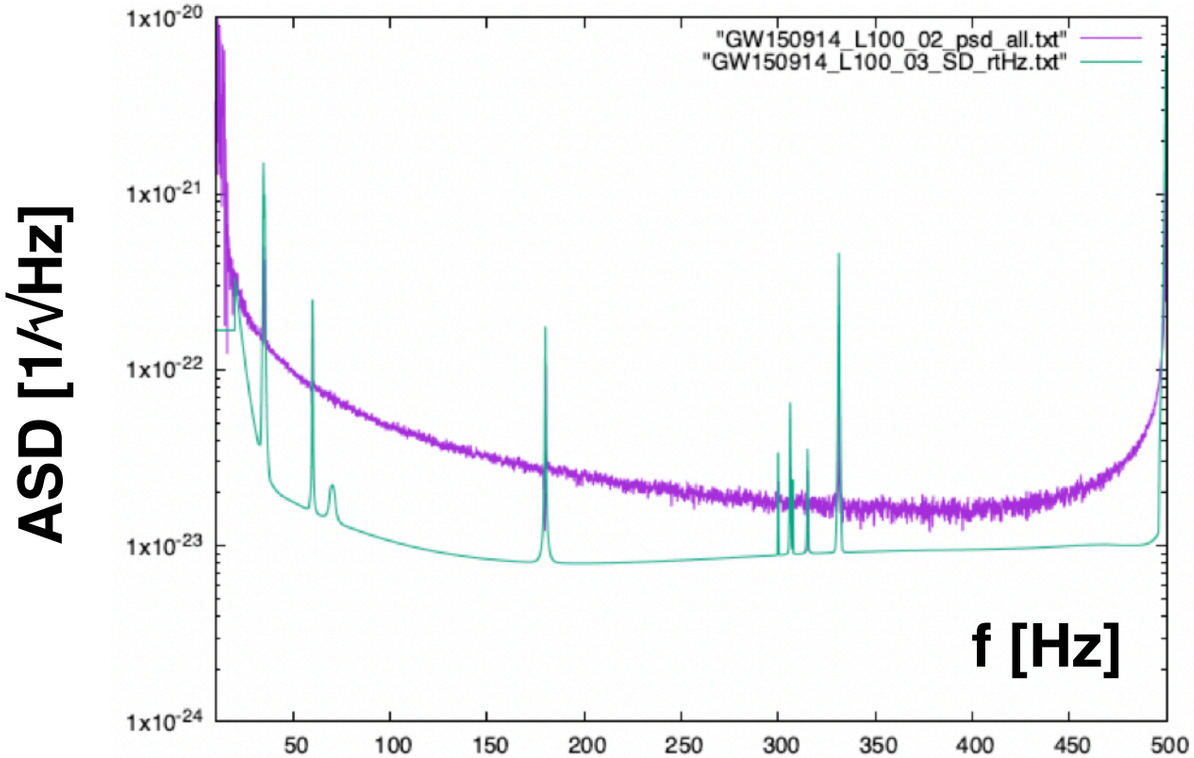

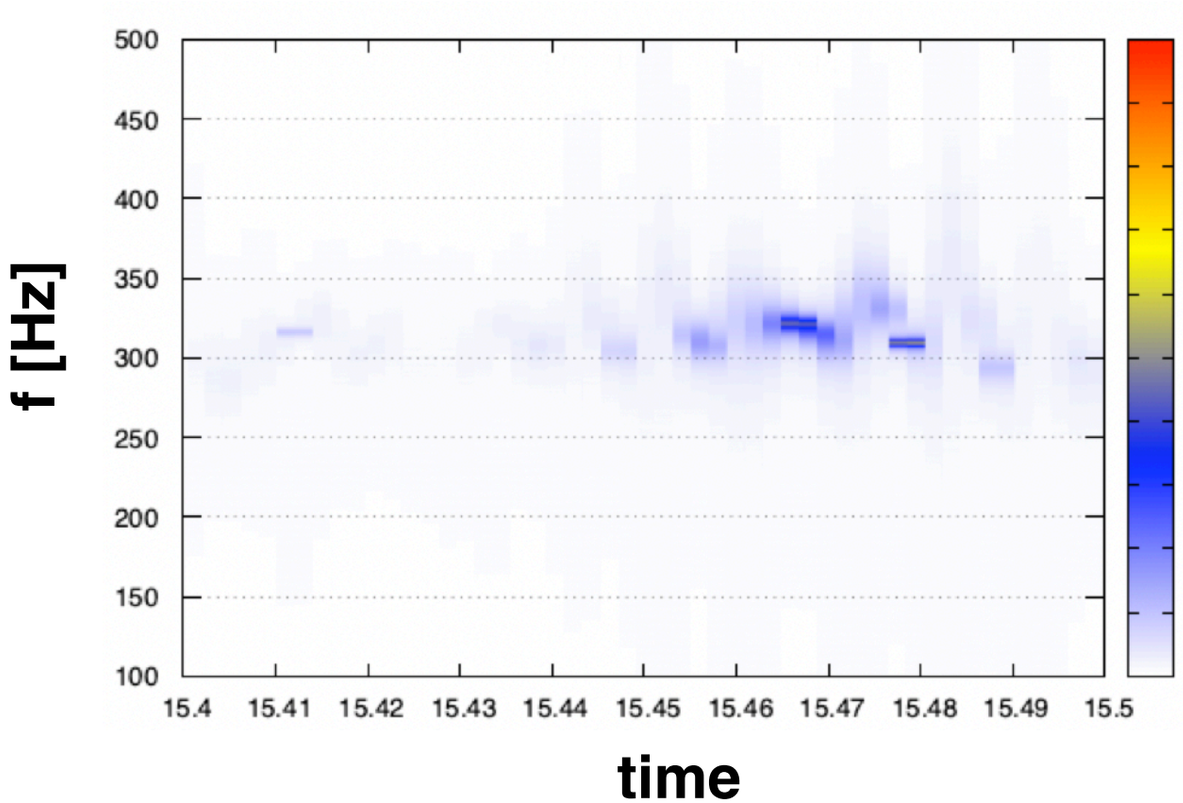

GW150914

LV paper ▶ $(M, a) = (63.1^{+3.4}_{-3.0}, 0.69^{+0.05}_{-0.04})$

fQNM ▶
$f_{220} = 271.8$ Hz, $f_{221} = 266.0$ Hz, $f_{222} = 254.7$ Hz
$f_{210} = 380.7$ Hz, $f_{211} = 225.7$ Hz, $f_{200} = 252.8$ Hz
$f_{330} = 430.9$ Hz, $f_{331} = 427.4$ Hz, $f_{332} = 421.1$ Hz
$f_{320} = 387.9$ Hz, $f_{310} = 351.1$ Hz, $f_{300} = 320.3$ Hz

Hanford (SNR=20.6) H100_SpectrogramAR

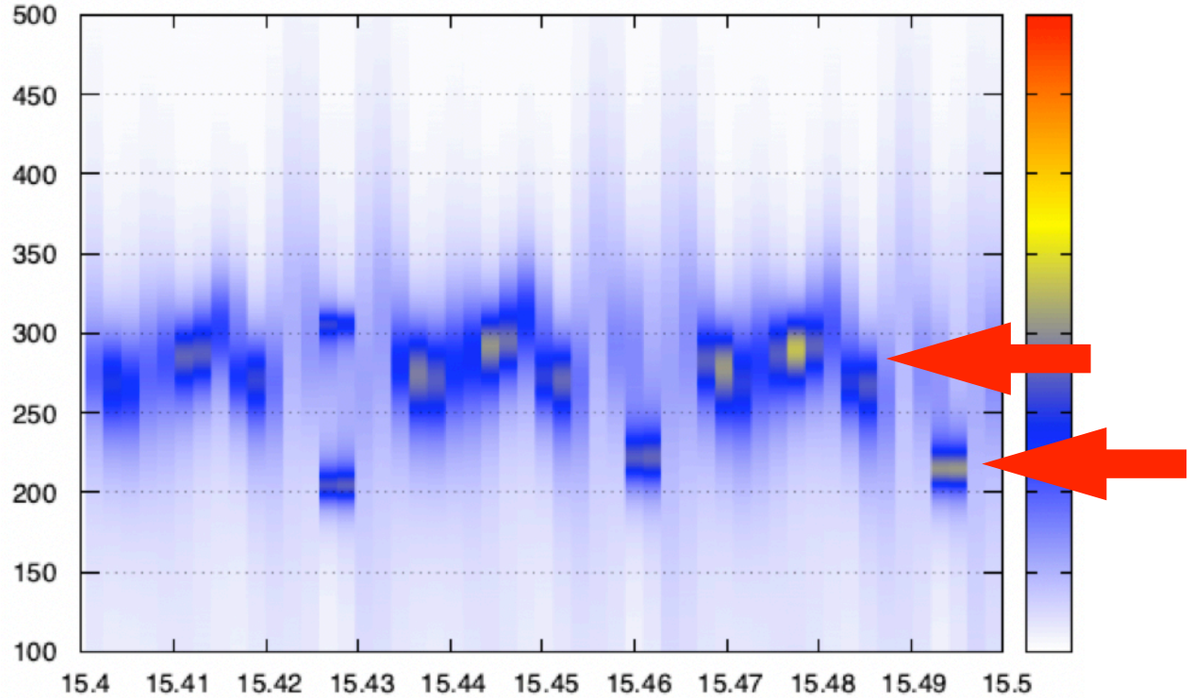

Livingston (SNR=14.2) L100_SpectrogramAR

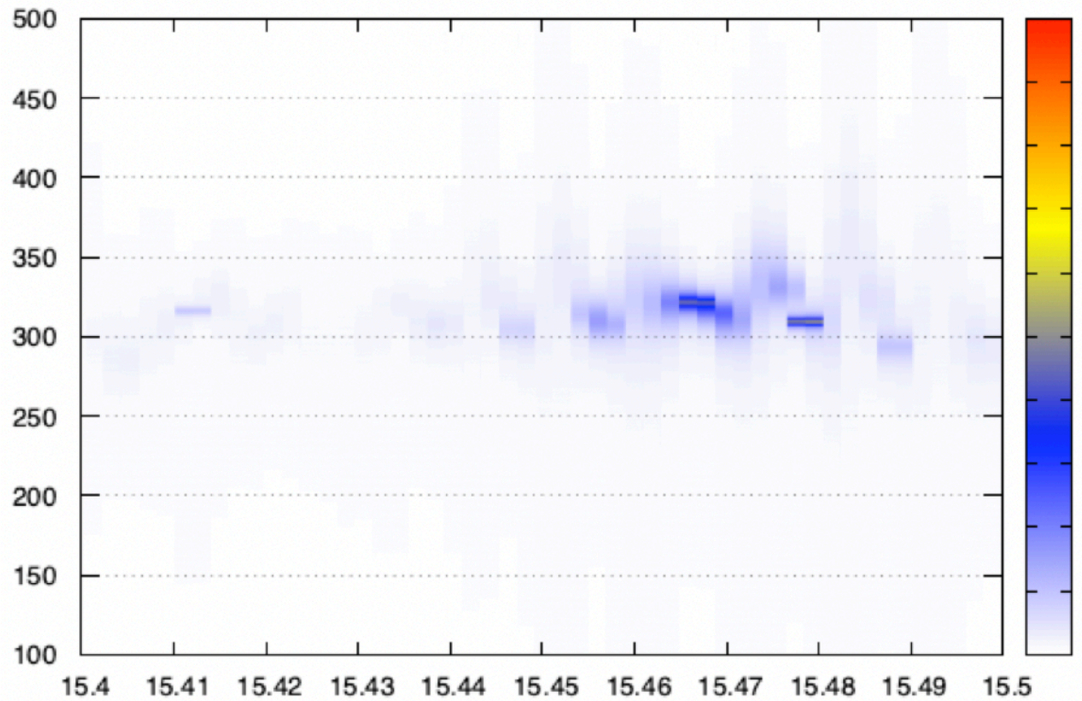

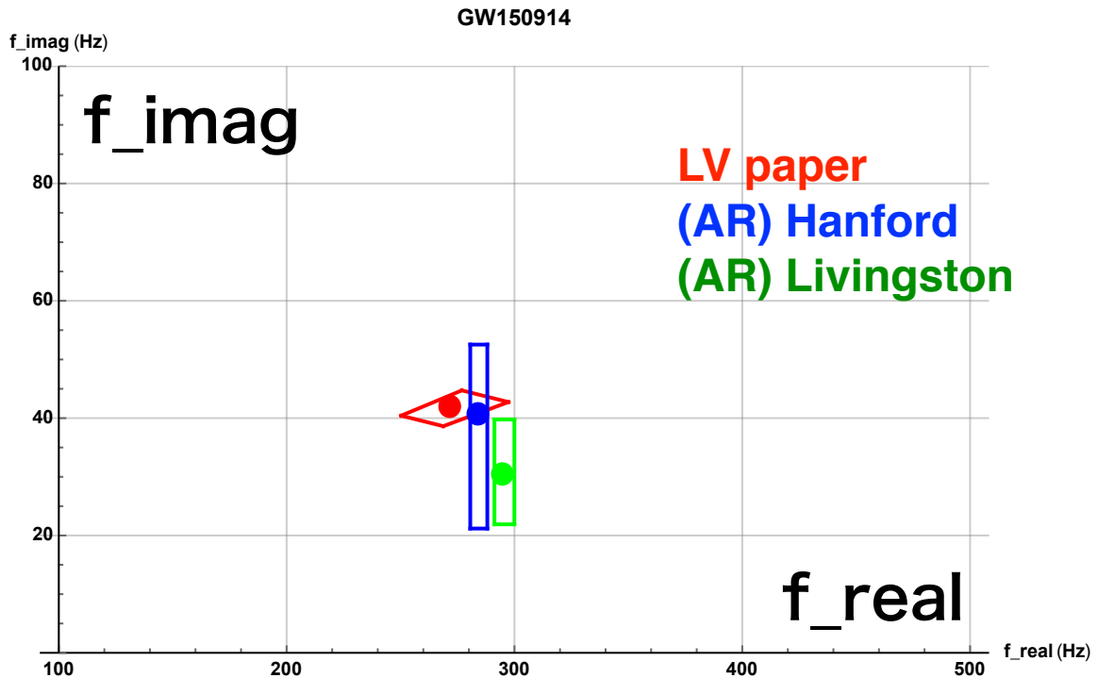

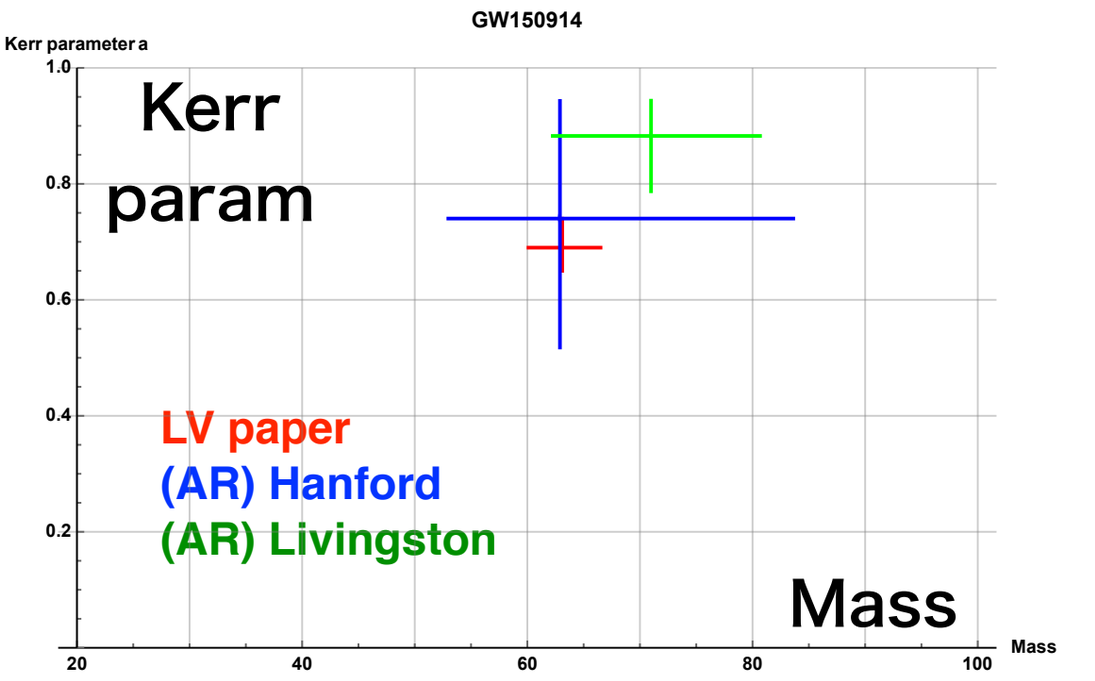

GW150914

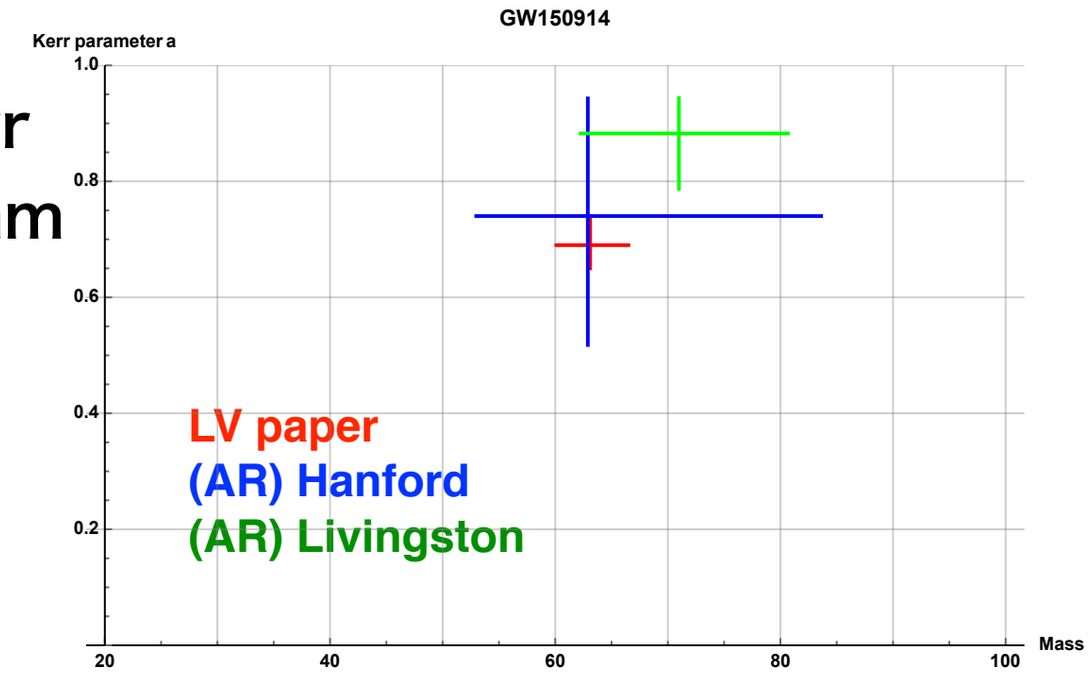

Kerr param

Mass

Hanford (SNR=20.6)
Livingston (SNR=14.2)

GW170809

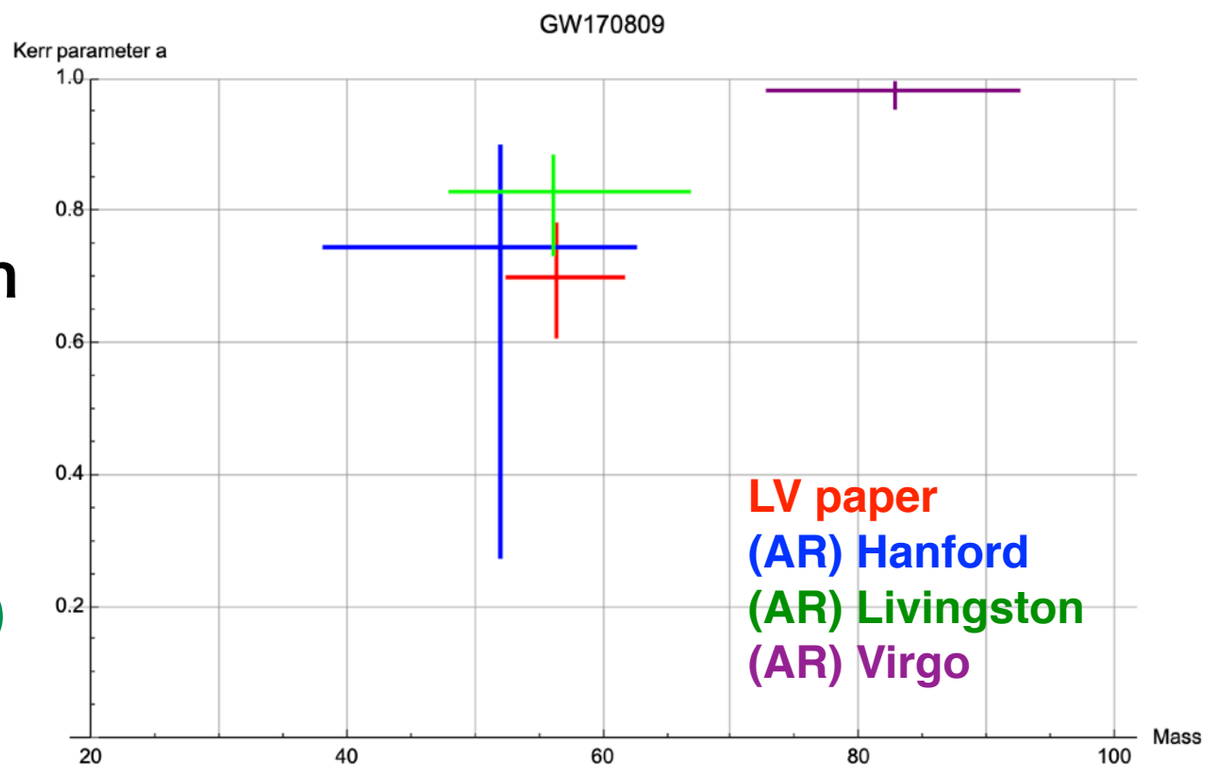

Kerr param

Mass

Hanford (SNR=5.9)
Livingston (SNR=10.7)
Virgo (SNR=1.1)

Event List ordered by SNR

Name	Release	Network SNR ↓	Distance (Mpc)	Total Mass ($M_\odot$)	
GW170817	GWTC-1-confident	33.0	40^{+7}_{-15}	--	
GW200129_065458	GWTC-3-confident	$26.8^{+0.2}_{-0.2}$	900^{+290}_{-380}	$63.4^{+4.3}_{-3.6}$	
GW190814	O3_Discovery_Papers	$25.0^{+0.1}_{-0.2}$	241^{+41}_{-45}	$25.8^{+1.0}_{-0.9}$	
GW150914	GWTC-1-confident	24.4	440^{+150}_{-170}	--	
GW190521_074359	GWTC-2	24.4	1240^{+400}_{-570}	$74.7^{+7.0}_{-4.8}$	
GW190814	GWTC-2	22.2	240^{+40}_{-50}	$25.8^{+1.0}_{-0.9}$	
GW190521_074359	GWTC-2.1-confident	22.2	--	--	
GW190814	GWTC-2.1-confident	20.4	--	--	
GW200224_222234	GWTC-3-confident	$20.0^{+0.2}_{-0.2}$	1710^{+490}_{-640}	$72.2^{+7.2}_{-5.1}$	
GW200112_155838	GWTC-3-confident	$19.8^{+0.1}_{-0.2}$	1250^{+430}_{-460}	$63.9^{+5.7}_{-4.6}$	
GW190412	O3_Discovery_Papers	$19.0^{+0.2}_{-0.3}$	740^{+130}_{-160}	$38.4^{+3.8}_{-3.9}$	
GW190412	GWTC-2	18.9	740^{+140}_{-170}	$38.4^{+3.8}_{-3.7}$	
GW191216_213338	GWTC-3-confident	$18.6^{+0.2}_{-0.2}$	340^{+120}_{-130}	$19.81^{+2.69}_{-0.94}$	AR filtering N/A (due to small *M*)
GW190412	GWTC-2.1-confident	18.2	--	--	
191225_215715	O3_IMBH_marginal	17.9	--	--	
GW200311_115853	GWTC-3-confident	$17.8^{+0.2}_{-0.2}$	1170^{+280}_{-400}	$61.9^{+5.3}_{-4.2}$	
GW191204_171526	GWTC-3-confident	$17.5^{+0.2}_{-0.2}$	650^{+190}_{-250}	$20.21^{+1.70}_{-0.96}$	AR filtering N/A (due to small *M*)
GW191109_010717	GWTC-3-confident	$17.3^{+0.5}_{-0.5}$	1290^{+1130}_{-650}	112^{+20}_{-16}	AR filtering N/A (due to large *M*)

★ tried in this study

☆ list overlapped

https://www.gw-openscience.org/eventapi/html/allevents/

Event List ordered by SNR (continued)

Name	Release	Network SNR ↓	Distance (Mpc)	Total Mass ($M_\odot$)
GW190828_063405	GWTC-2	16.0	2130^{+660}_{-930}	$58.0^{+7.7}_{-4.8}$
GW170814	GWTC-1-confident	15.9	600^{+150}_{-220}	--
GW190630_185205	GWTC-2	15.6	890^{+560}_{-370}	$59.1^{+4.6}_{-4.8}$
GW190630_185205	GWTC-2.1-confident	15.2	--	--
GW190828_063405	GWTC-2.1-confident	15.2	--	--
GW170608	GWTC-1-confident	14.9	320^{+120}_{-110}	--
GW190408_181802	GWTC-2	14.7	1550^{+400}_{-600}	$43.0^{+4.2}_{-3.0}$
GW190521	O3_Discovery_Papers	$14.6^{+0.4}_{-0.4}$	5300^{+2400}_{-2600}	150^{+29}_{-17}
200114_020818	O3_IMBH_marginal	14.5	--	--
GW190521	GWTC-2	14.4	3920^{+2190}_{-1950}	$163.9^{+39.2}_{-23.5}$
GW190408_181802	GWTC-2.1-confident	14.4	--	--
191223_014159	O3_IMBH_marginal	14.2	--	--
GW200105_162426	O3_Discovery_Papers	13.9	280^{+110}_{-110}	$10.9^{+1.1}_{-1.2}$
GW190519_153544	GWTC-2.1-confident	13.7	--	--
GW200105_162426	GWTC-3-marginal	$13.7^{+0.2}_{-0.4}$	270^{+120}_{-110}	$11.0^{+1.5}_{-1.4}$
GW190728_064510	GWTC-2	13.6	870^{+260}_{-370}	$20.6^{+4.5}_{-1.3}$
GW190521	GWTC-2.1-confident	13.6	--	--
200219_201407	GWTC-3-marginal	13.6	--	--
		$17.3^{}_{-0.5}$	$1290^{}_{-650}$	$112^{}_{-16}$

AR filtering N/A (due to small *M*)

AR filtering N/A (due to small *M*)

AR filtering N/A (due to small *M*)

GW190925

GW190910

GW190707

AR filtering N/A (due to small *M*)

https://www.gw-openscience.org/eventapi/html/allevents/

GW200129_065458

LVK paper $(M, a, z) = (60.3^{+4.}_{-3.3}, 0.73^{+0.06}_{-0.06}, 0.18^{+0.05}_{-0.07})$

Hanford

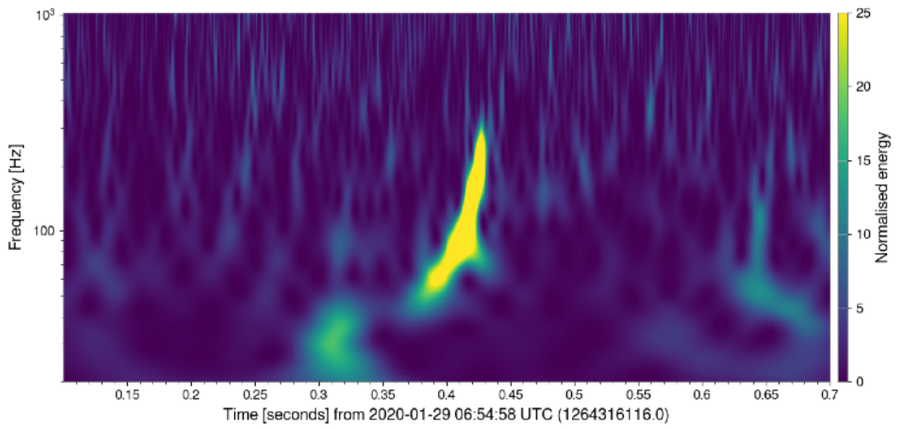

Livingston

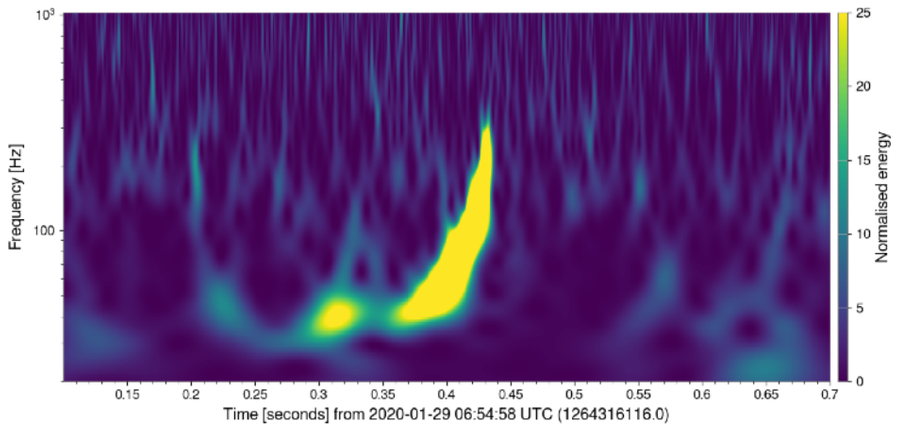

Virgo

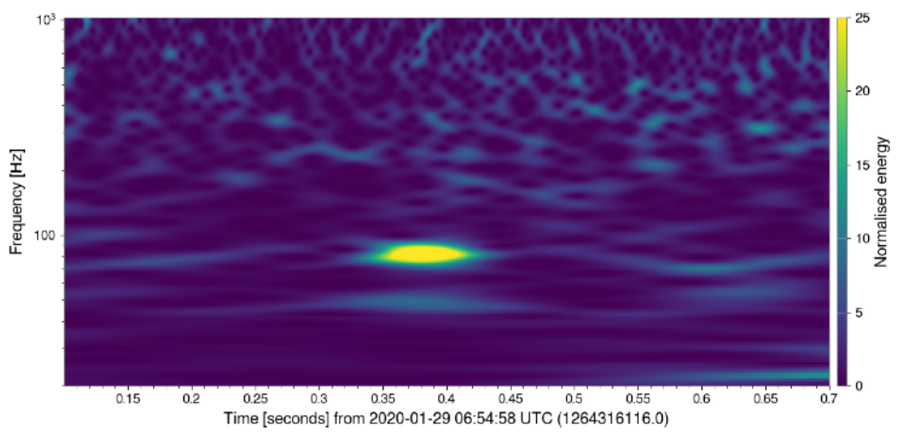

Network SNR=26.8

Expected f_{QNM} (detector frame)

$$f_{220} = 293.8 \text{ Hz}, f_{221} = 288.4 \text{ Hz}, f_{222} = 277.8 \text{ Hz}$$
$$f_{210} = 394.1 \text{ Hz}, f_{211} = 240.9 \text{ Hz}, f_{200} = 263.3 \text{ Hz}$$
$$f_{330} = 464.9 \text{ Hz}, f_{331} = 461.7 \text{ Hz}, f_{332} = 455.8 \text{ Hz}$$
$$f_{320} = 414.4 \text{ Hz}, f_{310} = 371.8 \text{ Hz}, f_{300} = 336.8 \text{ Hz}$$

GW200129_065458

LVK paper $(M, a, z) = (60.3^{+4.}_{-3.3}, 0.73^{+0.06}_{-0.06}, 0.18^{+0.05}_{-0.07})$

Hanford

H1_SpectrogramAR

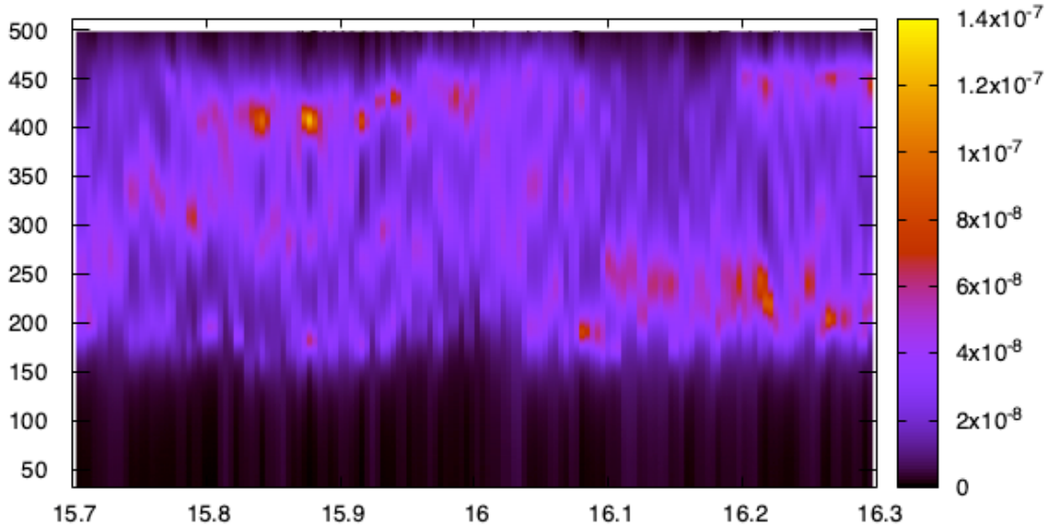

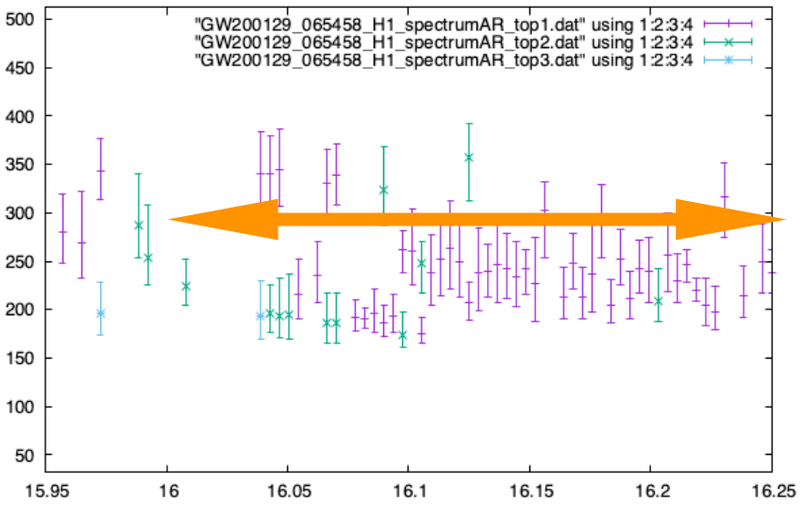

Network SNR=26.8

355Hz
◀323Hz
300Hz

Livingston

L1_SpectrogramAR

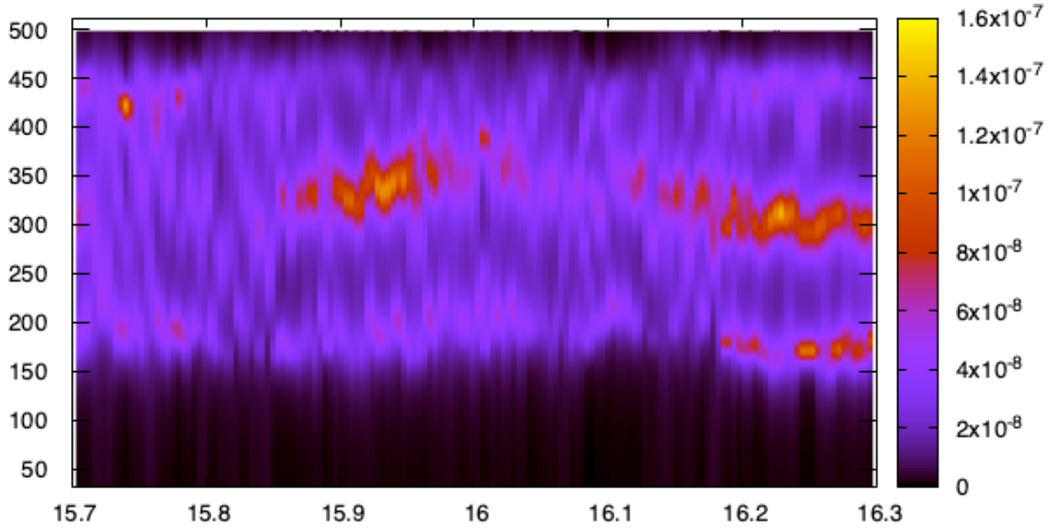

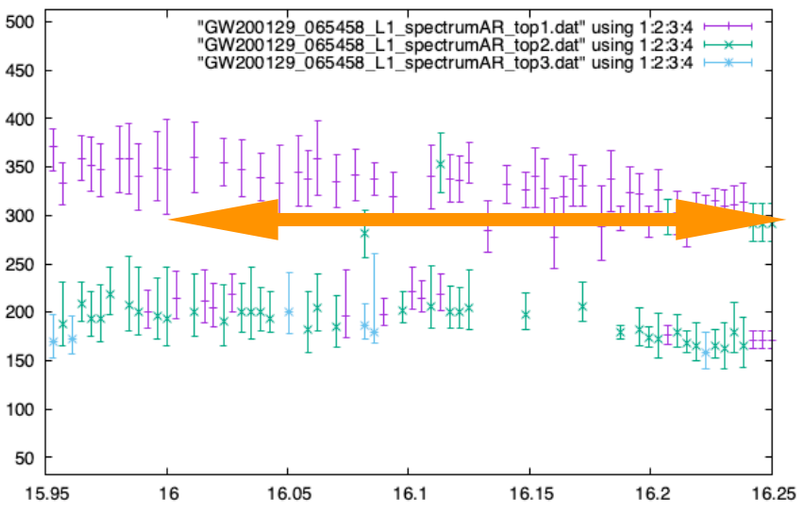

303 Hz
◀296 Hz
291 Hz

Virgo

V1_SpectrogramAR

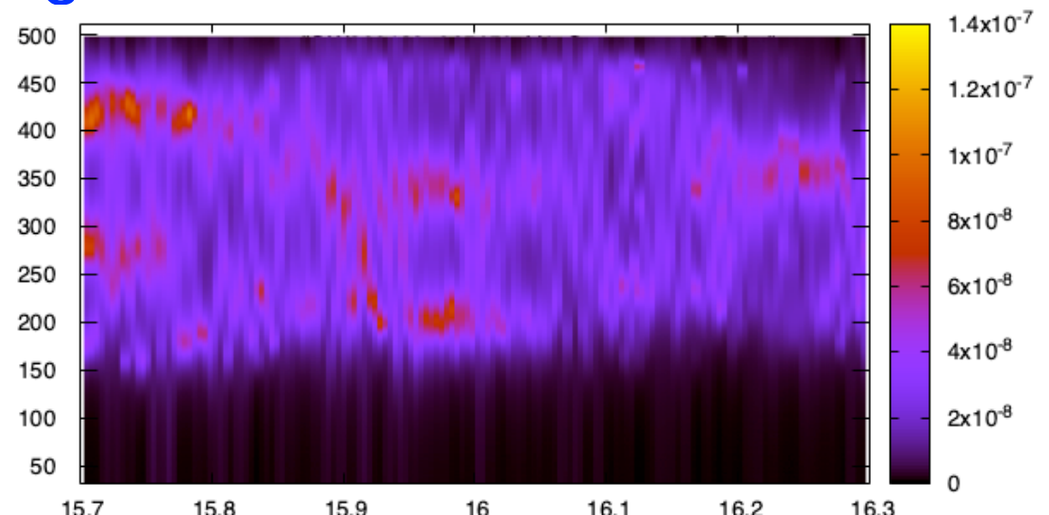

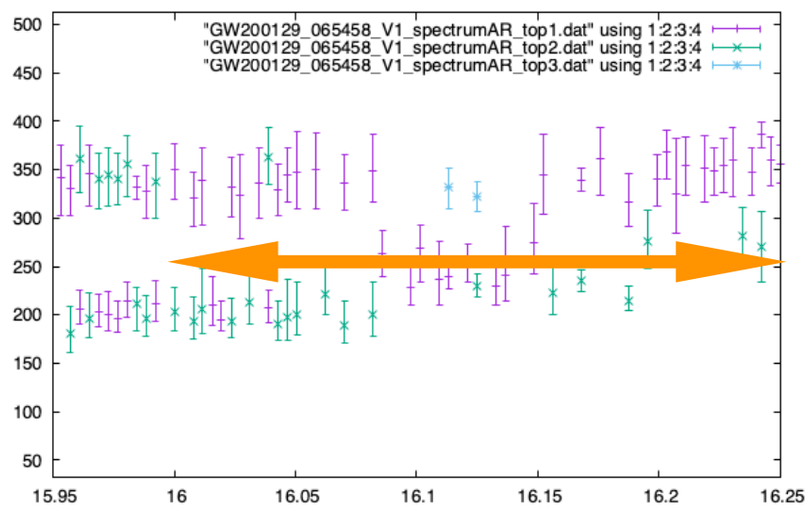

224 Hz
◀206 Hz
189 Hz

GW200129_065458

LVK paper $(M, a, z) = (60.3^{+4.}_{-3.3}, 0.73^{+0.06}_{-0.06}, 0.18^{+0.05}_{-0.07})$

Hanford

H1_SpectrogramAR

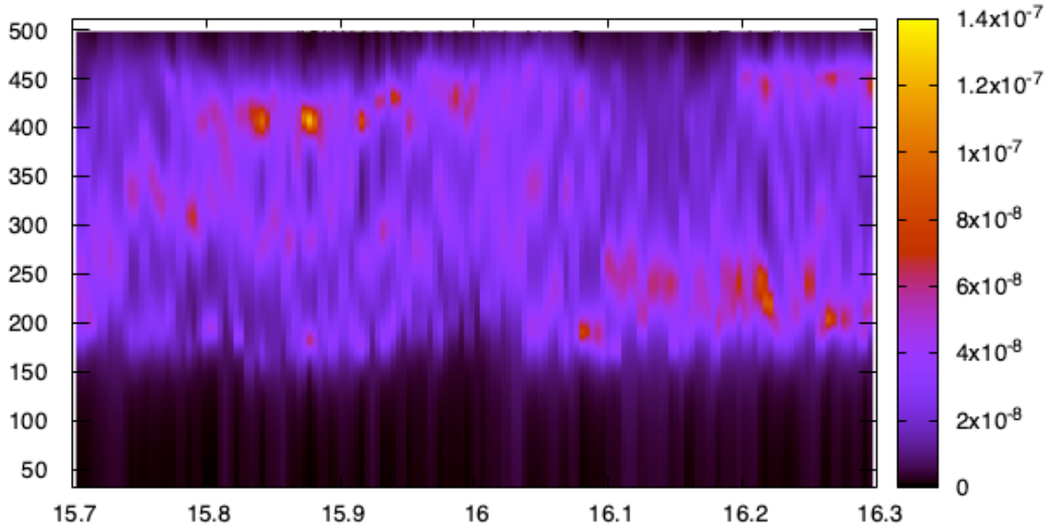

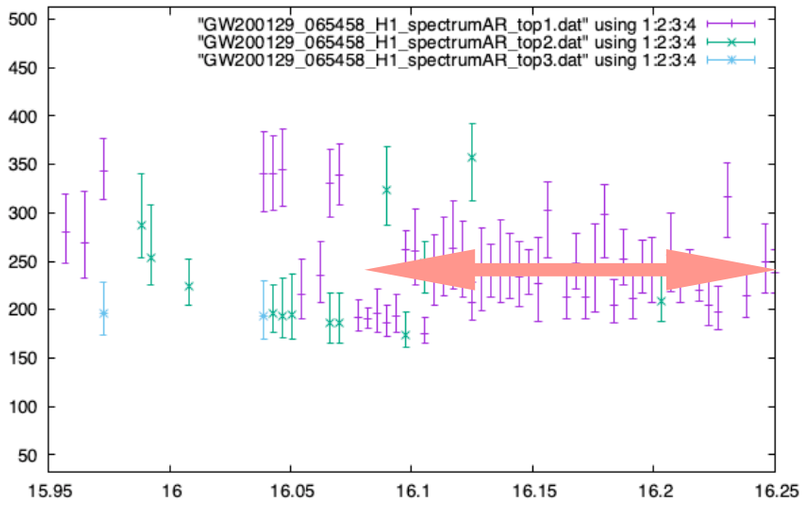

Network SNR=26.8

355Hz
◀323Hz
300Hz

252Hz
◀242Hz
234Hz

Livingston

L1_SpectrogramAR

303 Hz
◀296 Hz
291 Hz

208 Hz
◀192 Hz
183 Hz

Virgo

V1_SpectrogramAR

224 Hz
◀206 Hz
189 Hz

229 Hz
◀212 Hz
201 Hz

GW200129_065458

LVK paper $(M, a, z) = (60.3^{+4.}_{-3.3}, 0.73^{+0.06}_{-0.06}, 0.18^{+0.05}_{-0.07})$

Network SNR=26.8

Spin *a*

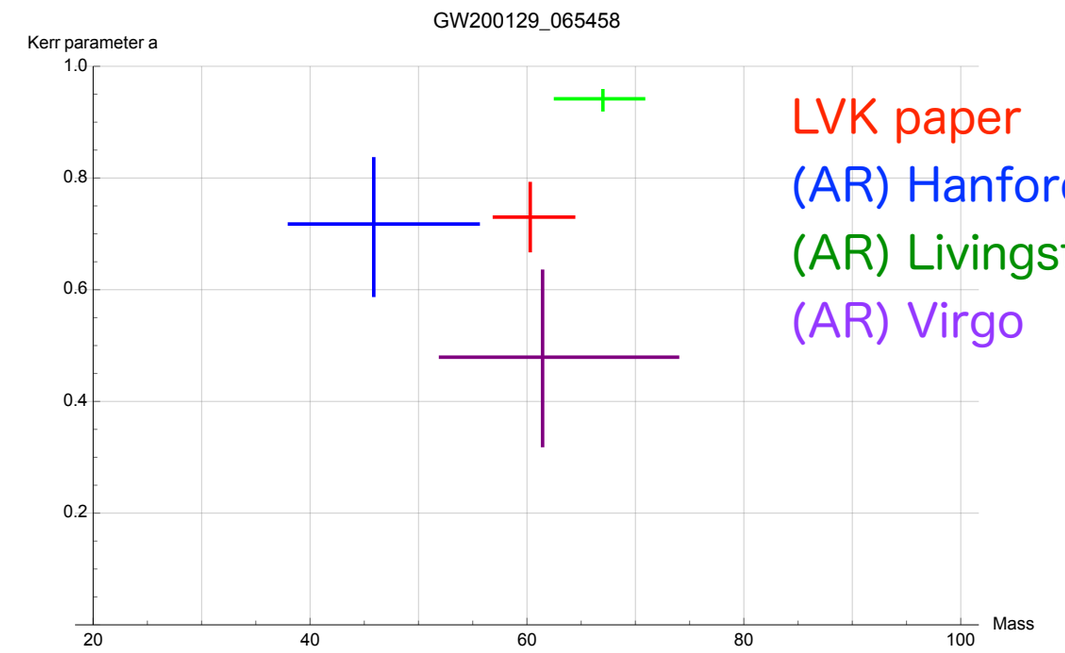

Mass *M*

Spin *a*

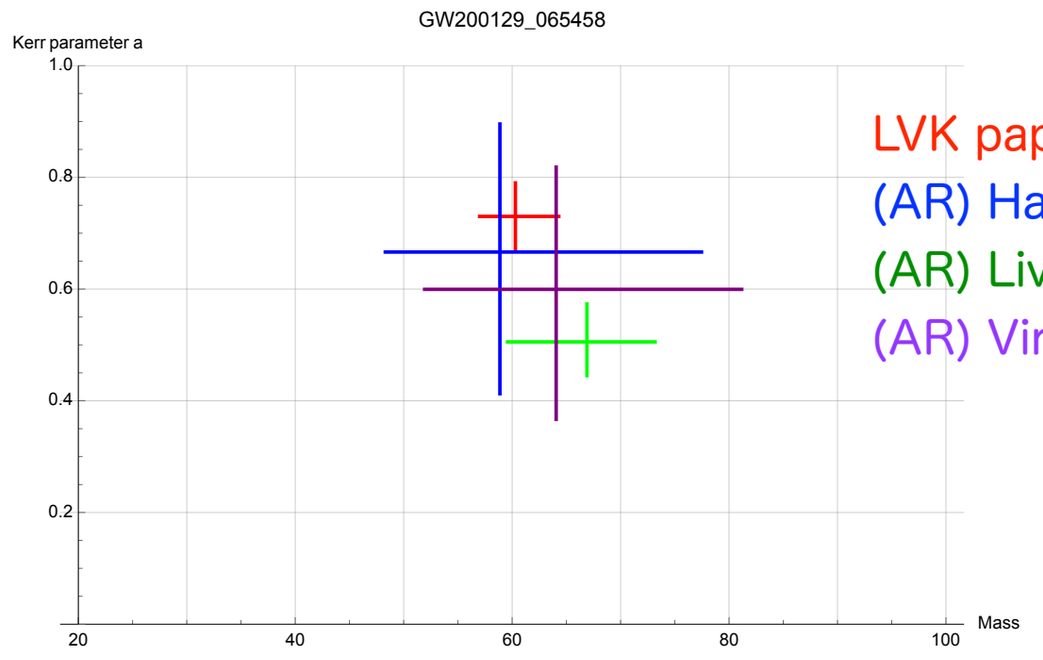

Mass *M*

estimated from the merger time for 0.25 sec

estimated from 0.10 sec after the merger for 0.15 sec

GW190828_063405

LV paper $(M, a, z) = (54.9^{+7.2}_{-4.3}, 0.61^{+0.18}_{-0.19}, 0.38^{+0.1}_{-0.15})$

Hanford

H1_SpectrogramAR

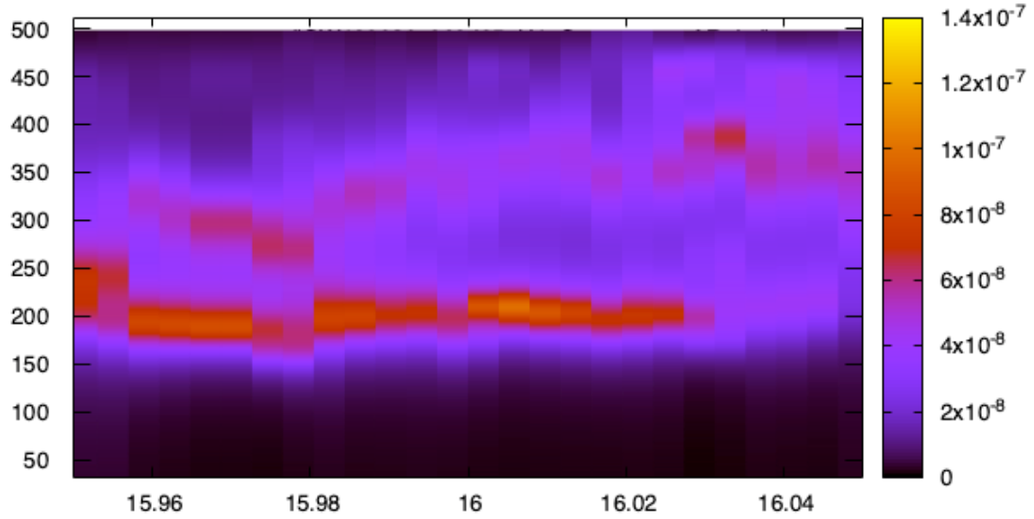

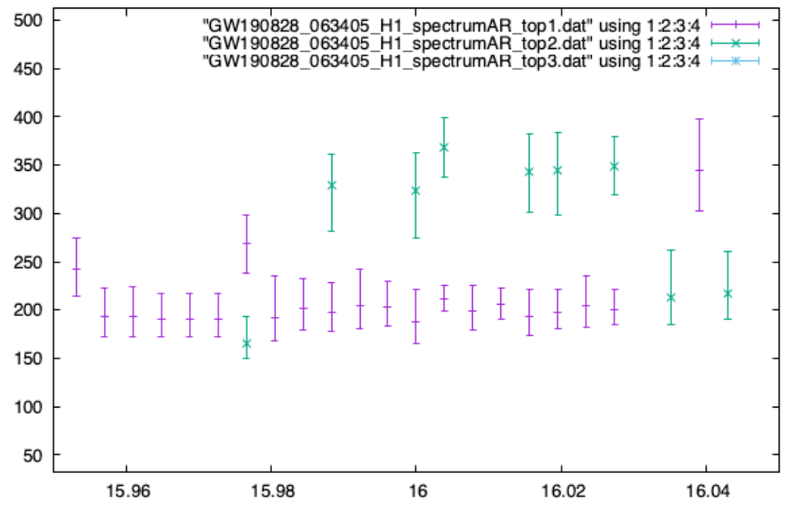

Network SNR=15.182

369Hz
◀354Hz
344Hz

203Hz
◀198Hz
195Hz

Livingston

L1_SpectrogramAR

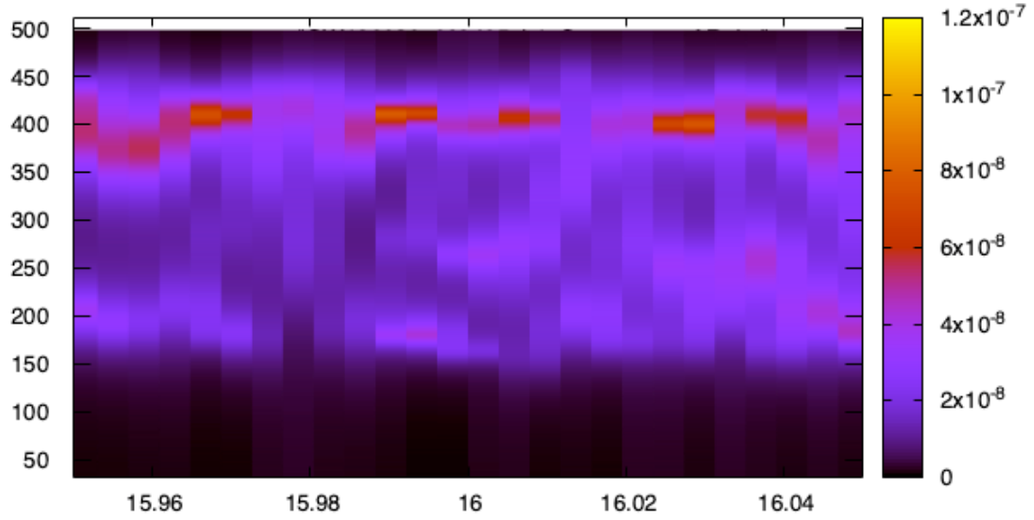

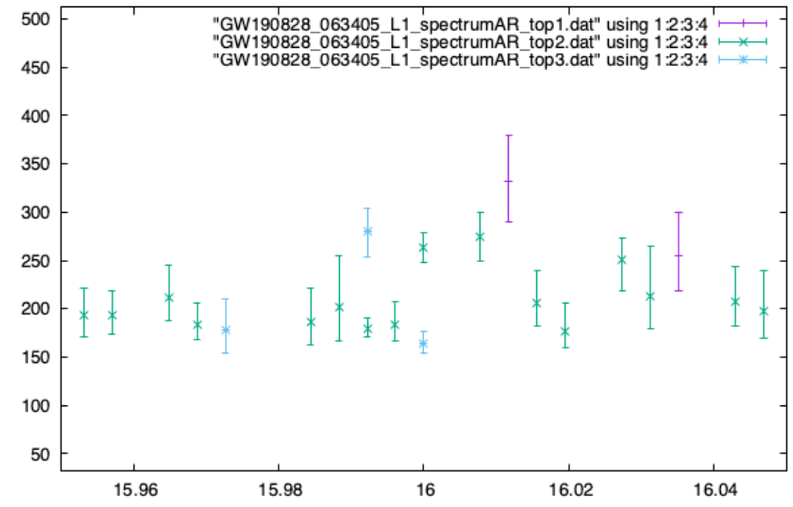

425Hz
◀407Hz
389Hz

210Hz
◀204Hz
200Hz

Virgo

V1_SpectrogramAR

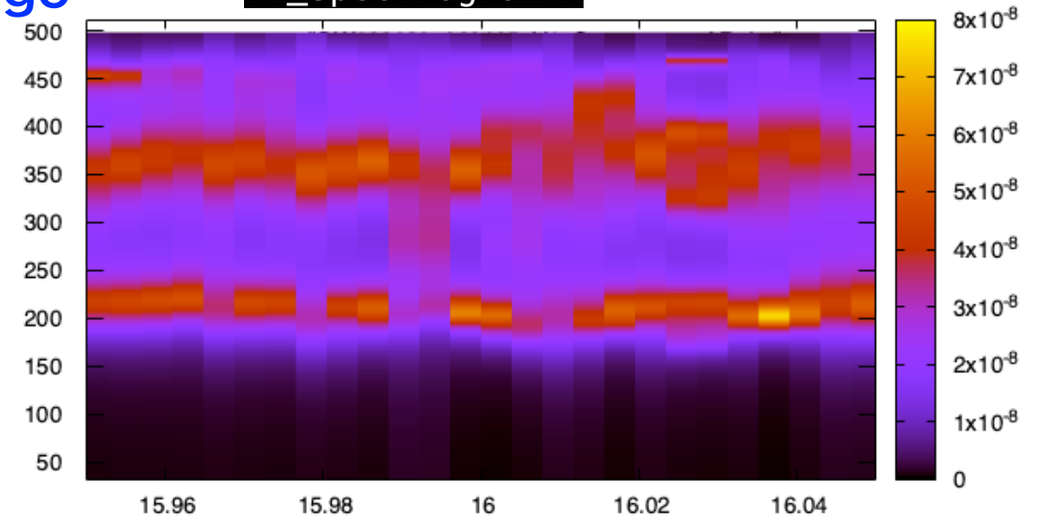

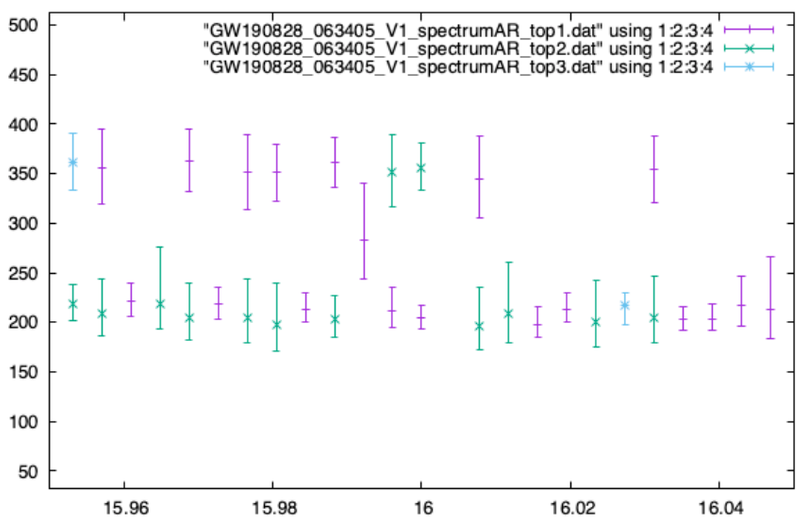

379Hz
◀366Hz
355Hz

214Hz
◀207Hz
201Hz

GW190828_063405

LV paper $(M, a, z) = (54.9^{+7.2}_{-4.3}, 0.61^{+0.18}_{-0.19}, 0.38^{+0.1}_{-0.15})$

Network SNR=15.182

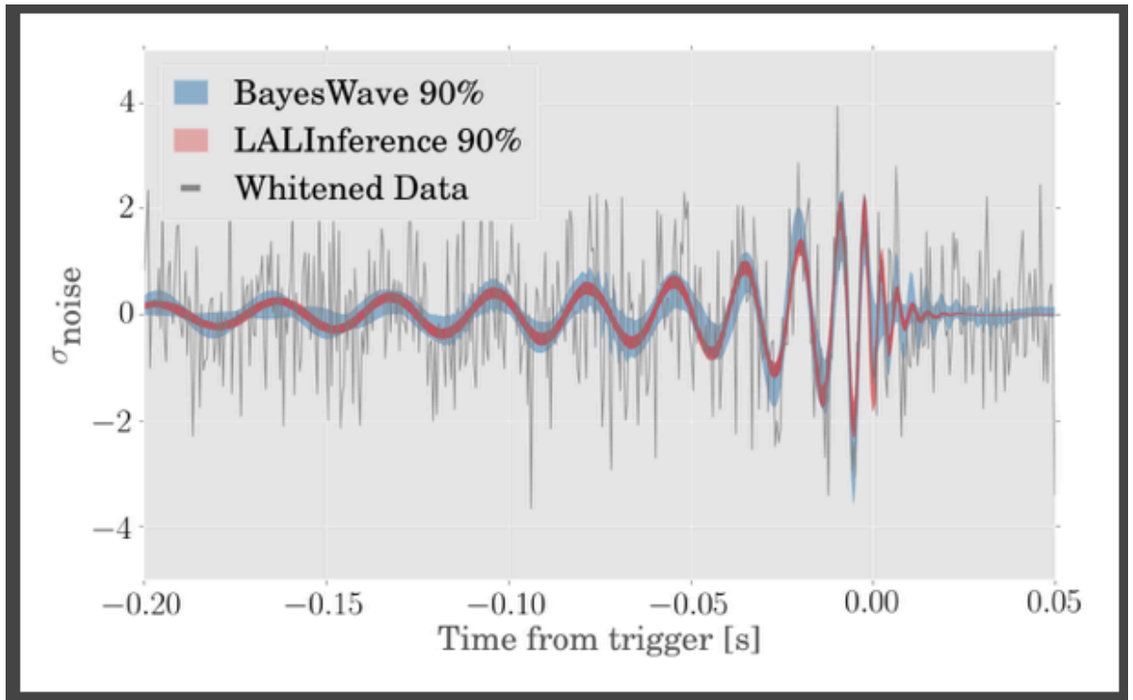

Waveform Reconstruction for GW190828_063405

Expected f_{QNM} (source frame)

$f_{220} = 213.6$ Hz, $f_{221} = 207.8$ Hz, $f_{222} = 196.8$ Hz
$f_{210} = 323.2$ Hz, $f_{211} = 181.2$ Hz, $f_{200} = 212.2$ Hz
$f_{330} = 339.7$ Hz, $f_{331} = 336.2$ Hz, $f_{332} = 329.7$ Hz
$f_{320} = 311.2$ Hz, $f_{310} = 286.2$ Hz, $f_{300} = 264.6$ Hz

Expected f_{QNM} (detector frame)

$f_{220} = 294.8$ Hz, $f_{221} = 286.7$ Hz, $f_{222} = 271.6$ Hz
$f_{210} = 446.1$ Hz, $f_{211} = 250.1$ Hz, $f_{200} = 292.9$ Hz
$f_{330} = 468.8$ Hz, $f_{331} = 463.9$ Hz, $f_{332} = 455.0$ Hz
$f_{320} = 429.4$ Hz, $f_{310} = 394.9$ Hz, $f_{300} = 365.2$ Hz

Spin *a*

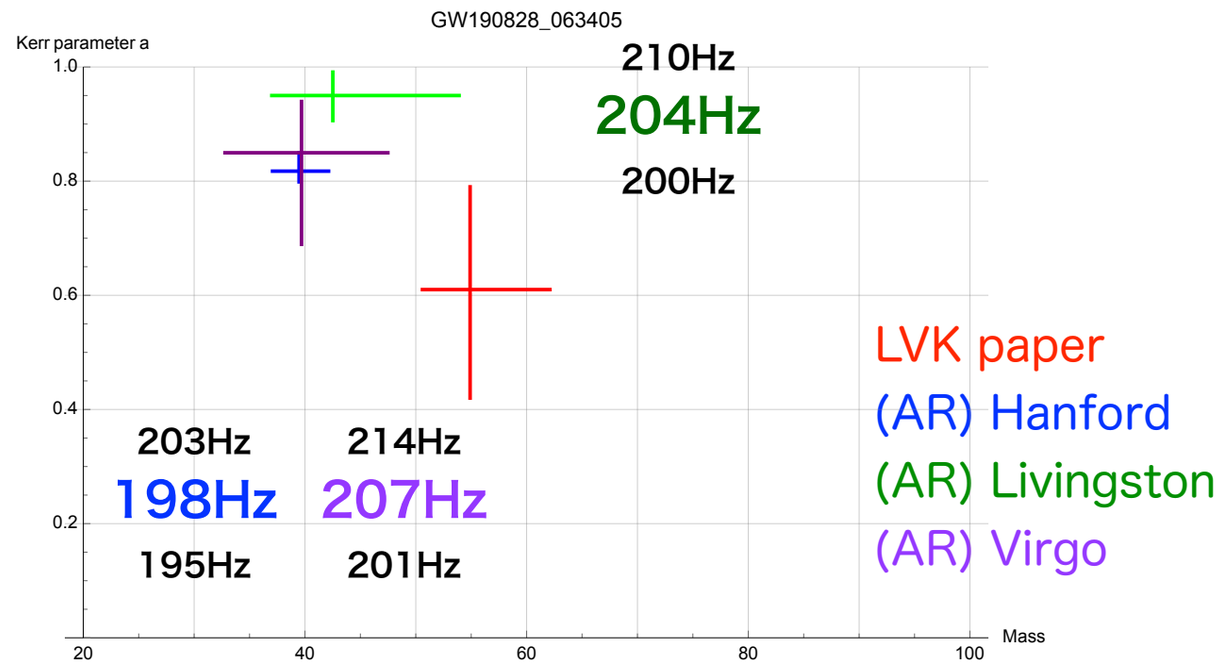

Mass *M*

Spin *a*

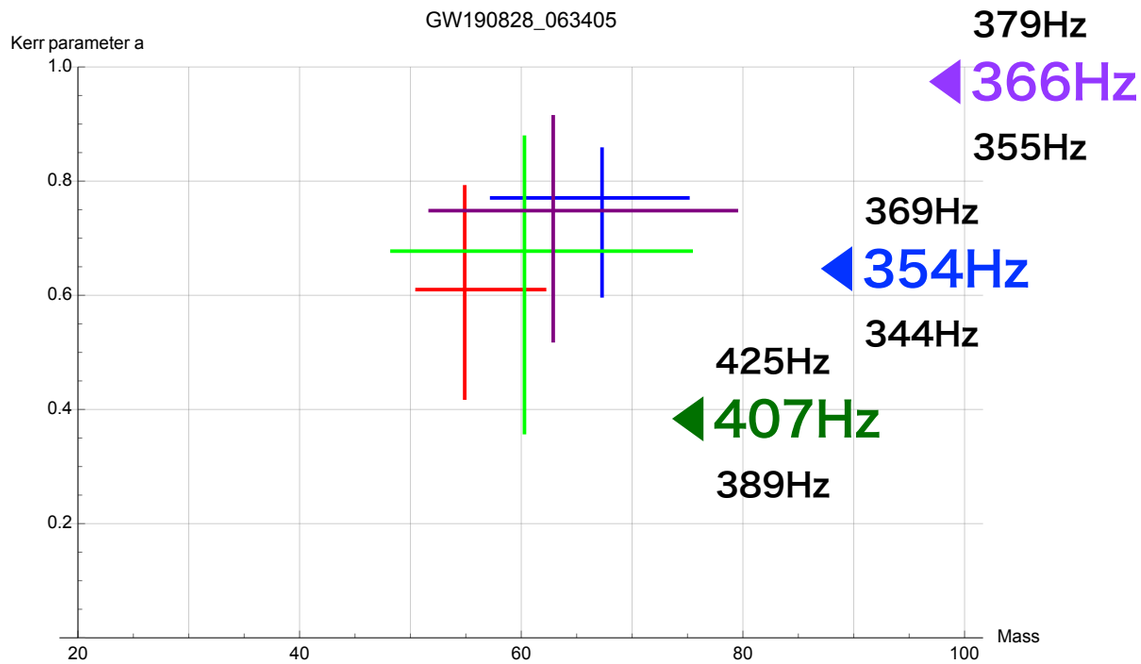

Mass *M*

GW200311_115853

LVK paper $(M, a, z) = (59.0^{+4.8}_{-3.9}, 0.69^{+0.07}_{-0.07}, 0.23^{+0.05}_{-0.07})$

Hanford

H1_SpectrogramAR

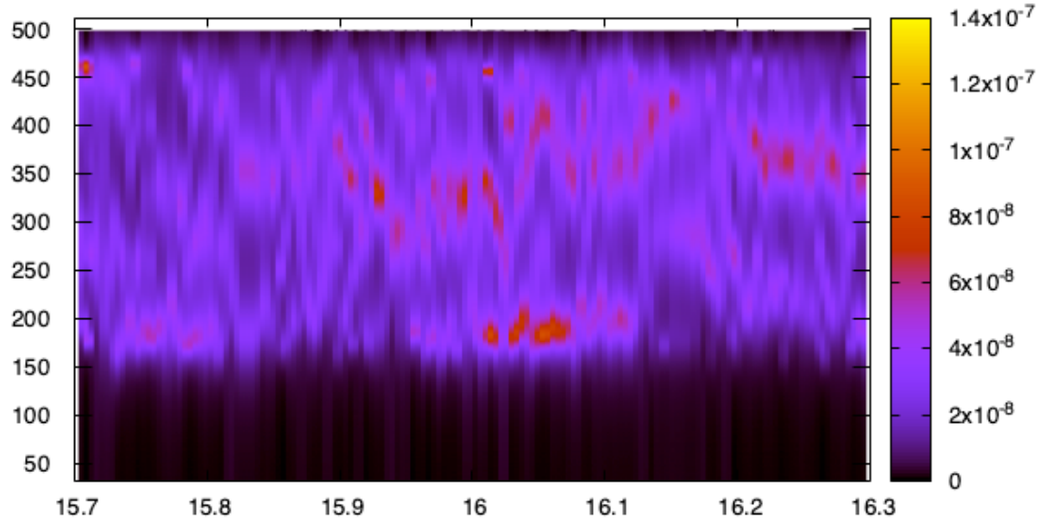

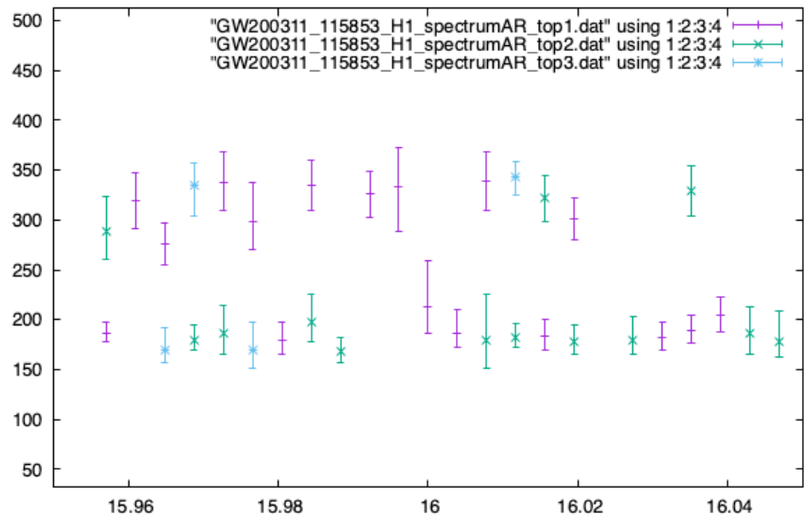

363Hz
◀350Hz
337Hz

206Hz
◀196Hz
191Hz

Livingston

L1_SpectrogramAR

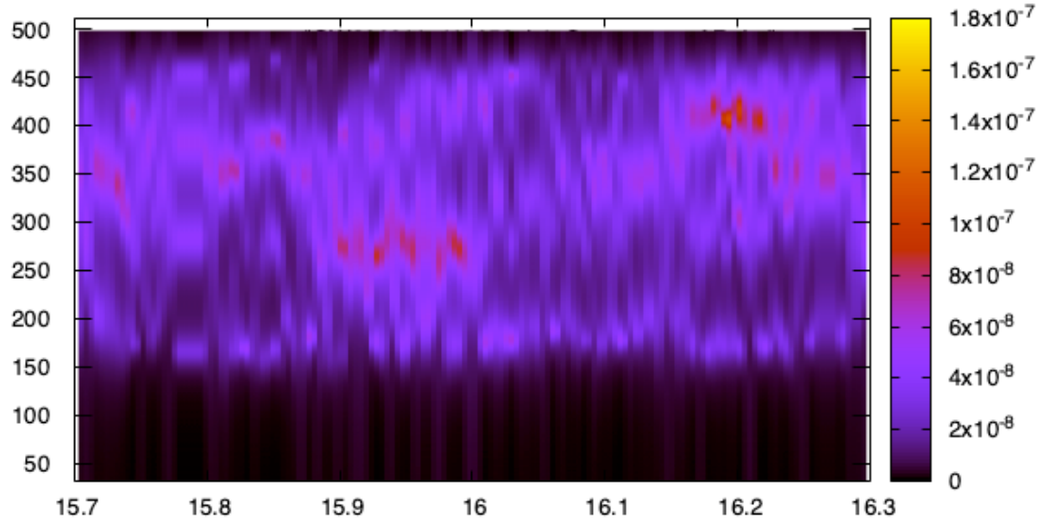

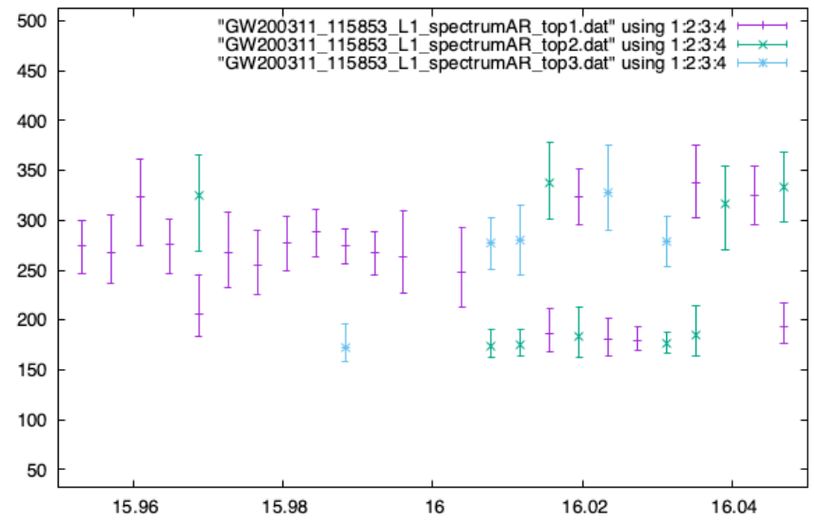

357Hz
◀341Hz
327Hz

190Hz
◀185Hz
180Hz

Virgo

V1_SpectrogramAR

GW200311_115853

LVK paper $(M, a, z) = (59.0^{+4.8}_{-3.9}, 0.69^{+0.07}_{-0.07}, 0.23^{+0.05}_{-0.07})$

Network SNR=17.8

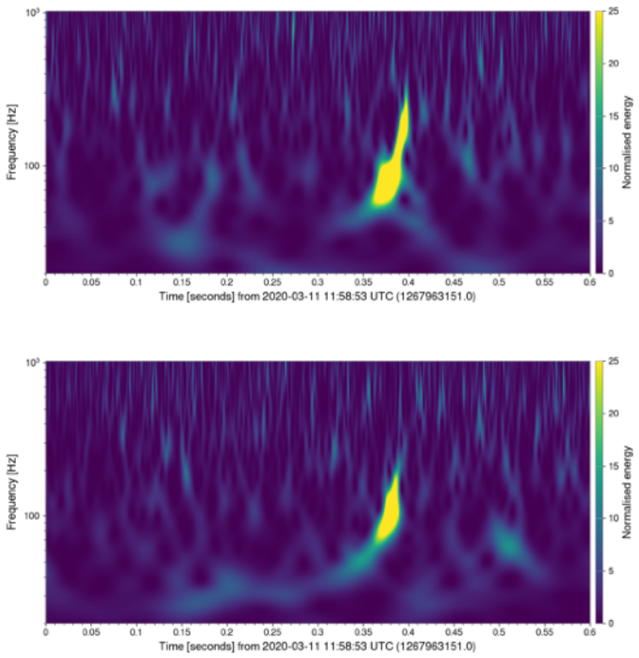

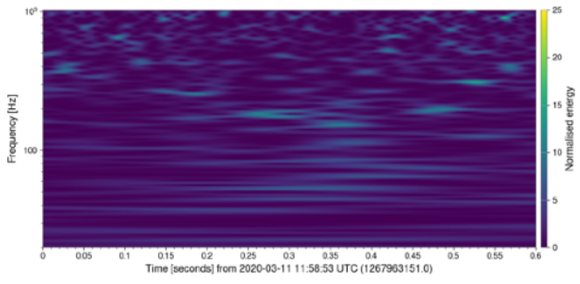

Expected f_{QNM} (detector frame)

$f_{220} = 290.7$ Hz, $f_{221} = 284.5$ Hz, $f_{222} = 272.4$ Hz
$f_{210} = 407.2$ Hz, $f_{211} = 241.4$ Hz, $f_{200} = 270.4$ Hz
$f_{330} = 460.9$ Hz, $f_{331} = 457.1$ Hz, $f_{332} = 450.3$ Hz
$f_{320} = 414.9$ Hz, $f_{310} = 375.5$ Hz, $f_{300} = 342.6$ Hz

Spin *a*

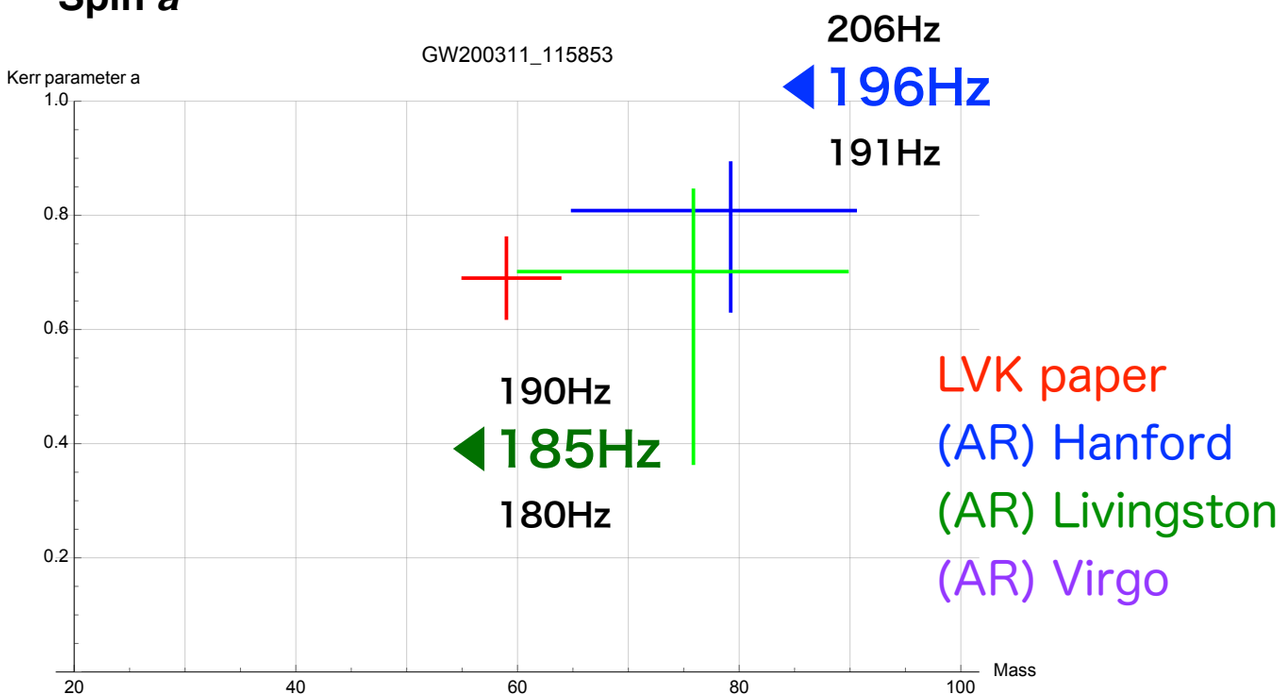

Mass *M*

Spin *a*

Mass *M*

GW190630_185205

LV paper $(M, a, z) = (56.4^{+4.4}_{-4.6}, 0.70^{+0.05}_{-0.07}, 0.18^{+0.1}_{-0.07})$

Hanford

H1_SpectrogramAR

Network SNR=15.6

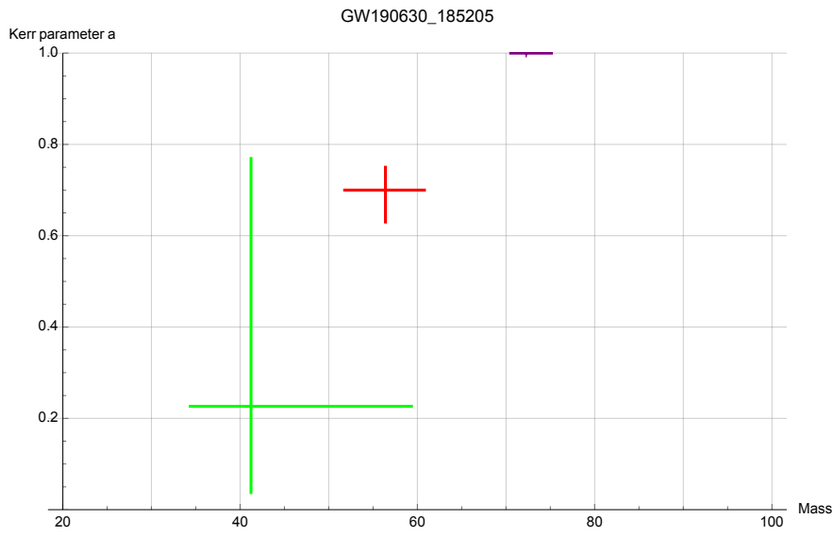

Livingston

L1_SpectrogramAR

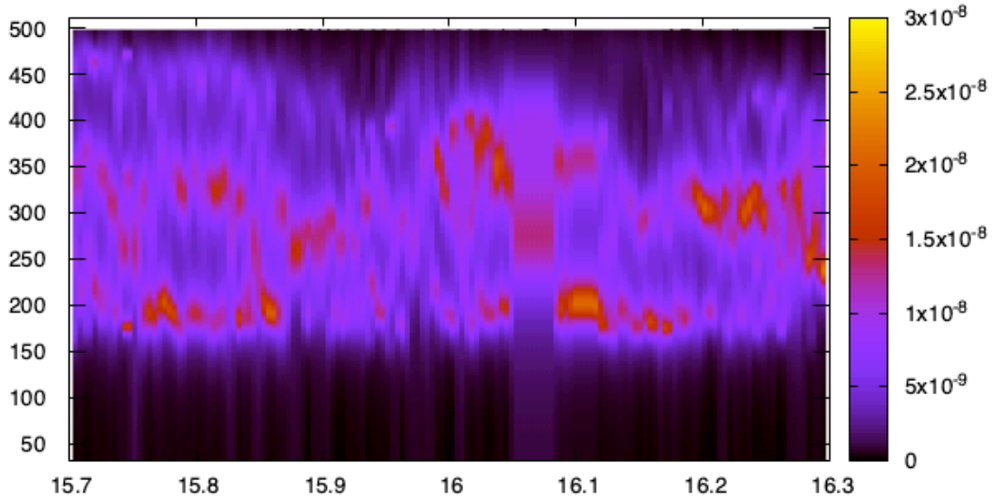

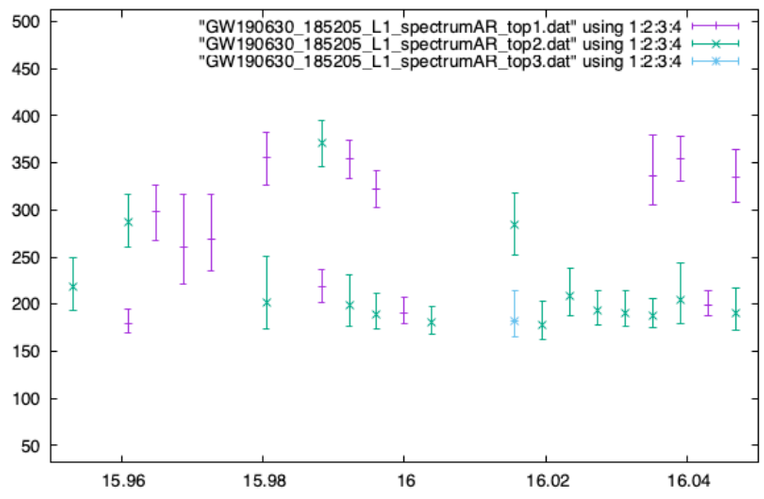

298 Hz
◀270Hz
262 Hz

206 Hz
◀197 Hz
187 Hz

Virgo

V1_SpectrogramAR

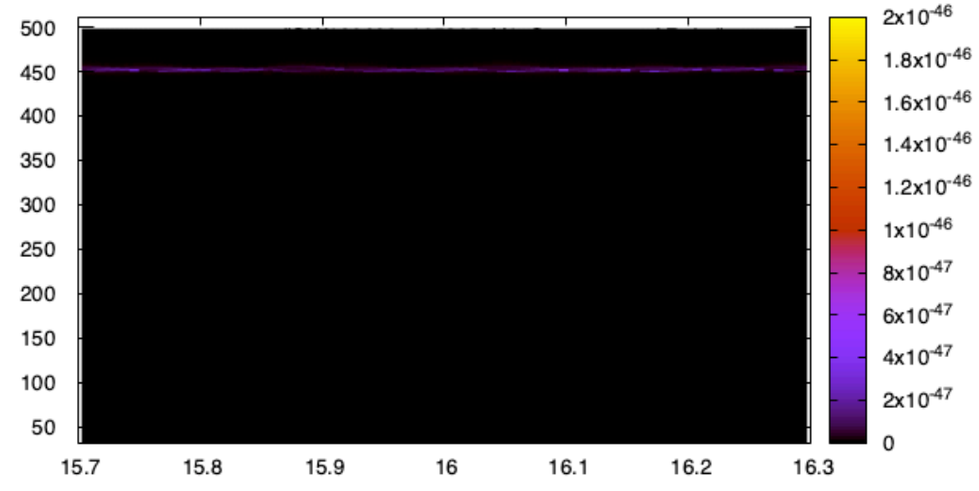

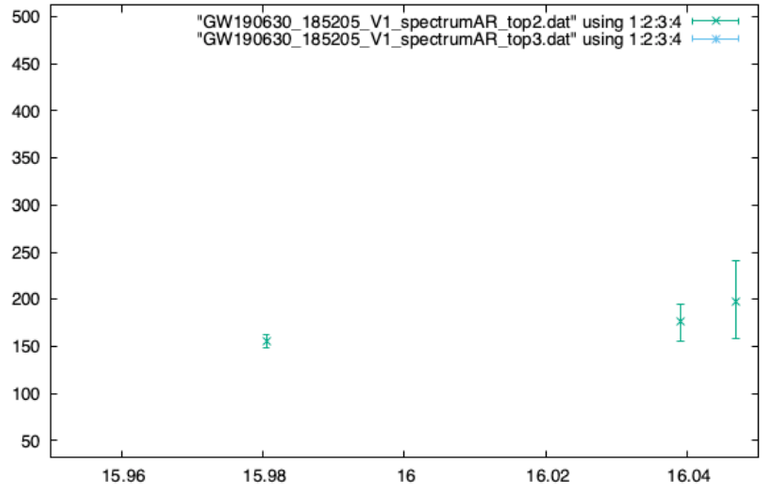

◀filter

GW200112_155838

LVK paper $(M, a, z) = (60.8^{+5.3}_{-4.3}, 0.71^{+0.06}_{-0.06}, 0.24^{+0.07}_{-0.08})$

Hanford

H1_SpectrogramAR

Network SNR=19.8

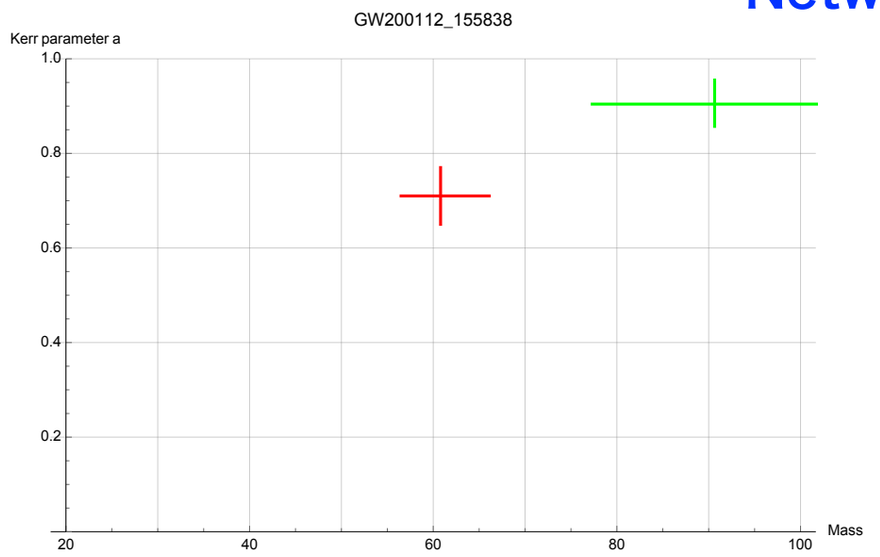

Livingston

L1_SpectrogramAR

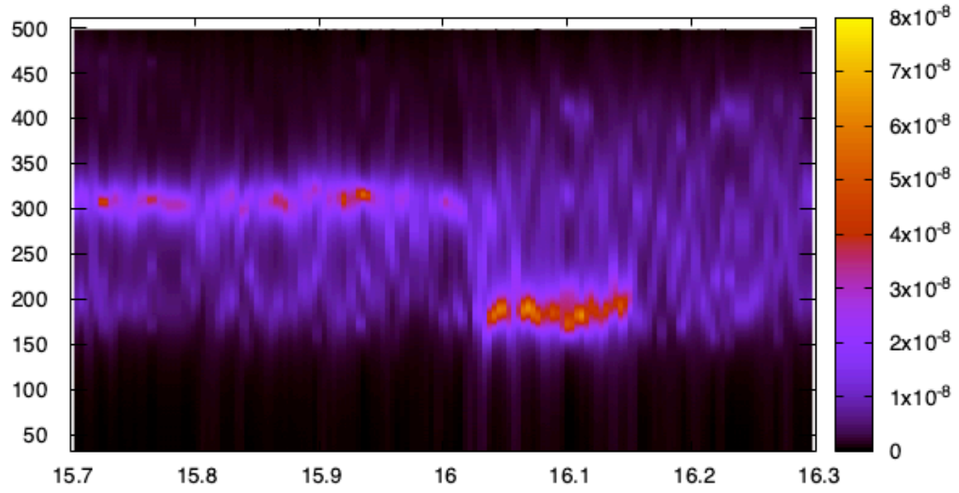

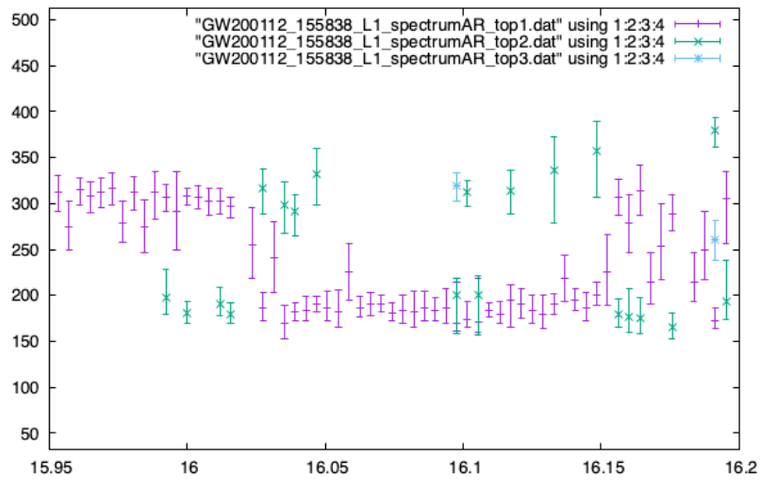

210 Hz
◀193 Hz
183 Hz

Virgo

V1_SpectrogramAR

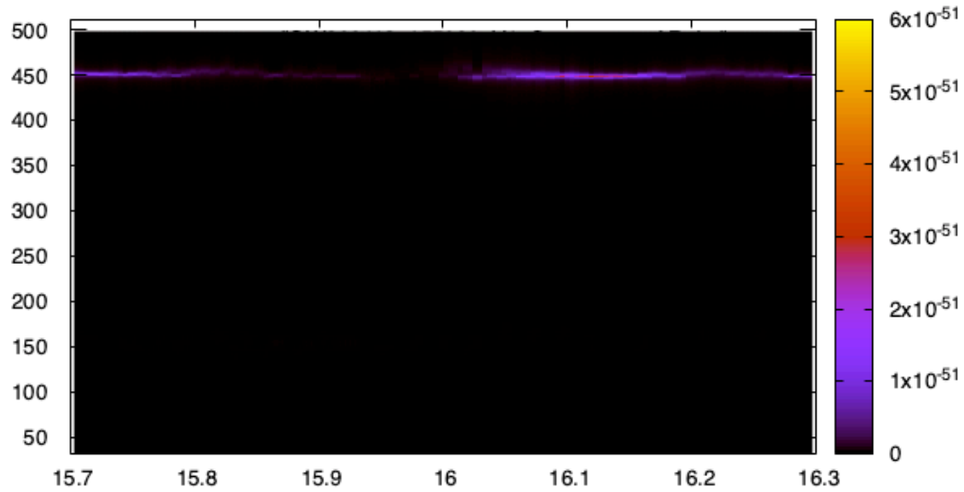

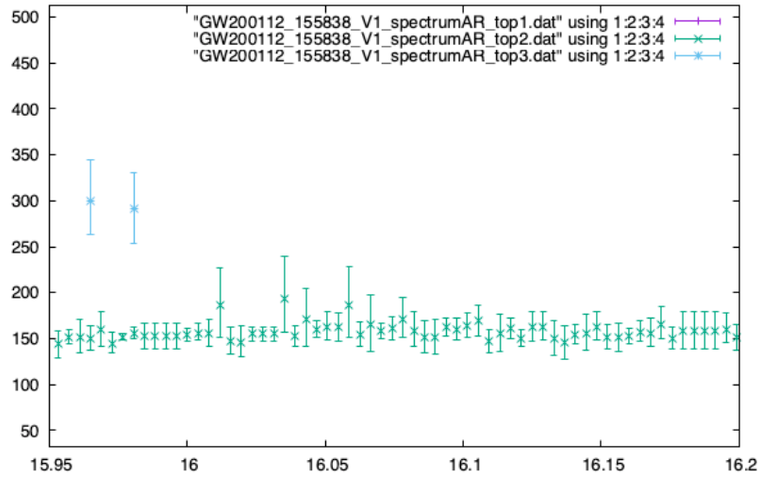

◀filter

◀filter

190 Hz
◀185 Hz
182 Hz

GW190910_112807

LV paper $(M, a, z) = (75.8^{+8.5}_{-8.6}, 0.70^{+0.08}_{-0.07}, 0.28^{+0.16}_{-0.1})$

Hanford

H1_SpectrogramAR

Network SNR=13.4

Livingston

L1_SpectrogramAR

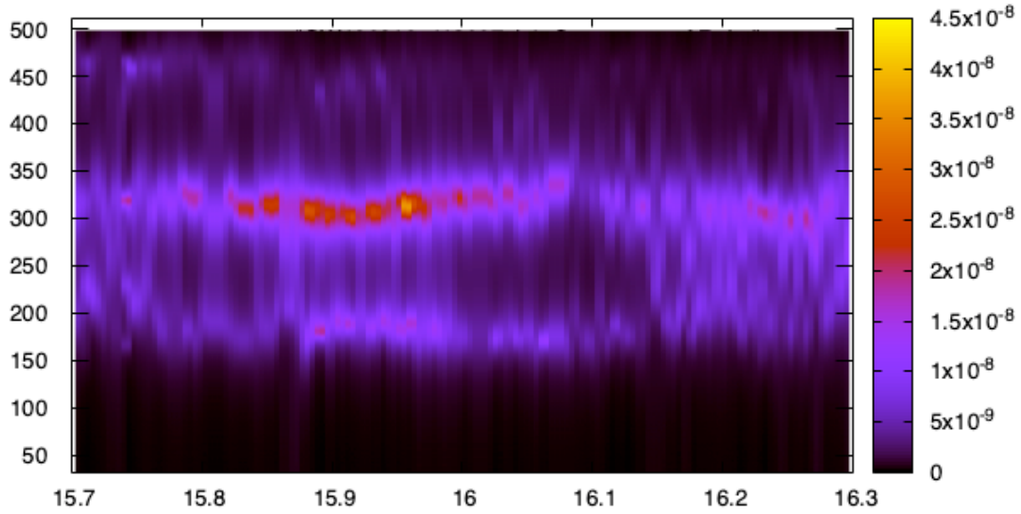

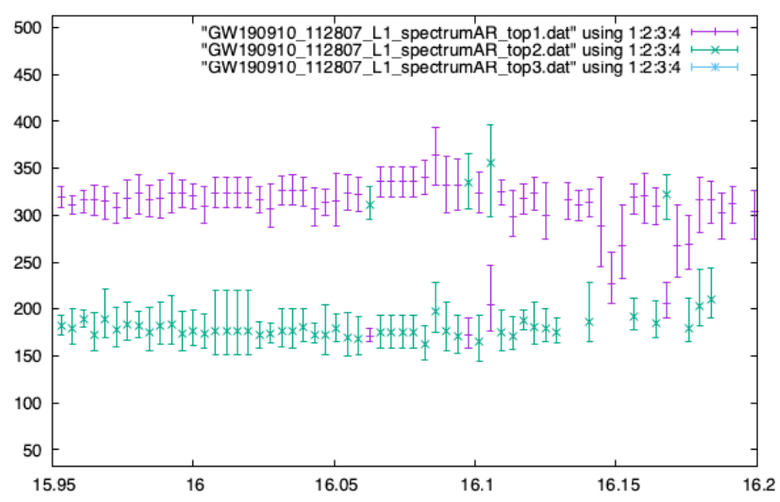

324 Hz

◀314 Hz

304 Hz

174 Hz

◀172 Hz

169 Hz

Virgo

V1_SpectrogramAR

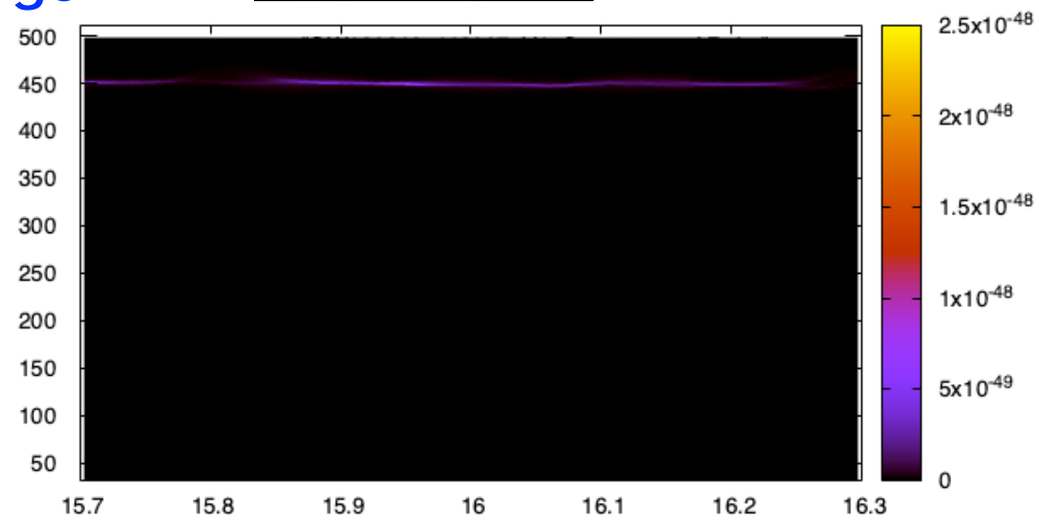

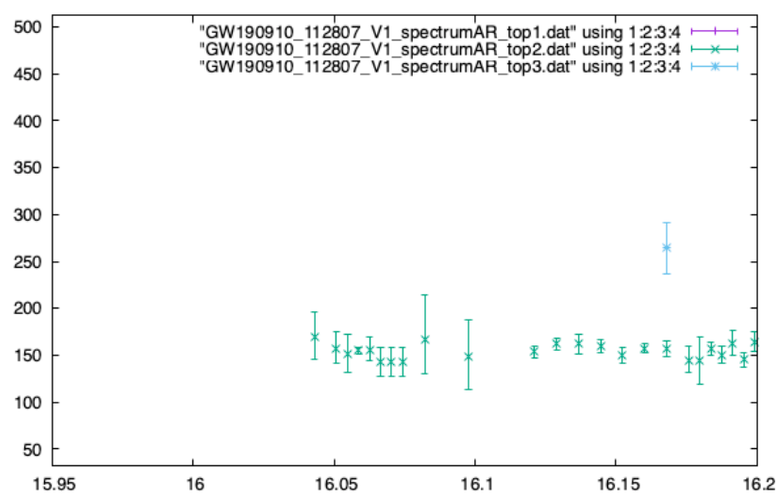

◀filter

◀filter

167 Hz

◀165 Hz

163 Hz

GW190910_112807

LV paper $(M, a, z) = (75.8^{+8.5}_{-8.6}, 0.70^{+0.08}_{-0.07}, 0.28^{+0.16}_{-0.1})$

Network SNR=13.4

Livingston

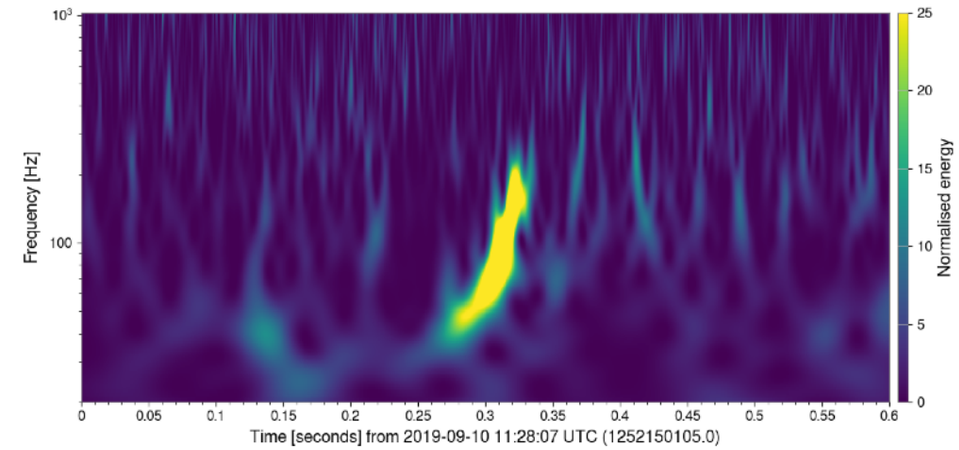

Virgo

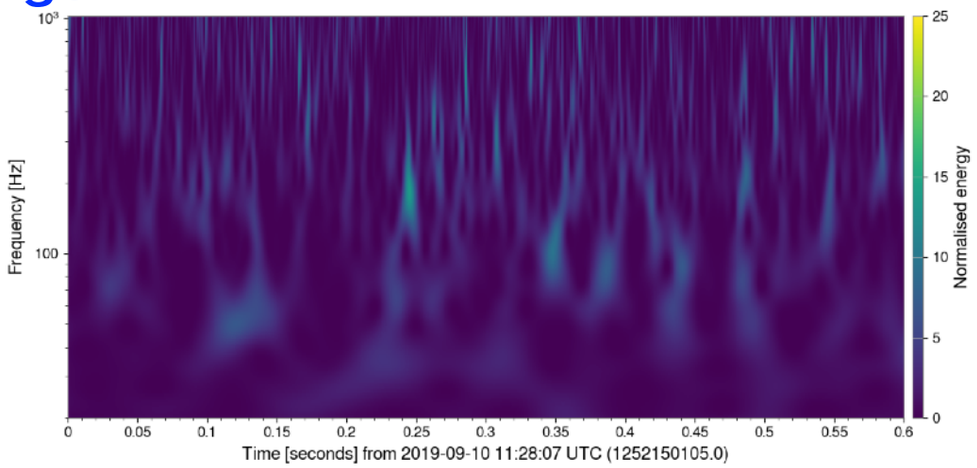

Expected f_{QNM}

(detector frame)

$$f_{220} = 228.1 \text{ Hz}, f_{221} = 223.4 \text{ Hz}, f_{222} = 214.2 \text{ Hz}$$
$$f_{210} = 316.1 \text{ Hz}, f_{211} = 188.8 \text{ Hz}, f_{200} = 210.2 \text{ Hz}$$
$$f_{330} = 361.4 \text{ Hz}, f_{331} = 358.6 \text{ Hz}, f_{332} = 353.4 \text{ Hz}$$
$$f_{320} = 324.5 \text{ Hz}, f_{310} = 293.1 \text{ Hz}, f_{300} = 267.0 \text{ Hz}$$

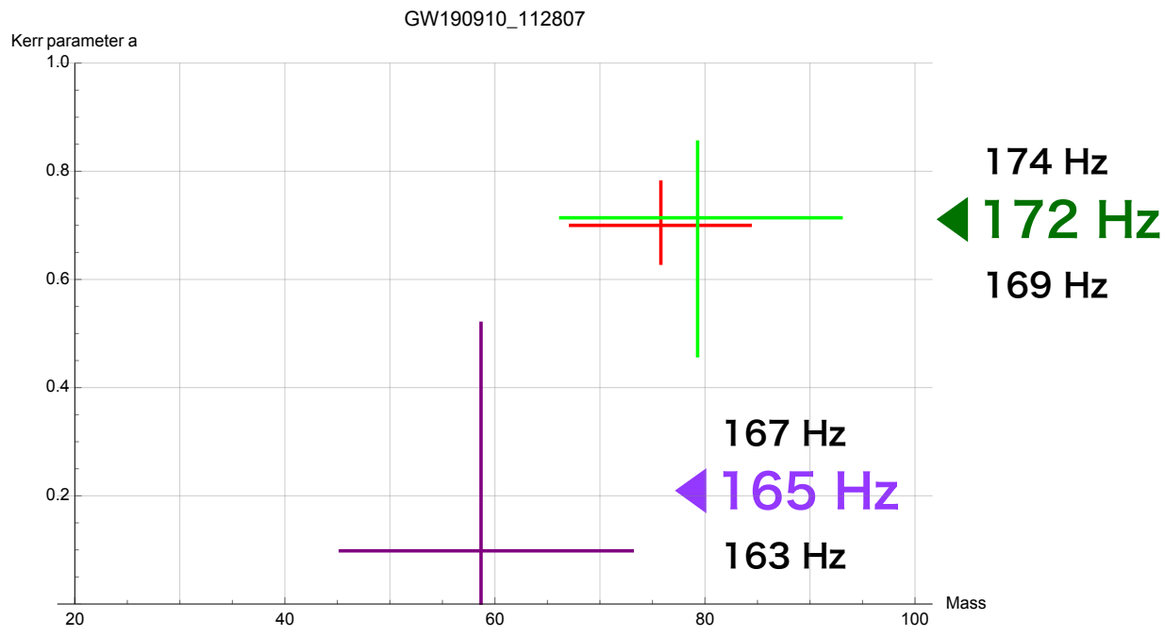

GW190408_181802

LV paper $(M, a, z) = (41.1^{+3.9}_{-2.8}, 0.67^{+0.06}_{-0.07}, 0.29^{+0.06}_{-0.1})$

Hanford

H1_SpectrogramAR

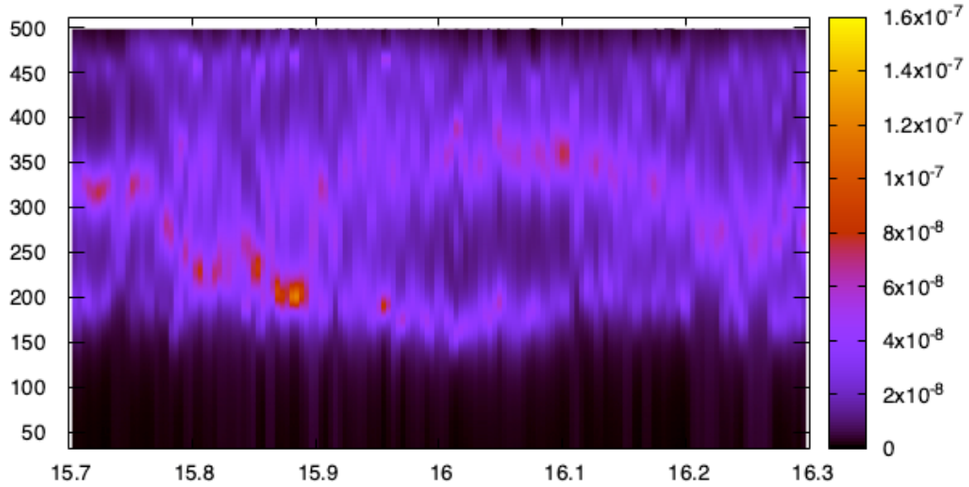

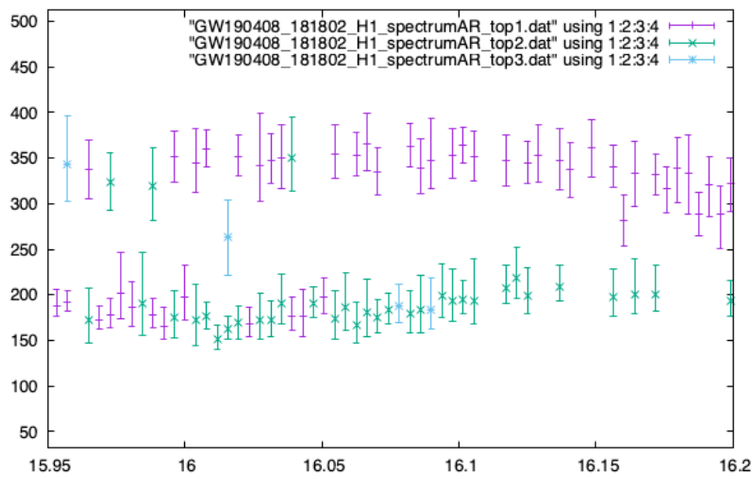

Network SNR=14.7

367Hz
◀349Hz
337Hz

Livingston

L1_SpectrogramAR

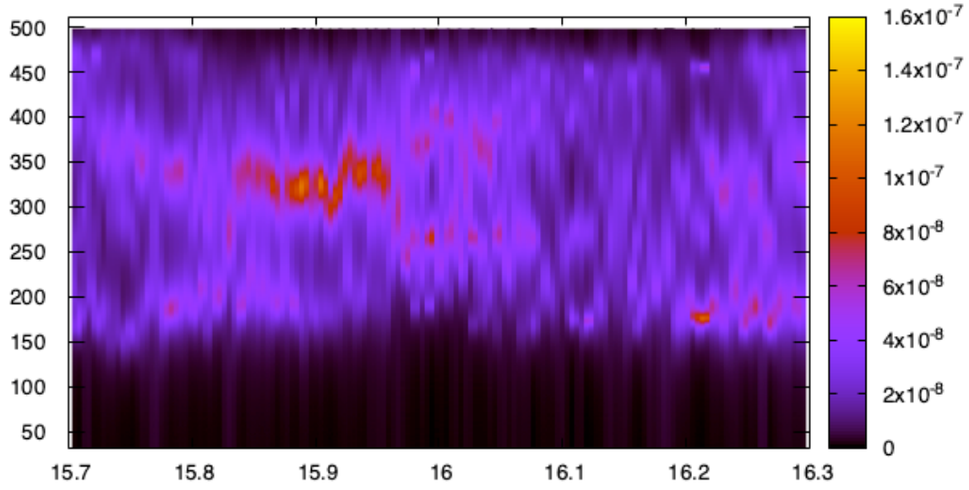

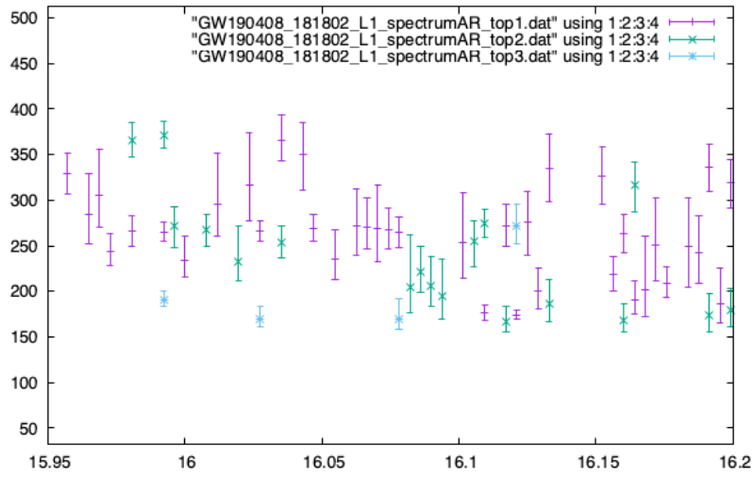

388 Hz
◀356 Hz
334 Hz

Virgo

V1_SpectrogramAR

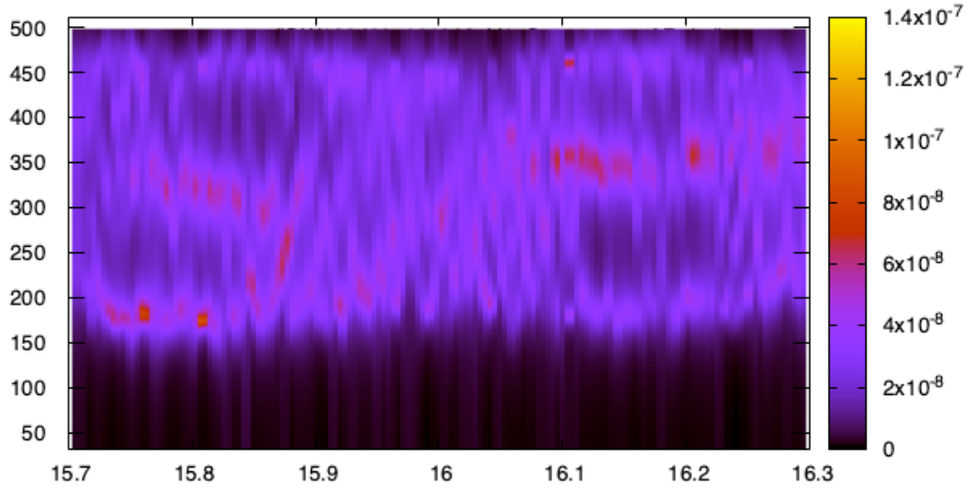

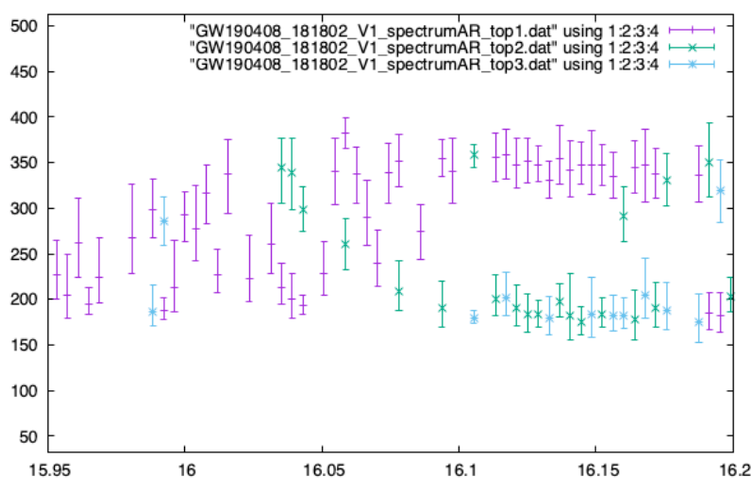

358 Hz
◀347 Hz
337 Hz

GW190408_181802

LV paper $(M, a, z) = (41.1^{+3.9}_{-2.8}, 0.67^{+0.06}_{-0.07}, 0.29^{+0.06}_{-0.1})$

Hanford

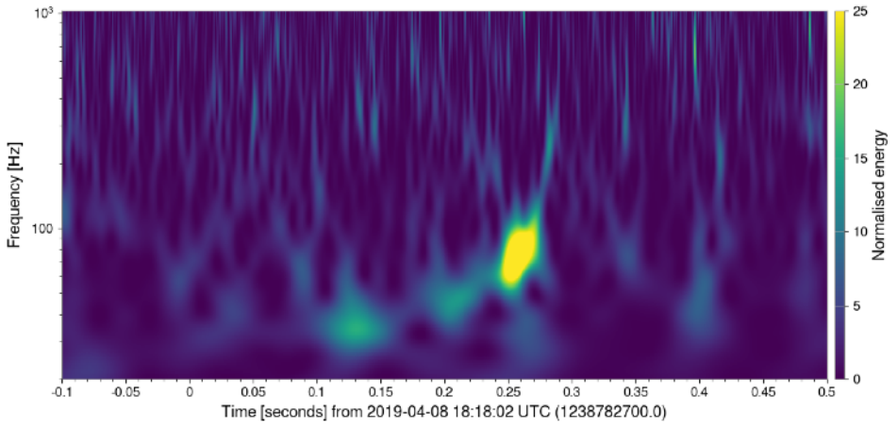

Livingston

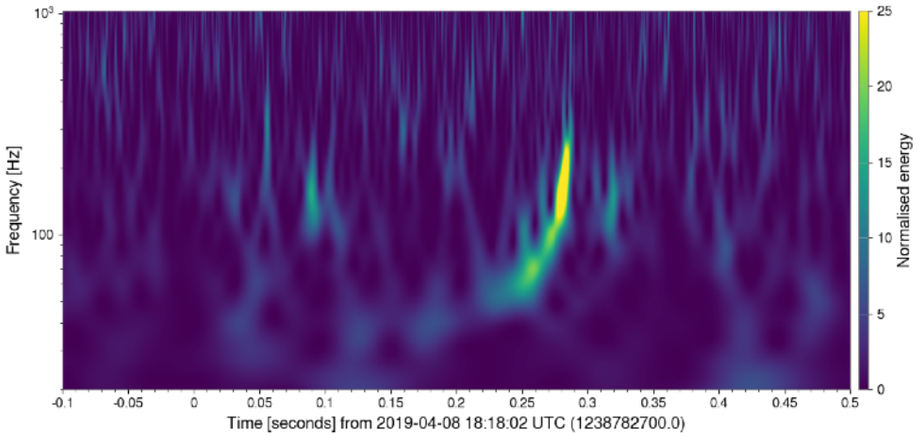

Virgo

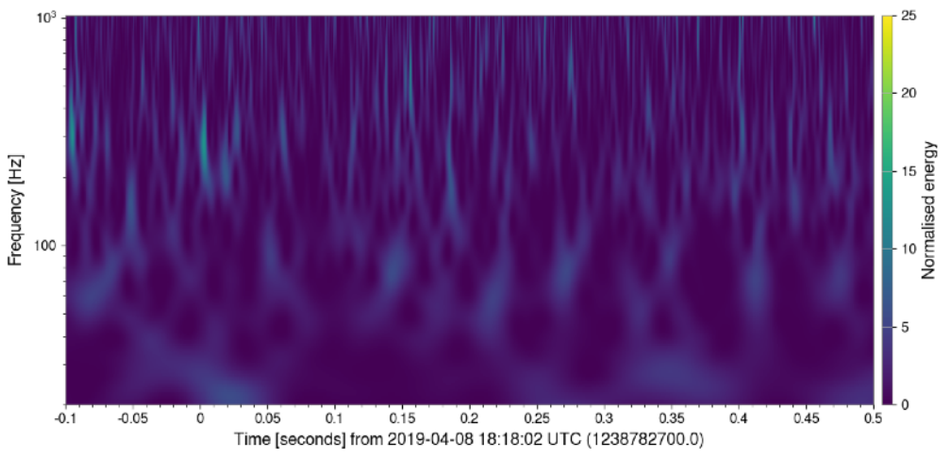

Network SNR=14.7

Expected f_{QNM} (detector frame)

$$f_{220} = 410.9 \text{ Hz}, f_{221} = 401.6 \text{ Hz}, f_{222} = 383.5 \text{ Hz}$$
$$f_{210} = 587.5 \text{ Hz}, f_{211} = 343.3 \text{ Hz}, f_{200} = 388.9 \text{ Hz}$$
$$f_{330} = 652.1 \text{ Hz}, f_{331} = 646.4 \text{ Hz}, f_{332} = 636.1 \text{ Hz}$$
$$f_{320} = 589.7 \text{ Hz}, f_{310} = 536.0 \text{ Hz}, f_{300} = 490.8 \text{ Hz}$$

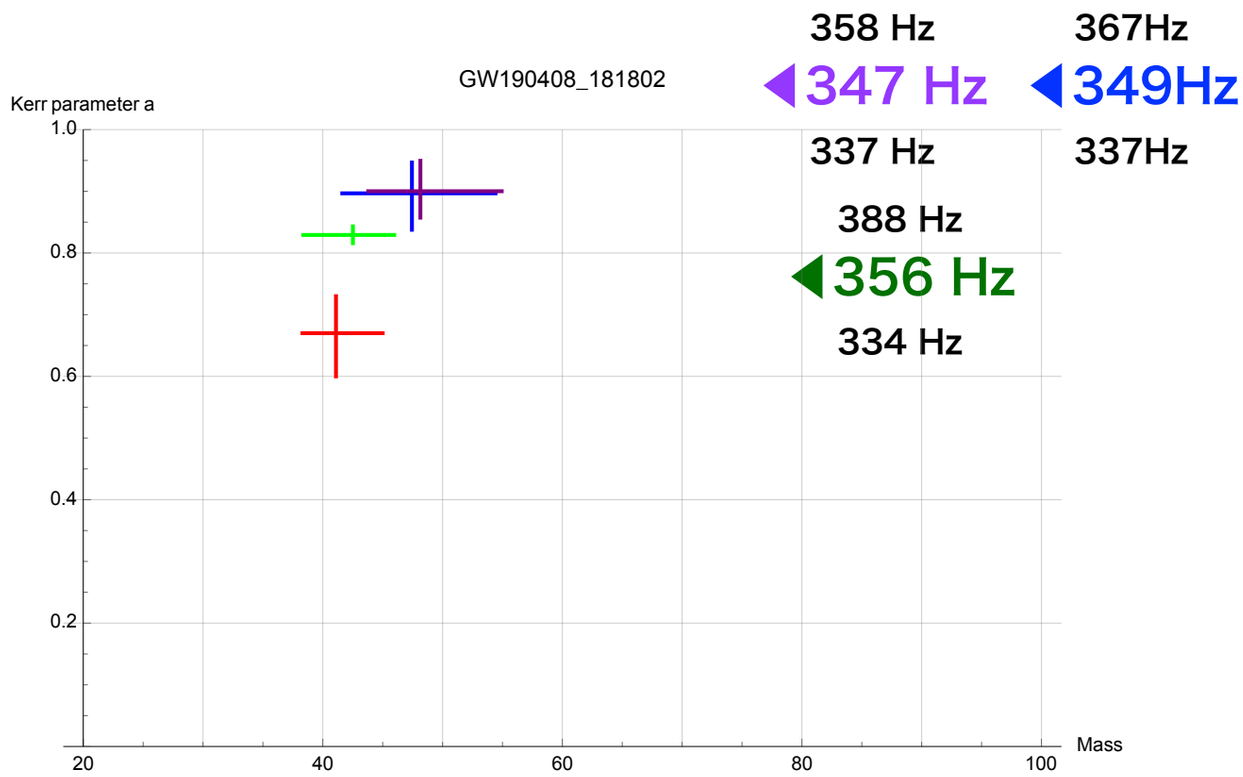

Summary & Outlook

AR model *x(t)*

$$
\begin{aligned}
x_n &= a_1 x_{n-1} + a_2 x_{n-2} + \cdots + a_M x_{n-M} + \varepsilon \\
&= \sum_{j=1}^{M} a_j x_{n-j} + \varepsilon
\end{aligned}
$$

Effective for finding frequencies and damping rates of short-time data (∼ 60 pts).

Data-base finding method, no templates are required.

Applied to LIGO/Virgo O1/O2/O3a & LVK O3b: Try to extract ring-down parts

Would be available for S/N >= 15, but some parameter tunings are necessary.

(Time width [merger time + X ms], Band Filterings [150-450Hz])

Analysis of GWTC-3 events are ongoing.
AR results of (M_final, a_final) are around the values of LV (LVK), i.e GR.